Quantum Monte Carlo simulations of ultracold fermions on optical lattices within dynamical mean-field theory

Nils Blümer and Elena Gorelik, Univ. Mainz

Outline

Systems with strong electronic (fermionic) correlations

Approaches for correlated Fermi systems

Auxiliary-field Hirsch-Fye QMC algorithm; Multigrid HF-QMC

Paramagnetic Mott transitions in 3-flavor mixtures

Melting of an antiferromagnet in an optical trap

Systems with strong electronic/fermionic correlations

Paramagnetic Mott metal-insulator transition

Prototype example: V_2O_3 doped with Cr/Ti and/or under pressure

Phase diagram

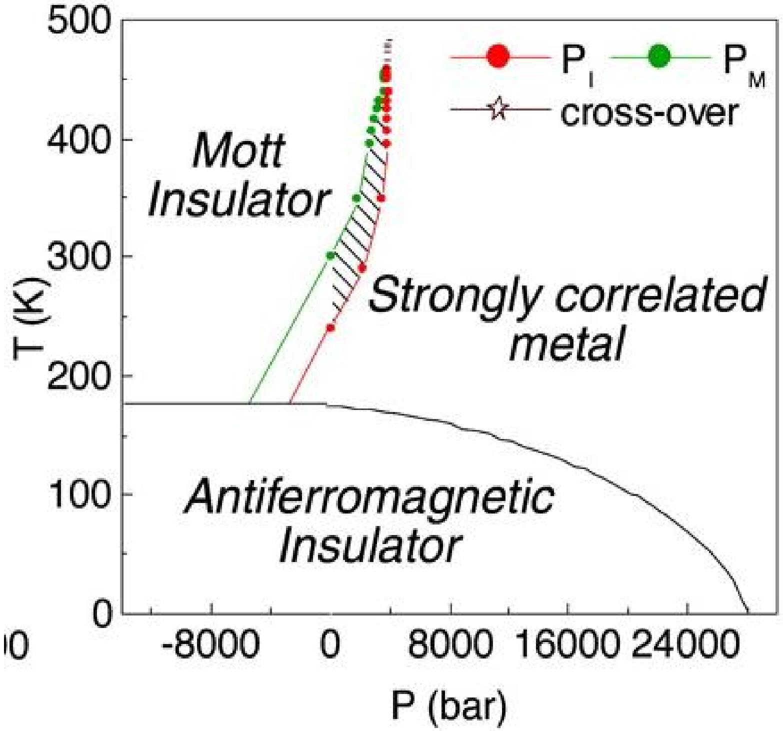

Systems with strong electronic/fermionic correlations

Paramagnetic Mott metal-insulator transition

Prototype example: V_2O_3 doped with Cr/Ti and/or under pressure

Phase diagram

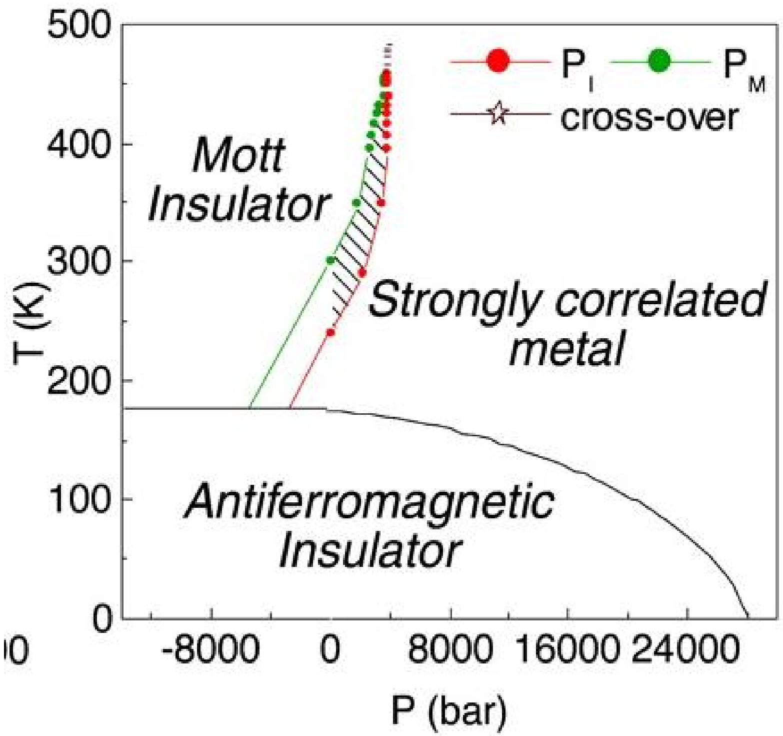

Electrical conductivity

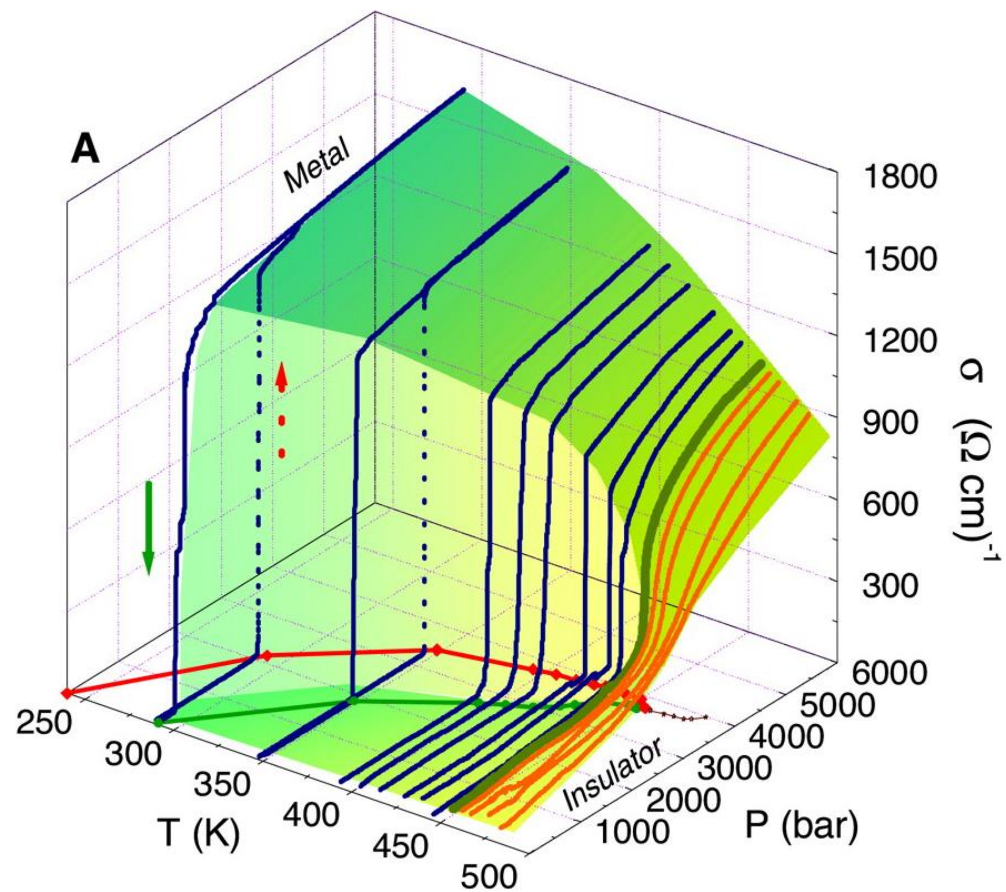

[Limelette et al., Science 302, 89 (2003)]

Ab initio calculations for correlated systems: LDA+DMFT

Recent "hot topic": kinks in photoemission spectra

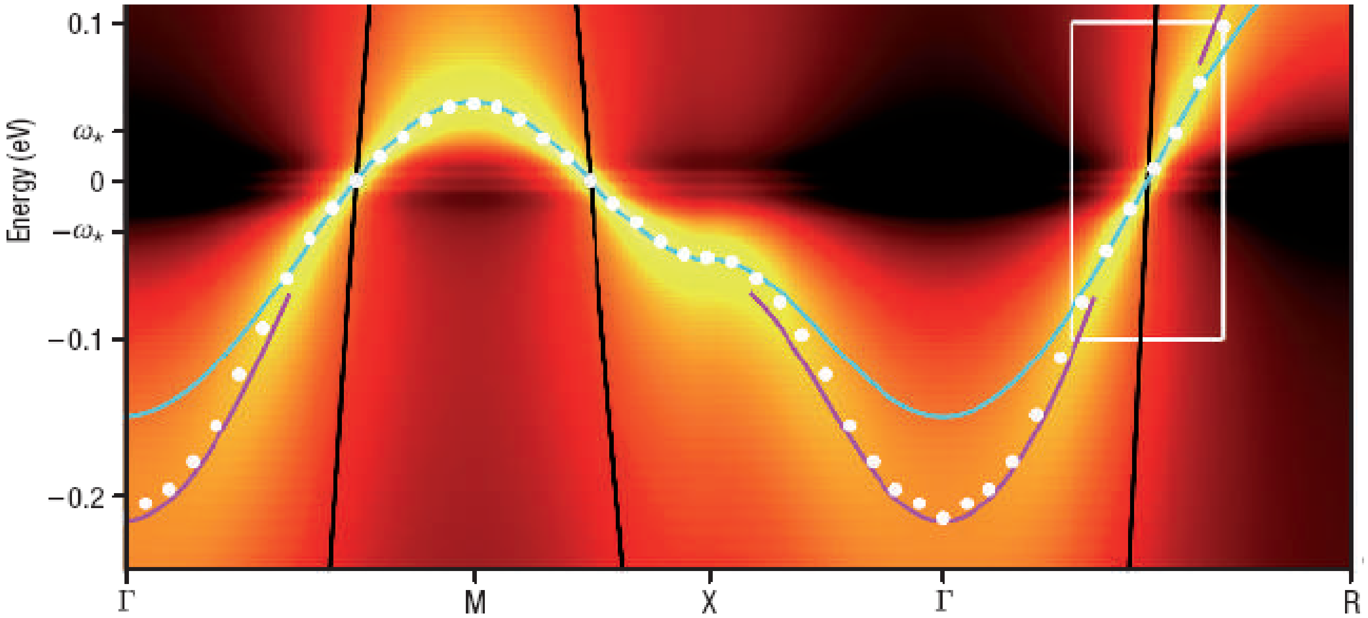

[Byzcuk et al., Nature Physics (2006)]

Strongly correlated electron systems – close to a Mott transition

Itinerant ferromagnetism and half-metallicity

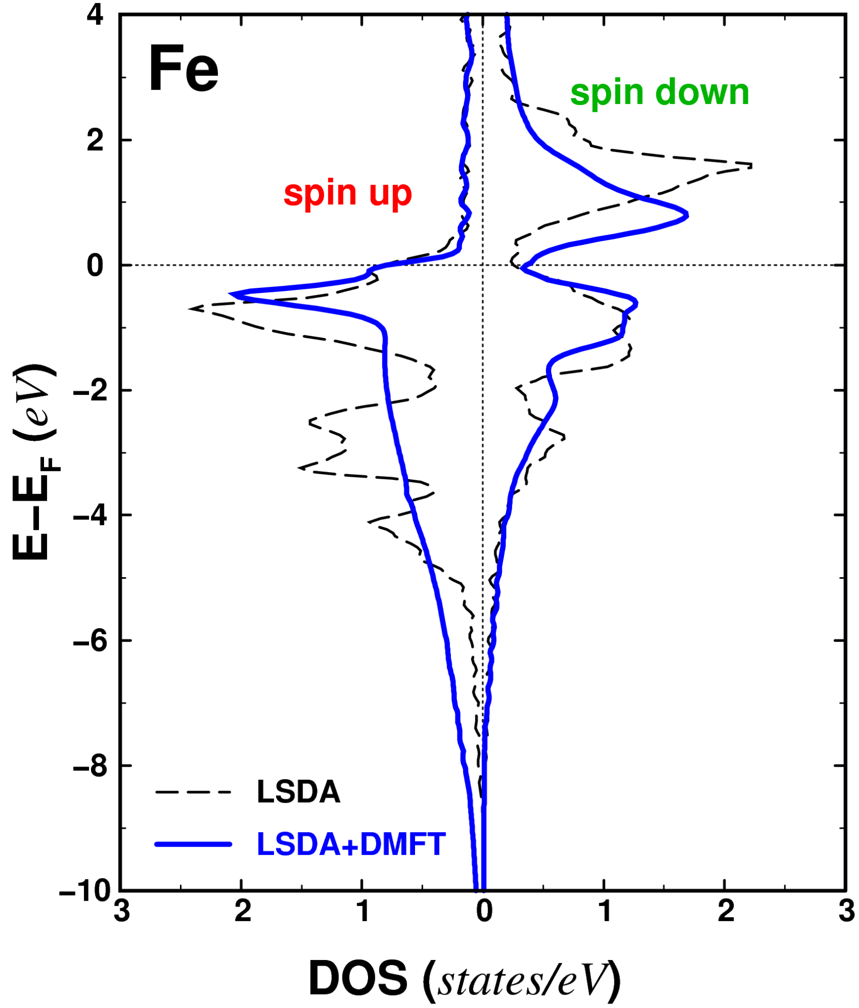

[Chioncel et. al, PRB (2003)]

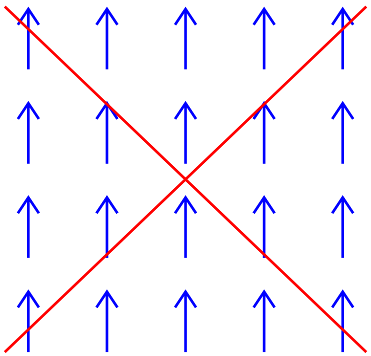

Spin models insufficient

Itinerant ferromagnetism and half-metallicity

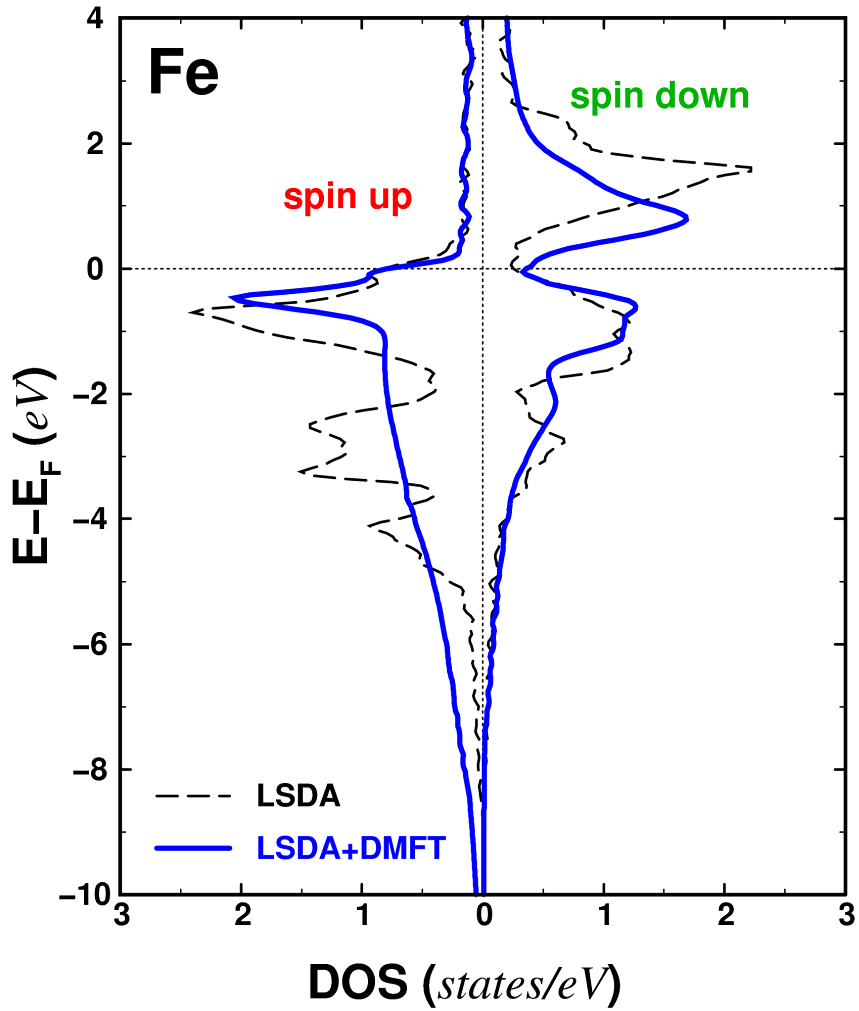

[Chioncel et. al, PRB (2003)]

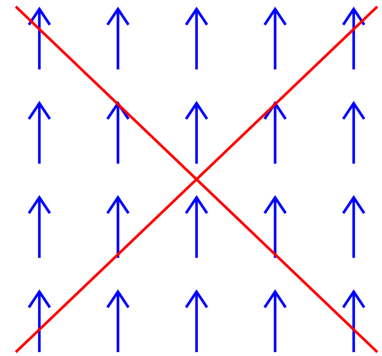

Spin models insufficient

Technological goal: TMR with half metals

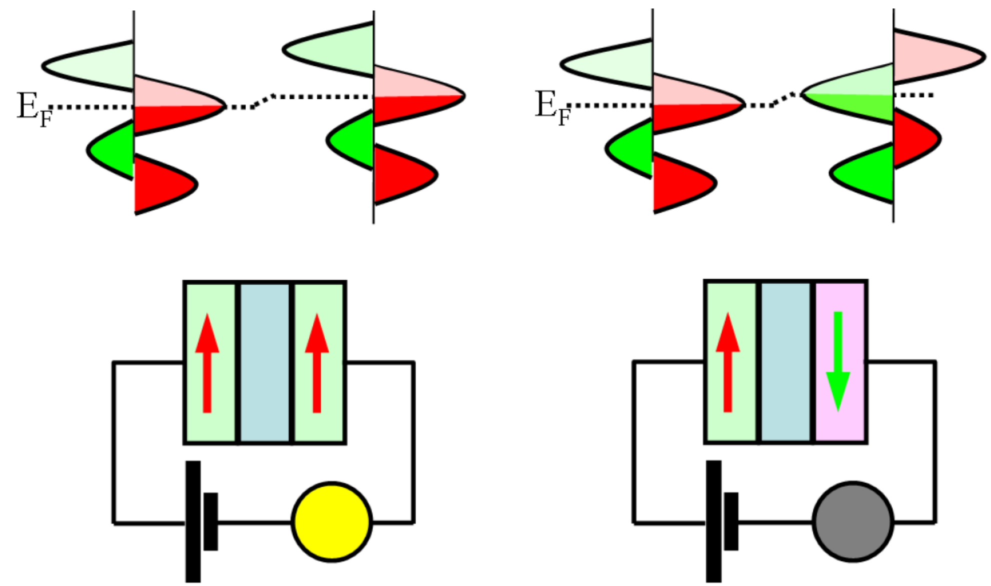

Complex phases of cuprate and organic superconductors

High-T_c physics contained in 2D Hubbard model?

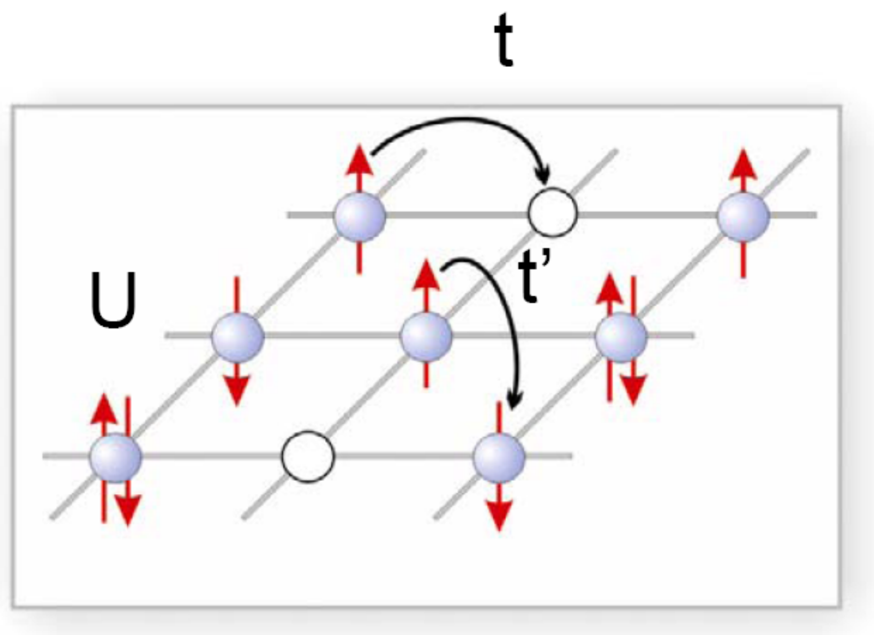

Are antiferromagnetic (AF) and Mott insulating phases essential for superconductivity?

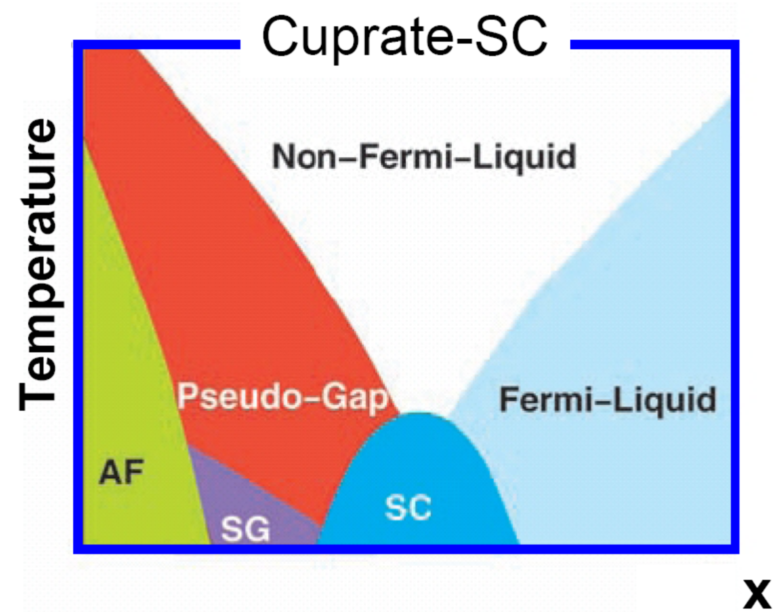

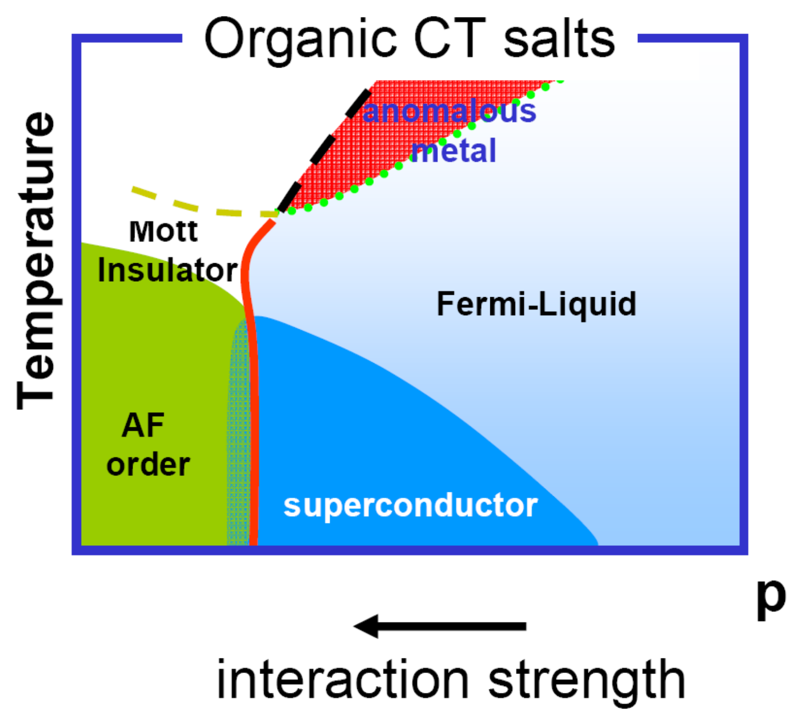

Correlated ultracold quantum gases on optical lattices: basics

Experimental systems: small dilute clouds of about 10^6 ultracold atoms $\rightsquigarrow$ need trap

Optical dipole trap (2 beams)

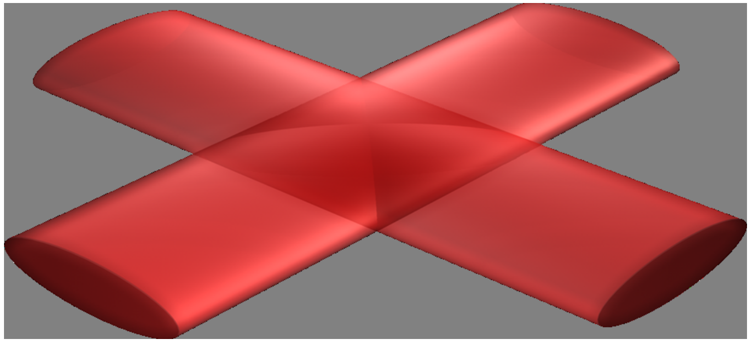

$$V_{\text{dipole}}(\boldsymbol{r}) = -\boldsymbol{d} \cdot \boldsymbol{E}(\boldsymbol{r}) \propto \alpha(\omega_{\text{L}}) \, |\boldsymbol{E}(\boldsymbol{r})|^2$$

time-averaged intensity $|\boldsymbol{E}(\boldsymbol{r})|^2$

Correlated ultracold quantum gases on optical lattices: basics

Experimental systems: small dilute clouds of about 10^6 ultracold atoms $\rightsquigarrow$ need trap

Optical dipole trap (2 beams)

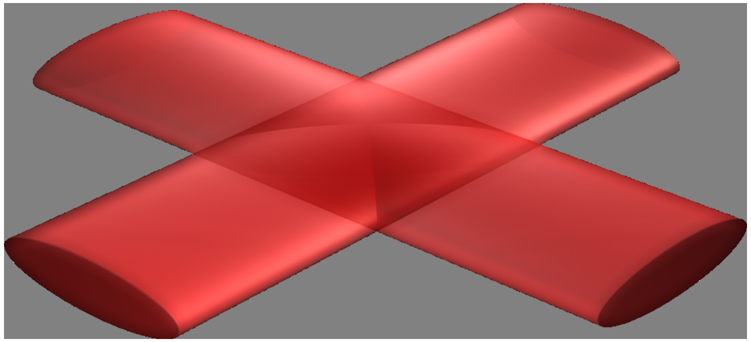

$$V_{\text{dipole}}(\boldsymbol{r}) = -\boldsymbol{d} \cdot \boldsymbol{E}(\boldsymbol{r}) \propto \alpha(\omega_{\text{L}})\,|\boldsymbol{E}(\boldsymbol{r})|^2$$

time-averaged intensity $|\boldsymbol{E}(\boldsymbol{r})|^2$

polarizability $\alpha(\omega_{\text{L}})$ changes sign at ω_0

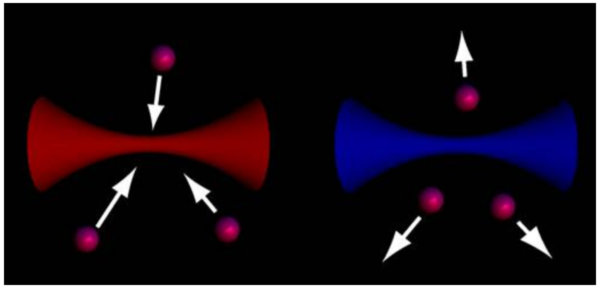

Correlated ultracold quantum gases on optical lattices: basics

Experimental systems: small dilute clouds of about 10^6 ultracold atoms $\rightsquigarrow$ need trap

Optical dipole trap (2 beams)

$$V_{\text{dipole}}(\boldsymbol{r}) = -\boldsymbol{d} \cdot \boldsymbol{E}(\boldsymbol{r}) \propto \alpha(\omega_{\text{L}})\,|\boldsymbol{E}(\boldsymbol{r})|^2$$

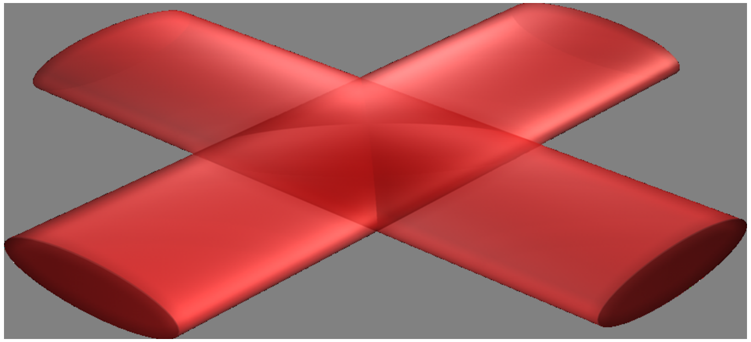

time-averaged intensity $|\boldsymbol{E}(\boldsymbol{r})|^2$

polarizability $\alpha(\omega_{\text{L}})$ changes sign at ω_0

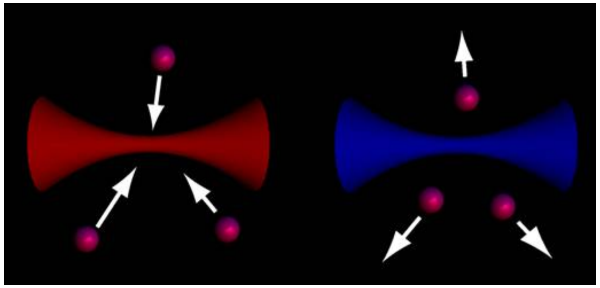

Standing wave (from coherent counterpropagating beams) $\rightsquigarrow$ modulated potential

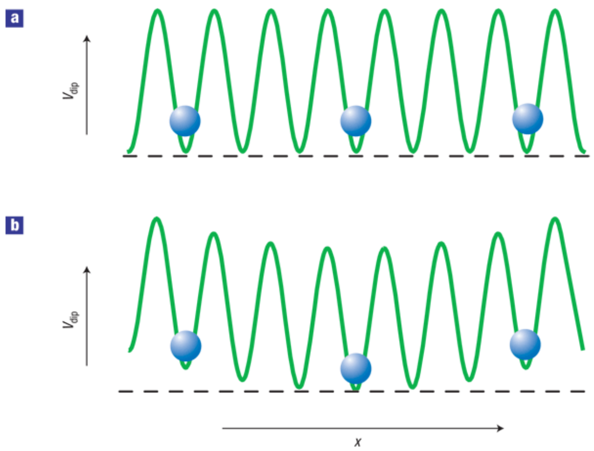

Beam profile: (anti) trapping

Correlated ultracold quantum gases on optical lattices: basics

Experimental systems: small dilute clouds of about 10^6 ultracold atoms $\rightsquigarrow$ need trap

Optical dipole trap (2 beams)

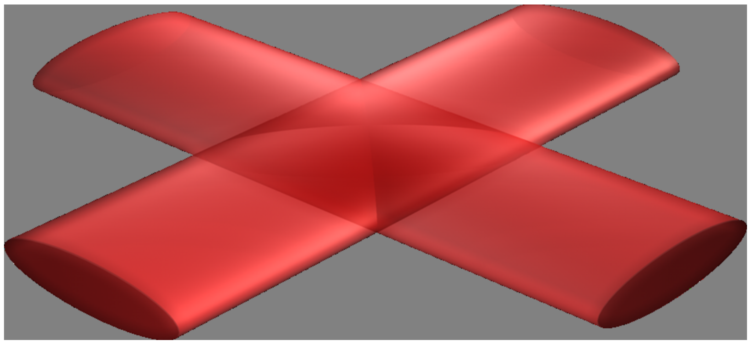

$$V_{\text{dipole}}(\boldsymbol{r}) = -\boldsymbol{d} \cdot \boldsymbol{E}(\boldsymbol{r}) \propto \alpha(\omega_{\text{L}})\,|\boldsymbol{E}(\boldsymbol{r})|^2$$

time-averaged intensity $|\boldsymbol{E}(\boldsymbol{r})|^2$

polarizability $\alpha(\omega_{\text{L}})$ changes sign at ω_0

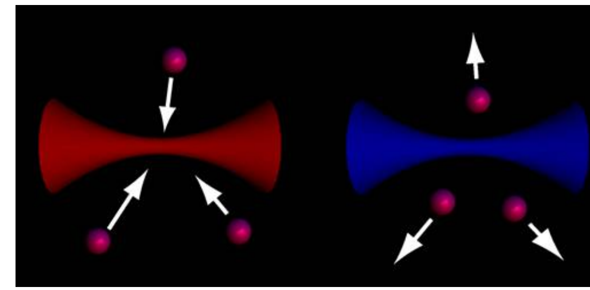

Standing wave (from coherent counterpropagating beams) $\rightsquigarrow$ modulated potential

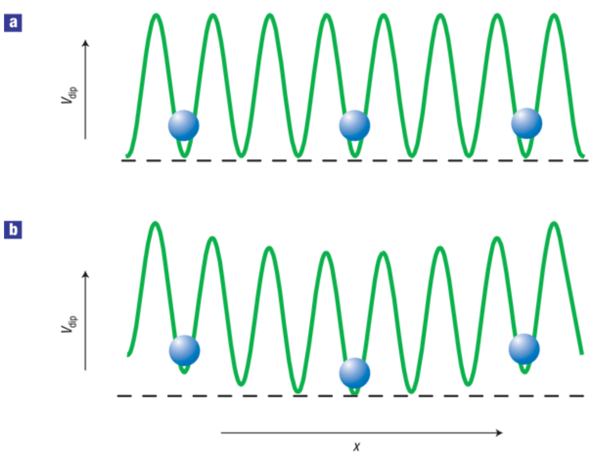

Beam profile: (anti) trapping

1 pair of lasers $\rightsquigarrow$ pancakes

2 pairs of lasers $\rightsquigarrow$ tubes

3 pairs of lasers $\rightsquigarrow$ lattice

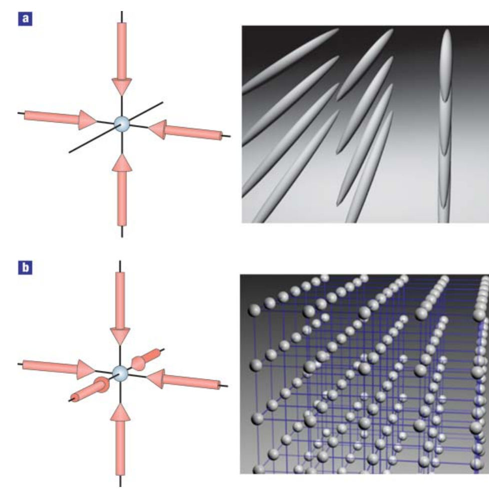

Interactions can be tuned via Feshbach resonances

Interactions can be tuned via Feshbach resonances (here in magnetic field $\boldsymbol{B}$)

short ranged: characterized by scattering length a – both signs possible!

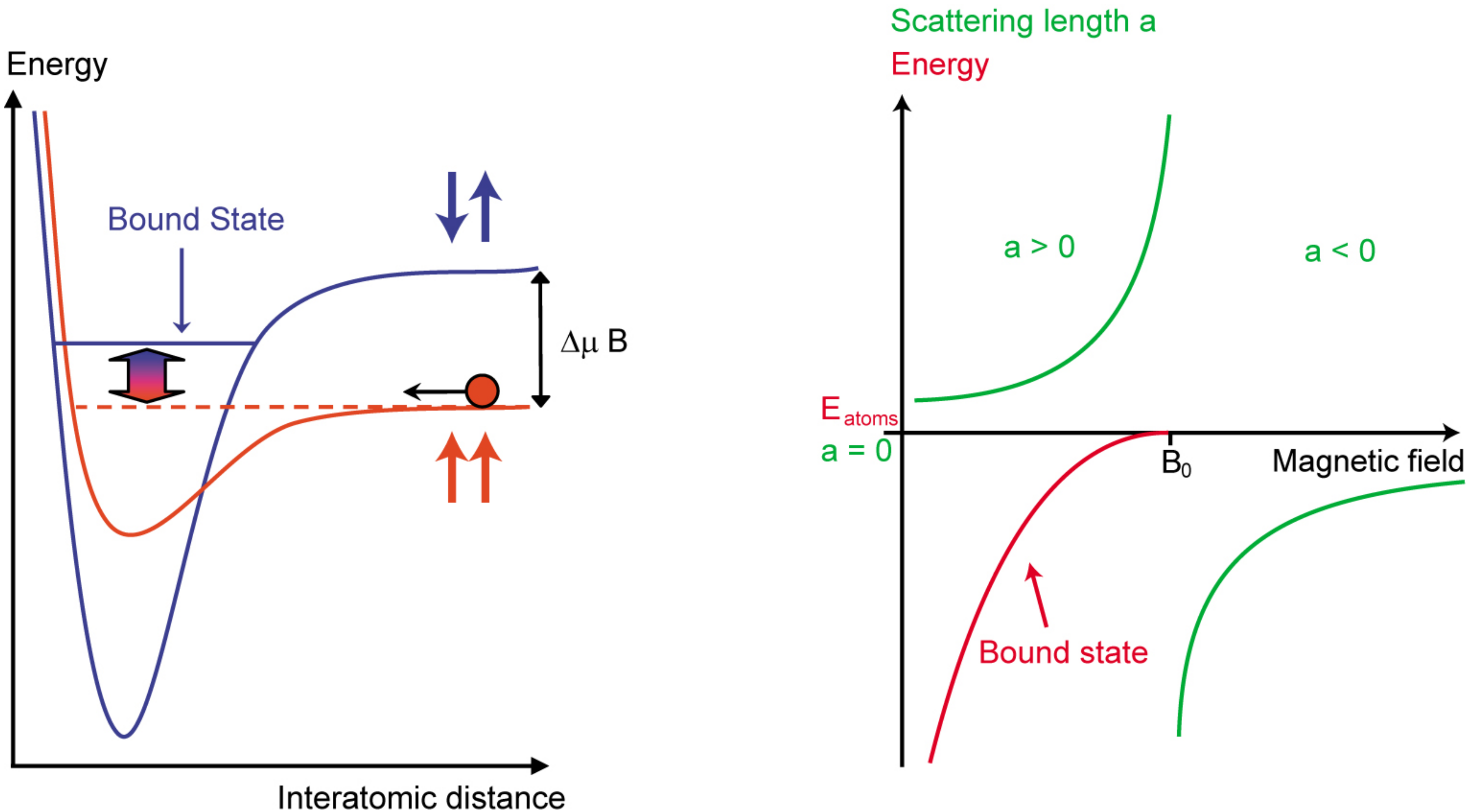

Correlated ultracold quantum gases on optical lattices: bosons

First evidence of strongly correlations in cold atoms: bosonic Mott transition

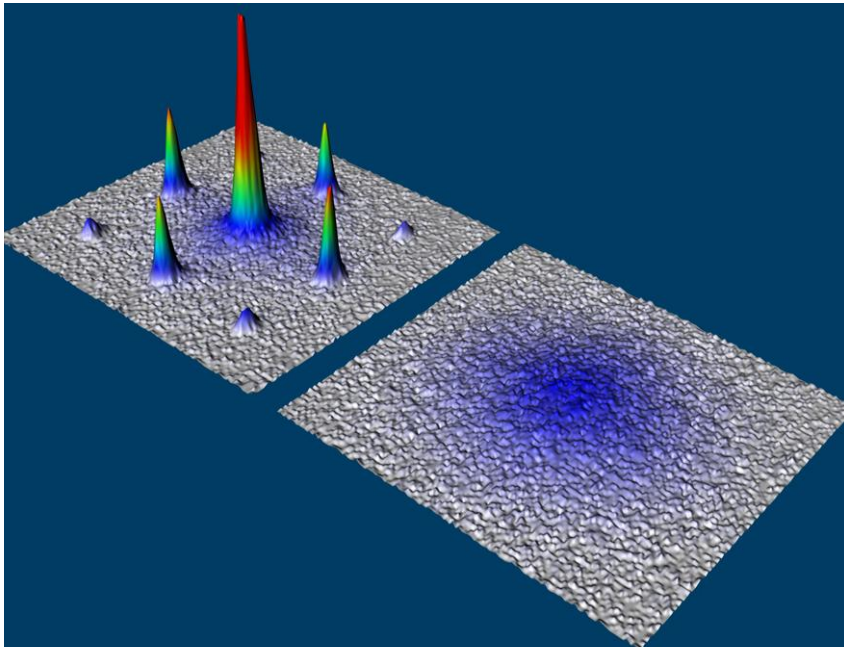

ultracold bosons on optical lattice (Bloch group, 2002)

Time-of-flight image – momentum distribution

Correlated ultracold quantum gases on optical lattices: bosons

First evidence of strongly correlations in cold atoms: bosonic Mott transition

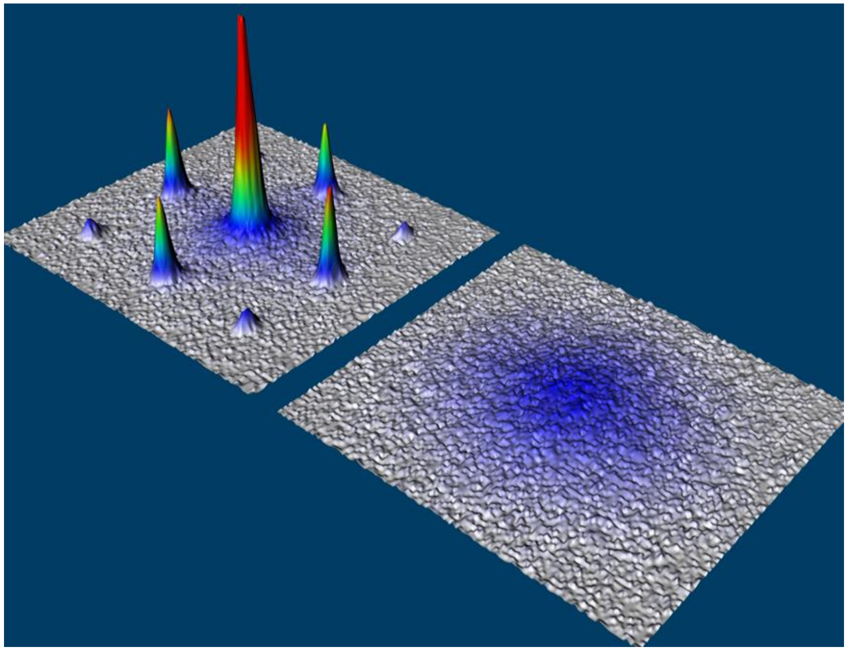

ultracold bosons on optical lattice (Bloch group, 2002)

Time-of-flight image – momentum distribution

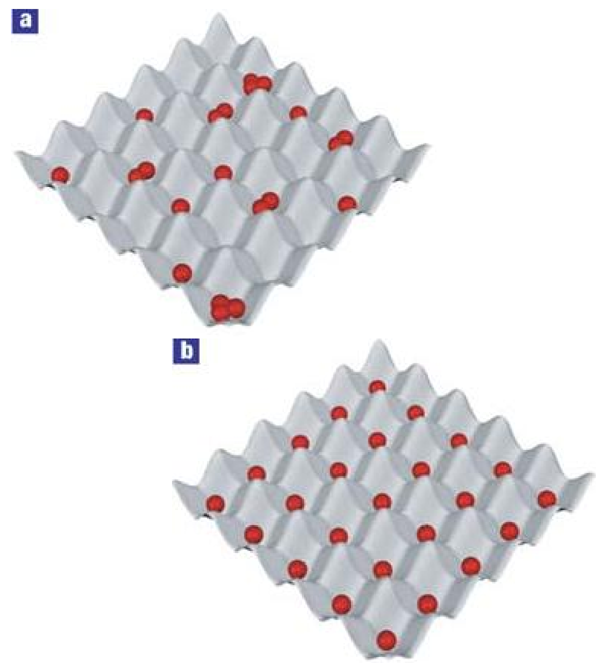

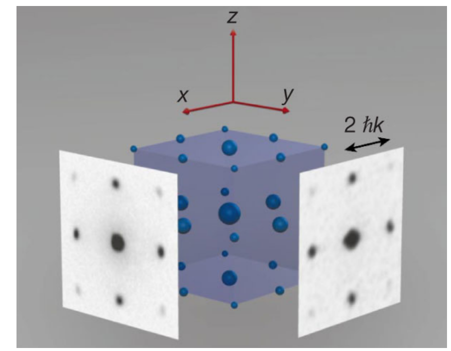

Correlated ultracold quantum gases on optical lattices: bosons

First evidence of strongly correlations in cold atoms: bosonic Mott transition

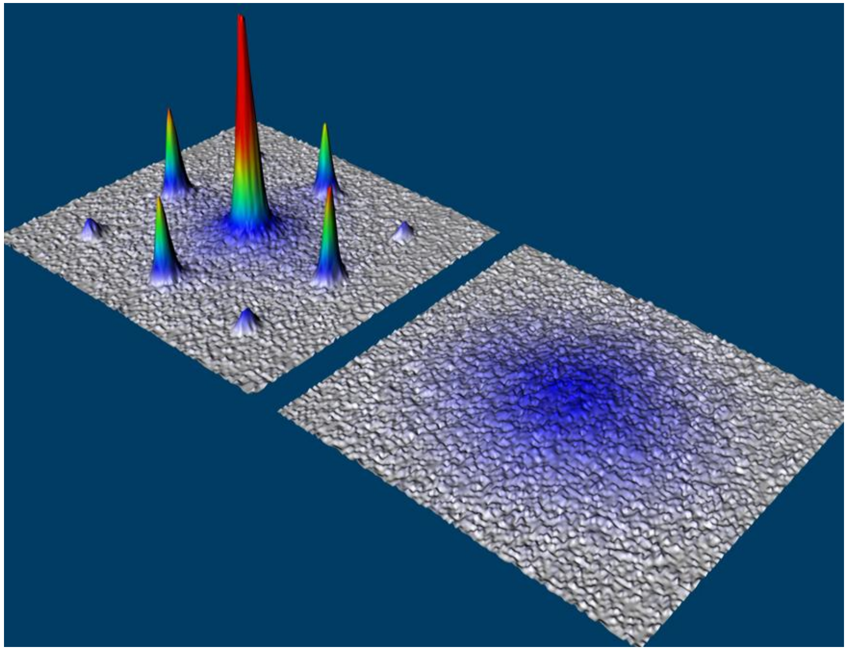

Time-of-flight image – momentum distribution

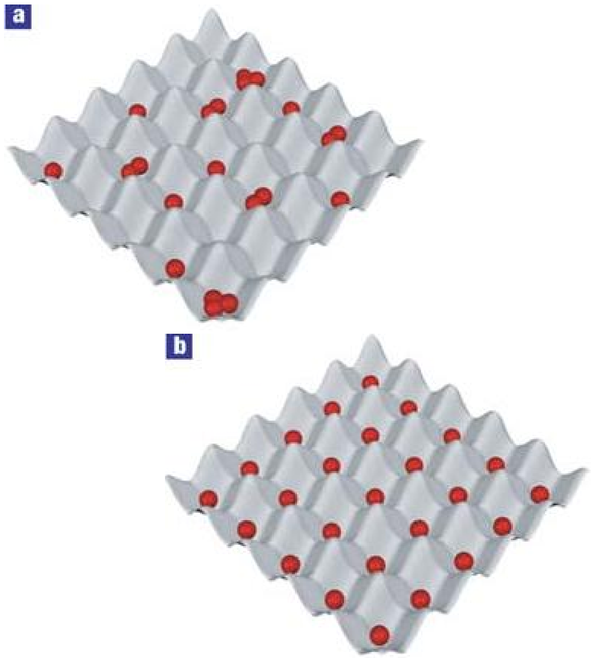

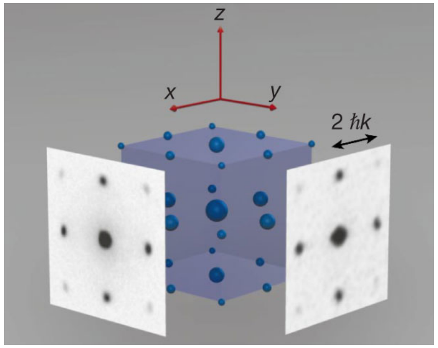

ultracold bosons on optical lattice (Bloch group, 2002)

superfluidity destroyed by density constraint at large U;
trapping potential $\rightsquigarrow$ wedding cake structure

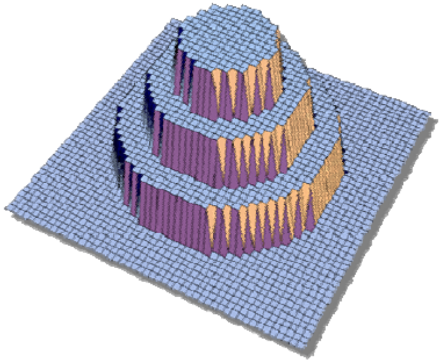

Correlated ultracold quantum gases on optical lattices: fermions

1st step: visualize (noninteracting) band structure in TOF experiment

Fermi surface mapping of 1-component system (**spinless fermions**)

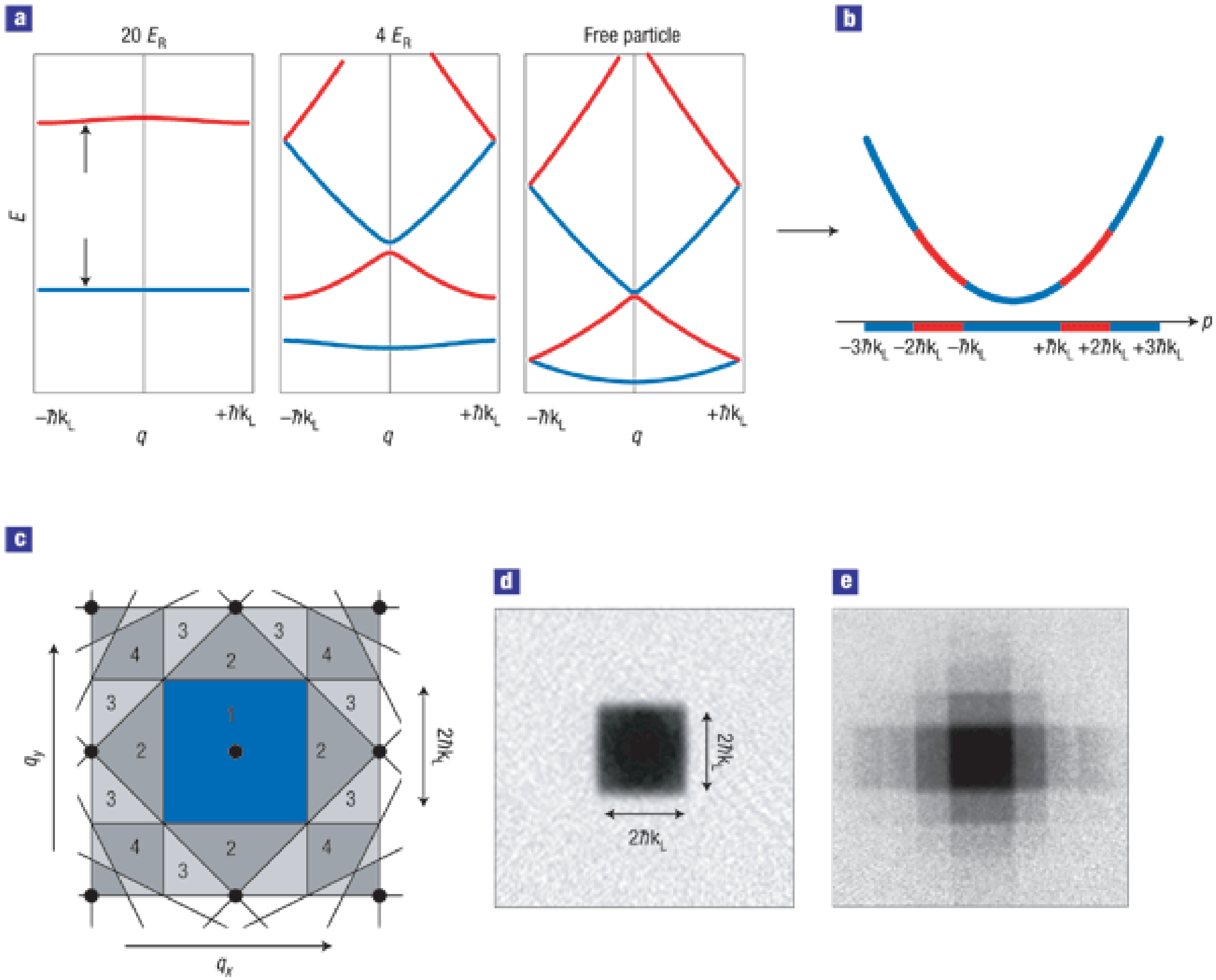

Correlated ultracold quantum gases on optical lattices: fermions

1st step: visualize (noninteracting) band structure in TOF experiment

Fermi surface mapping of 1-component system (**spinless fermions**)

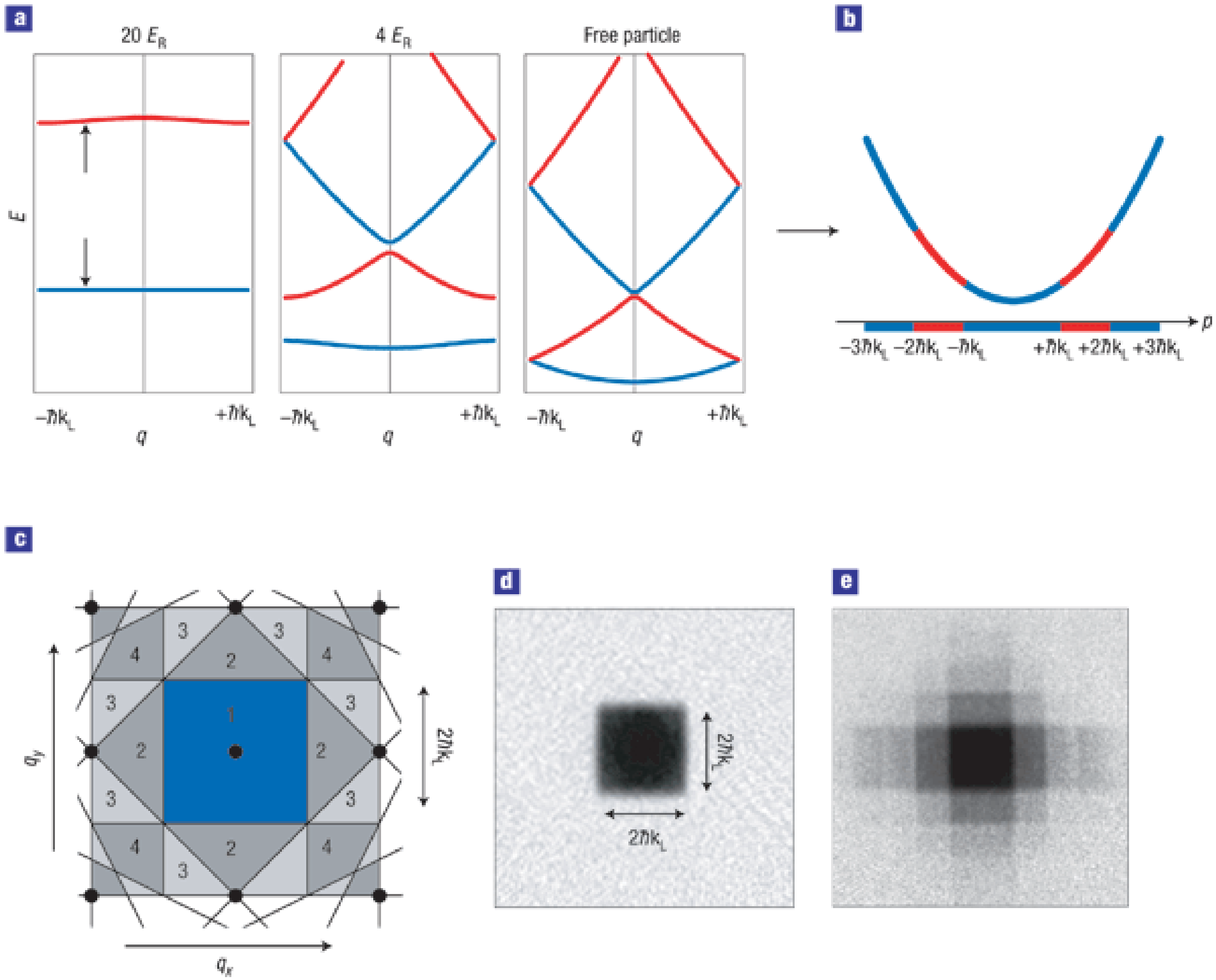

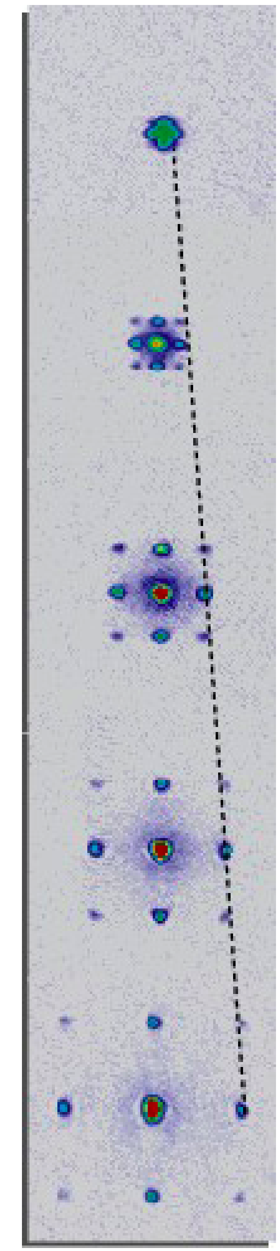

Filled 1st Brillouin zone: band insulator [Köhl et al, PRL (2005)]

Recent breakthrough: paramagnetic Mott transition in fermionic 2-flavor mixtures

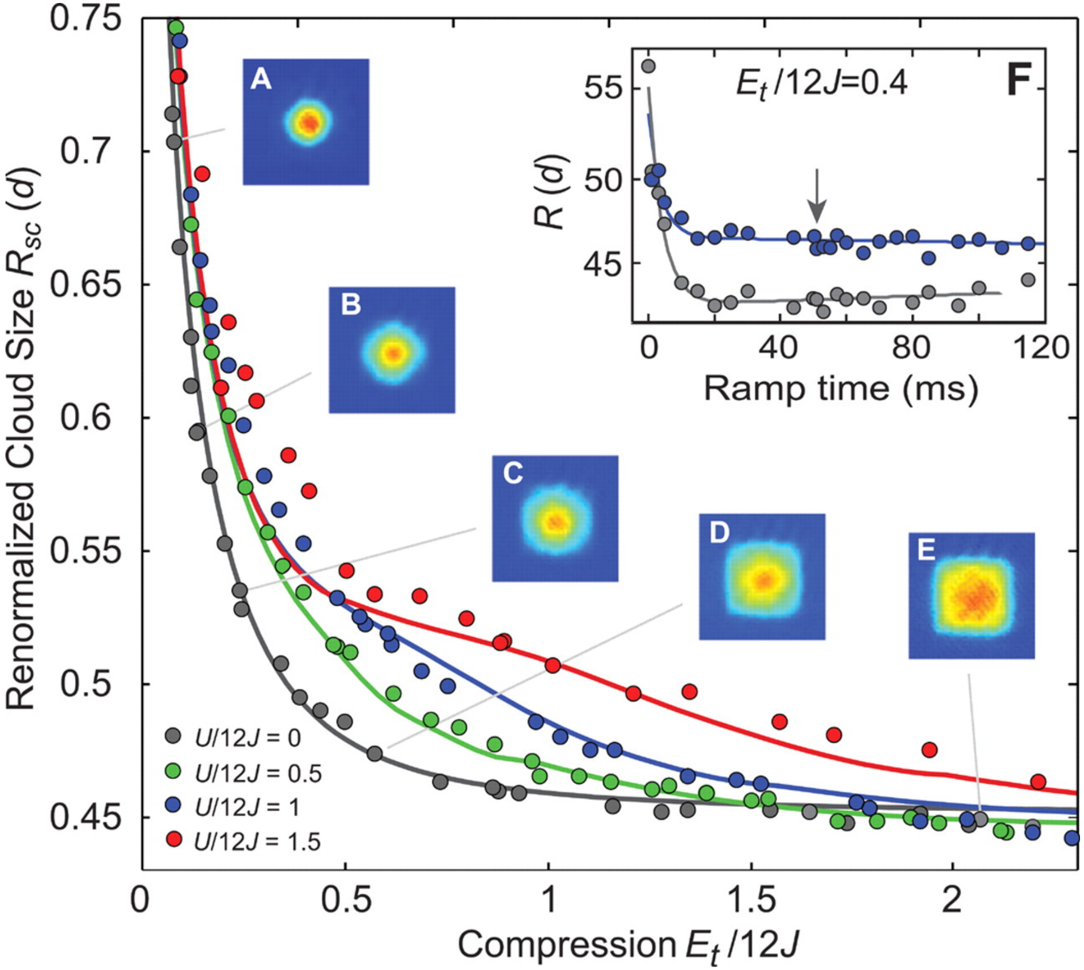

Concept: squeeze atomic cloud by variation of trapping potential (at constant interaction and hopping), measure cloud diameter

incompressible Mott phases should show up as plateaus in cloud size (for $U > U_c$)

[Schneider et al, Science **322**, 1520 (2008)]

Recent breakthrough: paramagnetic Mott transition in fermionic 2-flavor mixtures

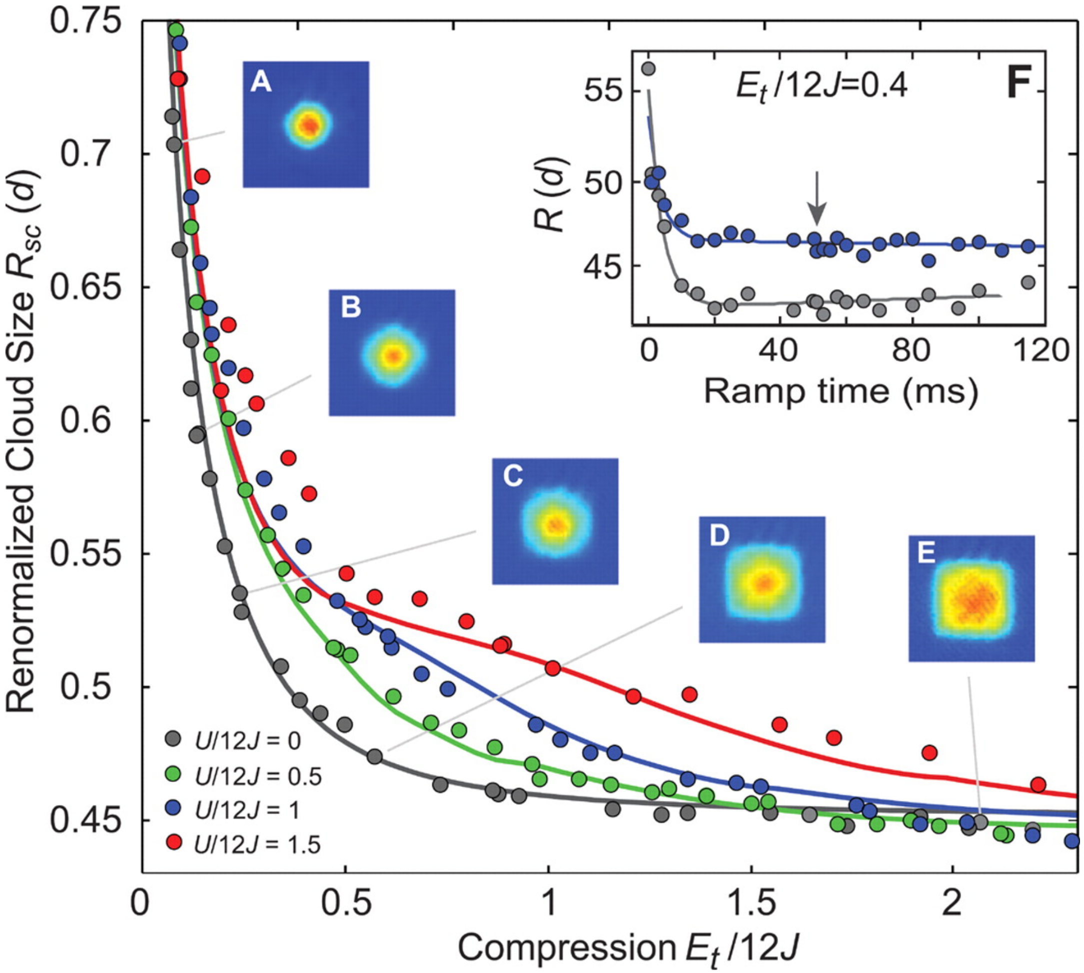

[Schneider et al, Science **322**, 1520 (2008)]

Concept: squeeze atomic cloud by variation of trapping potential (at constant interaction and hopping), measure cloud diameter

incompressible Mott phases should show up as plateaus in cloud size (for $U > U_c$)

Problem: measurements integrate over system, edges always metallic

Simulations (here DMFT+NRG) essential for interpretation of data!

Further MIT observables: column density, fraction of atoms with double occupations

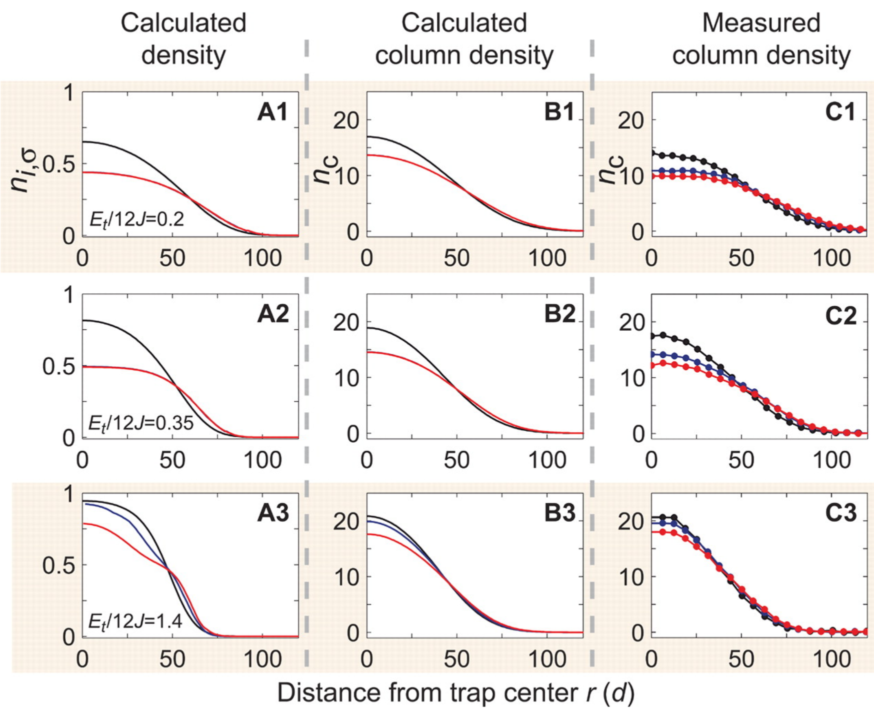

[Schneider et al, Science **322**, 1520 (2008)]

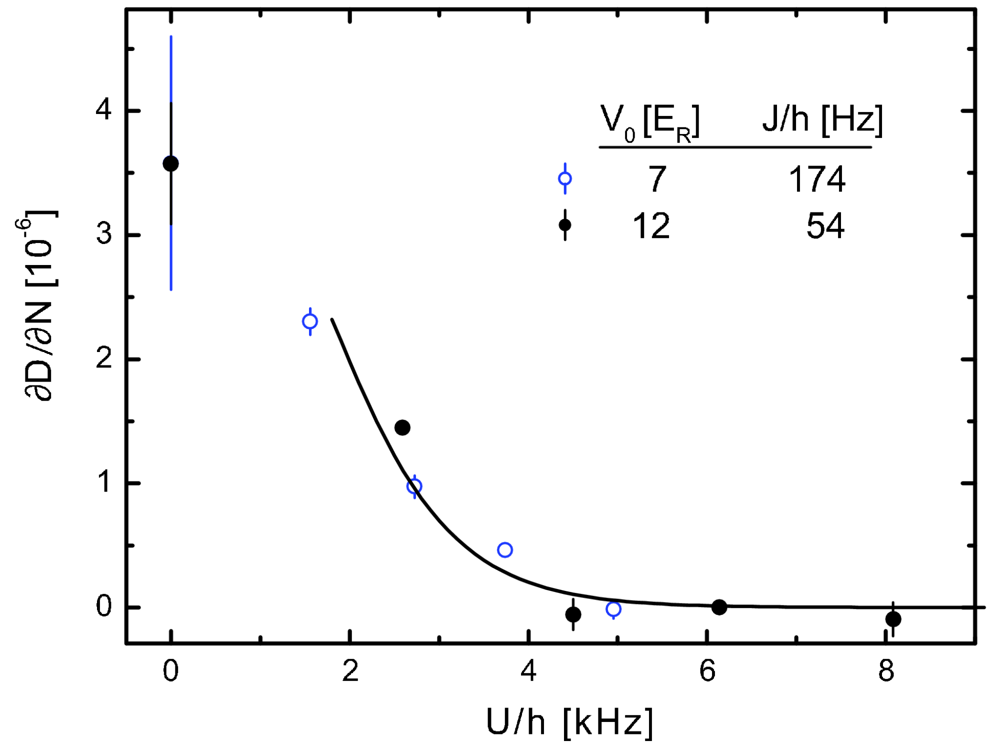

[Jördens et al., Nature (2008)]

Further MIT observables: column density, fraction of atoms with double occupations

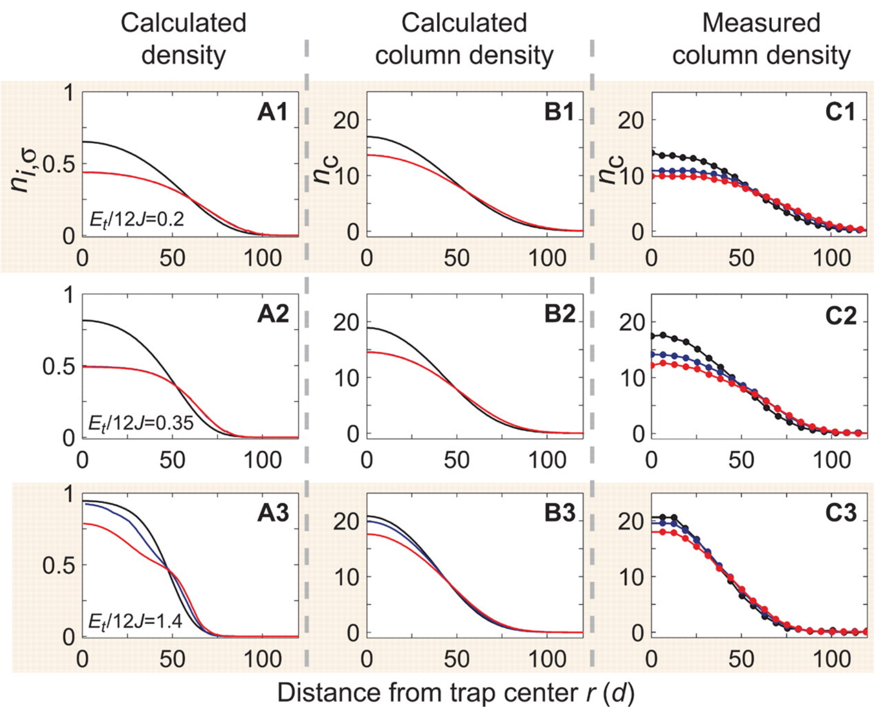

[Schneider et al, Science **322**, 1520 (2008)]

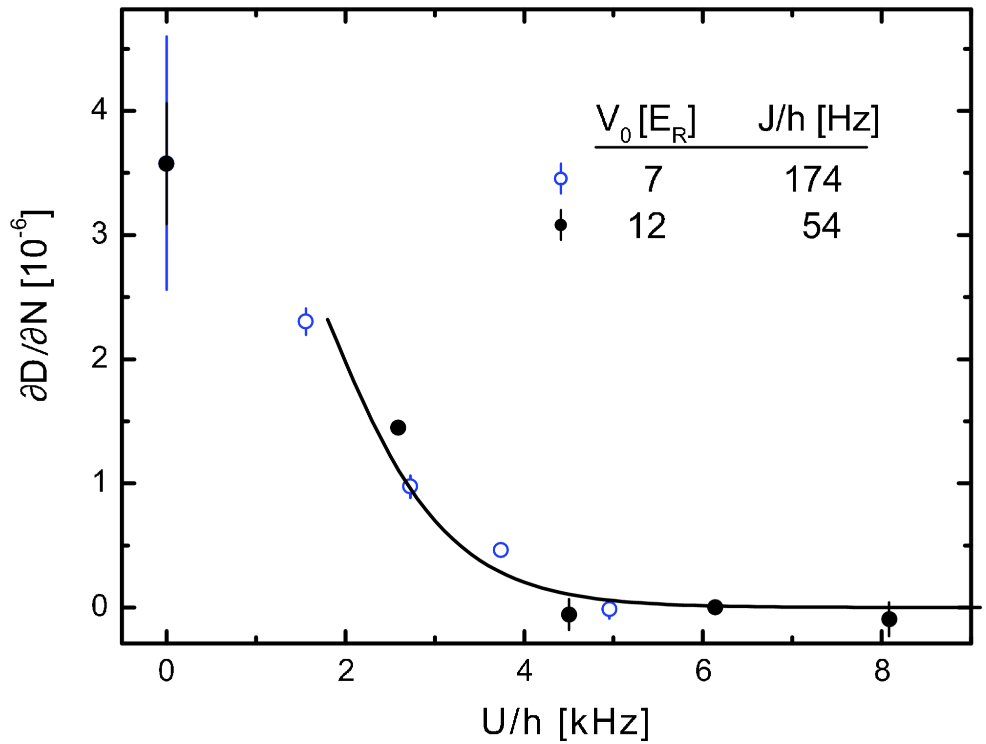

[Jördens et al., Nature (2008)]

Many other phenomena seen: superconductivity, vortices, BEC-BCS crossover, . . .

Urgent todo items:

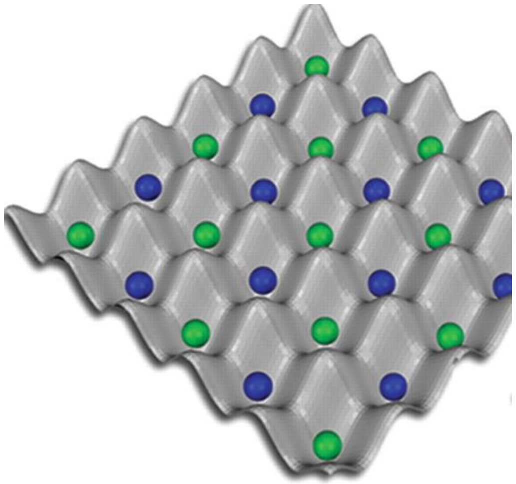

Antiferromagnetism (staggered order) in ultracold fermions

Problems:

(i) difficult to reach sufficiently low temperatures/entropies

(ii) detection of order parameter is not straightforward

Urgent todo items:

Antiferromagnetism (staggered order) in ultracold fermions

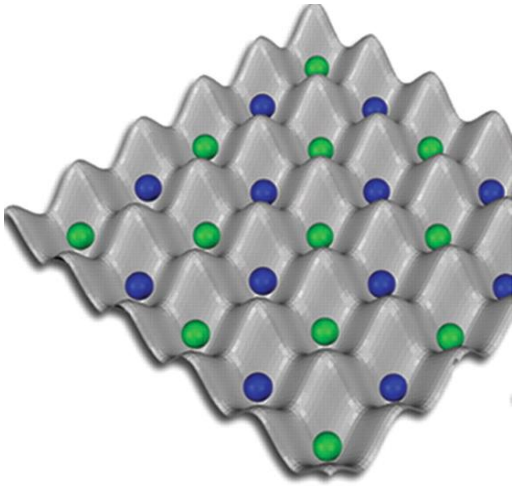

Problems:

(i) difficult to reach sufficiently low temperatures/entropies

(ii) detection of order parameter is not straightforward

Multiflavor phenomena, e.g. trions versus color superconductivity

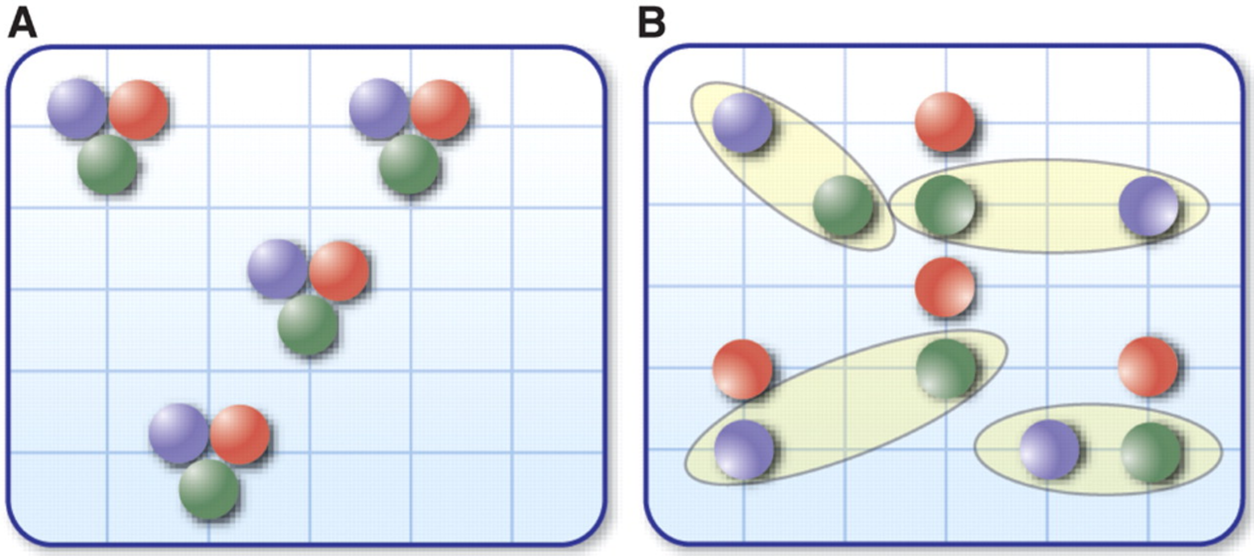

Approaches for correlated Fermi systems

General Hamiltonian for nuclei and electrons

$$H = \sum_{i=1}^{N_e} \frac{\mathbf{p}_i{}^2}{2m} + \sum_{k=1}^{L} \frac{\mathbf{P}_k{}^2}{2M_k} + \sum_{k<l} \frac{Z_k Z_l\, e^2}{|\mathbf{R}_k - \mathbf{R}_l|} - \sum_{i,k} \frac{Z_k\, e^2}{|\mathbf{r}_i - \mathbf{R}_k|} + \sum_{i<j} \frac{e^2}{|\mathbf{r}_i - \mathbf{r}_j|}$$

Approaches for correlated Fermi systems

General Hamiltonian for nuclei and electrons

$$H = \sum_{i=1}^{N_e} \frac{\boldsymbol{p}_i{}^2}{2m} + \sum_{k=1}^{L} \frac{\boldsymbol{P}_k{}^2}{2M_k} + \sum_{k<l} \frac{Z_k Z_l\, e^2}{|\boldsymbol{R}_k - \boldsymbol{R}_l|} - \sum_{i,k} \frac{Z_k\, e^2}{|\boldsymbol{r}_i - \boldsymbol{R}_k|} + \sum_{i<j} \frac{e^2}{|\boldsymbol{r}_i - \boldsymbol{r}_j|}$$

Born-Oppenheimer
approximation (0^{th}order)

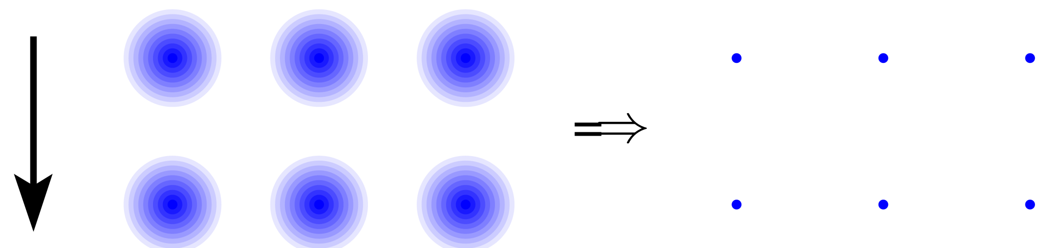

Approaches for correlated Fermi systems

General Hamiltonian for nuclei and electrons

$$H = \sum_{i=1}^{N_e} \frac{\mathbf{p}_i^{\,2}}{2m} + \sum_{k=1}^{L} \frac{\mathbf{P}_k^{\,2}}{2M_k} + \sum_{k<l} \frac{Z_k Z_l\, e^2}{|\mathbf{R}_k - \mathbf{R}_l|} - \sum_{i,k} \frac{Z_k\, e^2}{|\mathbf{r}_i - \mathbf{R}_k|} + \sum_{i<j} \frac{e^2}{|\mathbf{r}_i - \mathbf{r}_j|}$$

Born-Oppenheimer approximation (0^{th}order)

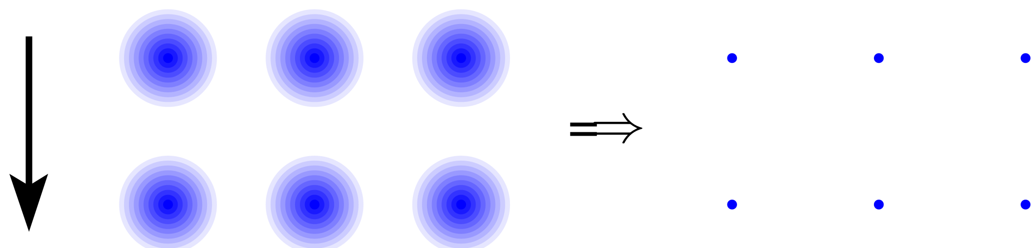

$$H = \sum_{i=1}^{N_e} \frac{\mathbf{p}_i^{\,2}}{2m} + \sum_{i} V(\mathbf{r}_i) + \sum_{i<j} \frac{e^2}{|\mathbf{r}_i - \mathbf{r}_j|}$$

Approaches for correlated Fermi systems

General Hamiltonian for nuclei and electrons

$$H = \sum_{i=1}^{N_e} \frac{\boldsymbol{p}_i^{\,2}}{2m} + \sum_{k=1}^{L} \frac{\boldsymbol{P}_k^{\,2}}{2M_k} + \sum_{k<l} \frac{Z_k Z_l\, e^2}{|\boldsymbol{R}_k - \boldsymbol{R}_l|} - \sum_{i,k} \frac{Z_k\, e^2}{|\boldsymbol{r}_i - \boldsymbol{R}_k|} + \sum_{i<j} \frac{e^2}{|\boldsymbol{r}_i - \boldsymbol{r}_j|}$$

Born-Oppenheimer
approximation (0^{th}order) $\downarrow$

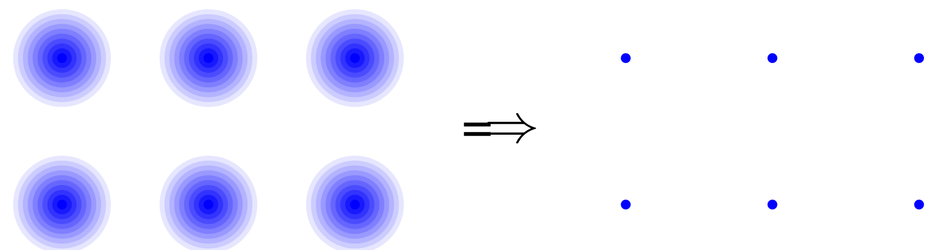

$$H = \sum_{i=1}^{N_e} \frac{\boldsymbol{p}_i^{\,2}}{2m} + \sum_{i} V(\boldsymbol{r}_i) + \sum_{i<j} \frac{e^2}{|\boldsymbol{r}_i - \boldsymbol{r}_j|}$$

Classes of theoretical approaches for electronic problem

- continuum methods: density functional theory, variational+diffusion QMC, . . .
- methods for lattice electrons

Derivation of lattice models

$$H = \sum_{i=1}^{N_e} \frac{\mathbf{p}_i^{\,2}}{2m} + \sum_i V(\mathbf{r}_i) + \sum_{i<j} \frac{e^2}{|\mathbf{r}_i - \mathbf{r}_j|}$$

reduction to valence electrons

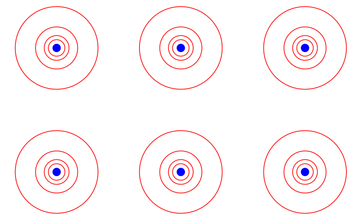

$\Longrightarrow$

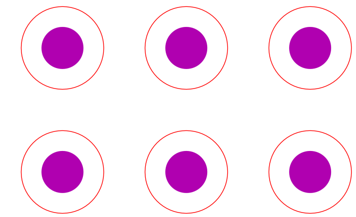

$$H = \sum_{i=1}^{N_v} \frac{\mathbf{p}_i^2}{2m} + \sum_{i=1}^{N_v} V^{\text{ion}}(\mathbf{r}_i) + \sum_{i=1}^{N_v-1} \sum_{j=i+1}^{N_v} V^{ee}(\mathbf{r}_i, \mathbf{r}_j)$$

Derivation of lattice models

$$H = \sum_{i=1}^{N_e} \frac{\boldsymbol{p}_i^{\,2}}{2m} + \sum_i V(\boldsymbol{r}_i) + \sum_{i<j} \frac{e^2}{|\boldsymbol{r}_i - \boldsymbol{r}_j|}$$

reduction to valence electrons $\downarrow$

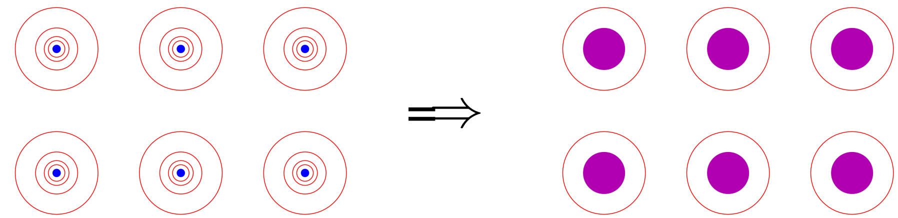

$$H = \sum_{i=1}^{N_v} \frac{\boldsymbol{p}_i^2}{2m} + \sum_{i=1}^{N_v} V^{\text{ion}}(\boldsymbol{r}_i) + \sum_{i=1}^{N_v-1} \sum_{j=i+1}^{N_v} V^{ee}(\boldsymbol{r}_i, \boldsymbol{r}_j)$$

occupation number formalism $\downarrow$ Wannier orbitals

$$\hat{H} = \sum_{i\nu j\sigma} t_{ij}^{\nu}\, \hat{c}_{i\nu\sigma}^{\dagger}\, \hat{c}_{j\nu\sigma} + \frac{1}{2} \sum_{\nu\nu'\mu\mu'} \sum_{ijmn} \sum_{\sigma\sigma'} \mathcal{V}_{ijmn}^{\nu\nu'\mu\mu'}\, \hat{c}_{i\nu\sigma}^{\dagger}\, \hat{c}_{j\nu'\sigma'}^{\dagger}\, \hat{c}_{n\mu'\sigma'}\, \hat{c}_{m\mu\sigma}$$

Derivation of lattice models

$$H = \sum_{i=1}^{N_e} \frac{\mathbf{p}_i^{\,2}}{2m} + \sum_i V(\mathbf{r}_i) + \sum_{i<j} \frac{e^2}{|\mathbf{r}_i - \mathbf{r}_j|}$$

reduction to valence electrons $\downarrow$

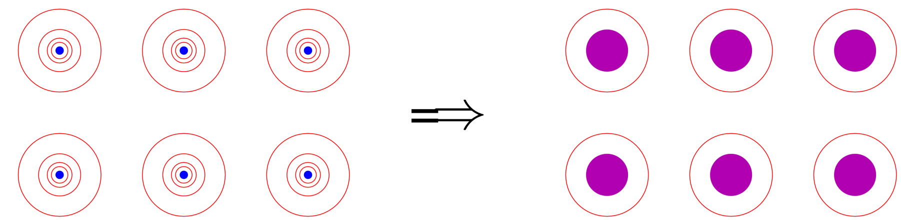

$$H = \sum_{i=1}^{N_v} \frac{\mathbf{p}_i^2}{2m} + \sum_{i=1}^{N_v} V^{\text{ion}}(\mathbf{r}_i) + \sum_{i=1}^{N_v-1} \sum_{j=i+1}^{N_v} V^{ee}(\mathbf{r}_i, \mathbf{r}_j)$$

occupation number formalism $\downarrow$ Wannier orbitals

$$\hat{H} = \sum_{i\nu j\sigma} t_{ij}^{\nu}\, \hat{c}_{i\nu\sigma}^{\dagger}\, \hat{c}_{j\nu\sigma} + \frac{1}{2} \sum_{\nu\nu'\mu\mu'} \sum_{ijmn} \sum_{\sigma\sigma'} \mathcal{V}_{ijmn}^{\nu\nu'\mu\mu'}\, \hat{c}_{i\nu\sigma}^{\dagger}\, \hat{c}_{j\nu'\sigma'}^{\dagger}\, \hat{c}_{n\mu'\sigma'}\, \hat{c}_{m\mu\sigma}$$

Hubbard model $\hat{H} = \sum_{(i,j),\sigma} t_{ij}\,(\hat{c}_{i\sigma}^{\dagger}\hat{c}_{j\sigma} + \text{h.c.}) + U \sum_i \hat{n}_{i\uparrow}\hat{n}_{i\downarrow}$

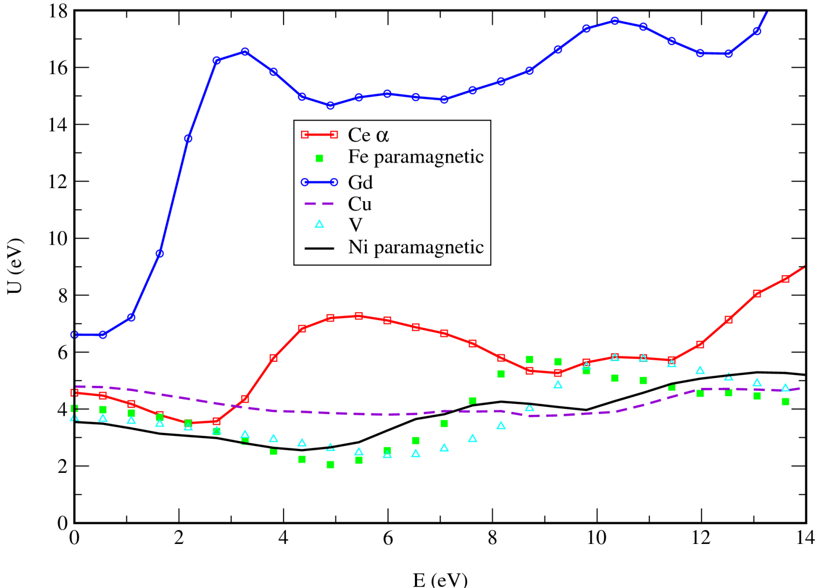

[Aryasetiawan et al, PRB 2006]

$$+ \sum_i V(\boldsymbol{r}_i) + \sum_{i<j} \frac{e^2}{|\boldsymbol{r}_i - \boldsymbol{r}_j|}$$

:rons $\downarrow$

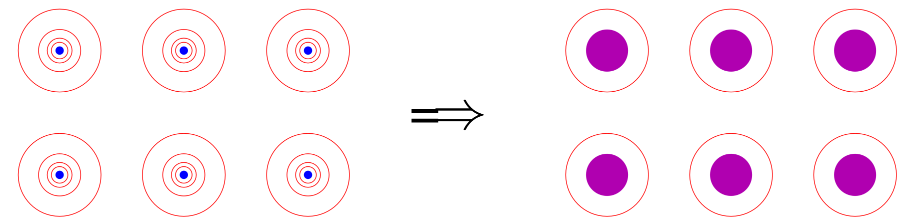

$$H = \sum_{i=1}^{N_v} \frac{\boldsymbol{p}_i^2}{2m} + \sum_{i=1}^{N_v} V^{\text{ion}}(\boldsymbol{r}_i) + \sum_{i=1}^{N_v-1} \sum_{j=i+1}^{N_v} V^{ee}(\boldsymbol{r}_i, \boldsymbol{r}_j)[\cancel{\omega}]$$

occupation number formalism $\downarrow$ Wannier orbitals

$$\hat{H} = \sum_{i\nu j\sigma} t_{ij}^{\nu}\, \hat{c}_{i\nu\sigma}^{\dagger}\, \hat{c}_{j\nu\sigma} + \frac{1}{2} \sum_{\nu\nu'\mu\mu'} \sum_{ijmn} \sum_{\sigma\sigma'} \mathcal{V}_{ijmn}^{\nu\nu'\mu\mu'}\, \hat{c}_{i\nu\sigma}^{\dagger}\, \hat{c}_{j\nu'\sigma'}^{\dagger}\, \hat{c}_{n\mu'\sigma'}\, \hat{c}_{m\mu\sigma}$$

Hubbard model $\hat{H} = \sum_{(i,j),\sigma} t_{ij} \left(\hat{c}_{i\sigma}^{\dagger} \hat{c}_{j\sigma} + \text{h.c.}\right) + U \sum_i \hat{n}_{i\uparrow} \hat{n}_{i\downarrow}$

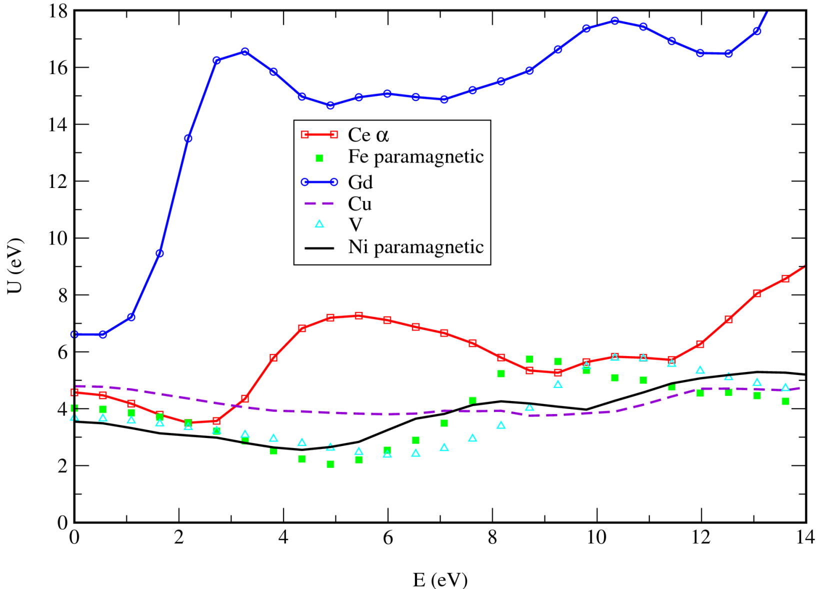

[Aryasetiawan et al, PRB 2006]

$$+ \sum_i V(\boldsymbol{r}_i) + \sum_{i<j} \frac{e^2}{|\boldsymbol{r}_i - \boldsymbol{r}_j|}$$

trons $\Big\downarrow$

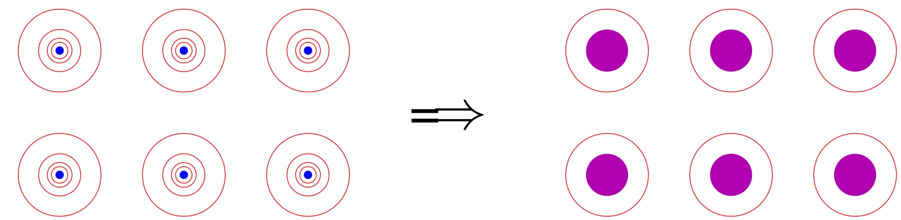

$$H = \sum_{i=1}^{N_v} \frac{\boldsymbol{p}_i^2}{2m} + \sum_{i=1}^{N_v} V^{\text{ion}}(\boldsymbol{r}_i) + \sum_{i=1}^{N_v-1} \sum_{j=i+1}^{N_v} V^{ee}(\boldsymbol{r}_i, \boldsymbol{r}_j)[\cancel{\omega}]$$

occupation number formalism $\Big\downarrow$ Wannier orbitals

$$\hat{H} = \sum_{i\nu j\sigma} t_{ij}^{\nu}\, \hat{c}_{i\nu\sigma}^{\dagger}\, \hat{c}_{j\nu\sigma} + \frac{1}{2} \sum_{\nu\nu'\mu\mu'} \sum_{ijmn} \sum_{\sigma\sigma'} \mathcal{V}_{ijmn}^{\nu\nu'\mu\mu'}\, \hat{c}_{i\nu\sigma}^{\dagger}\, \hat{c}_{j\nu'\sigma'}^{\dagger}\, \hat{c}_{n\mu'\sigma'}\, \hat{c}_{m\mu\sigma}$$

Hubbard model $$\hat{H} = \sum_{(i,j),\sigma} t_{ij}\,(\hat{c}_{i\sigma}^{\dagger}\hat{c}_{j\sigma} + \text{h.c.}) + U \sum_i \hat{n}_{i\uparrow}\hat{n}_{i\downarrow}$$

Note: no core states in quantum gas case!

Approaches for Hubbard-type models

$$\hat{H} = \sum_{(i,j),\sigma} t_{ij} \, (\hat{c}^{\dagger}_{i\sigma} \hat{c}_{j\sigma} + \text{h.c.}) + U \sum_{i} \hat{n}_{i\uparrow} \hat{n}_{i\downarrow}$$

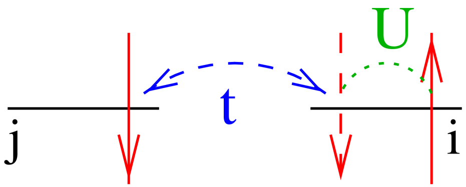

Perturbation theory

- $U \longrightarrow 0$: Hartree-Fock
  2^{nd} order PT, ...
- $t/U \longrightarrow 0$ (for $n = 1$)
  $\rightsquigarrow$ Heisenberg model

finite clusters: ED, QMC

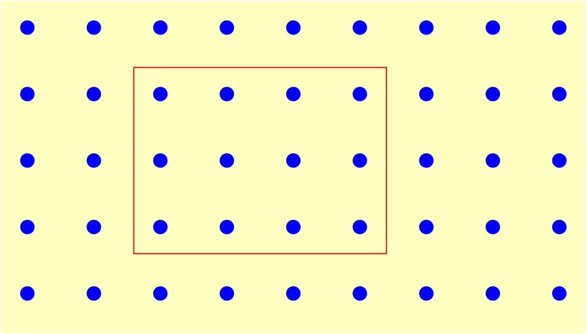

$d \rightarrow 1$: Bethe ansatz, DMRG

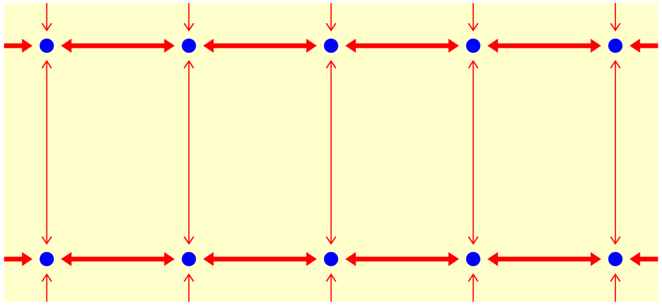

Approaches for Hubbard-type models

$$\hat{H} = \sum_{(i,j),\sigma} t_{ij} \, (\hat{c}^{\dagger}_{i\sigma} \hat{c}_{j\sigma} + \text{h.c.}) + U \sum_{i} \hat{n}_{i\uparrow} \hat{n}_{i\downarrow}$$

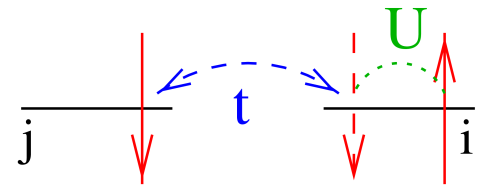

Perturbation theory

- $U \longrightarrow 0$: Hartree-Fock
  2nd order PT, . . .
- $t/U \longrightarrow 0$ (for $n = 1$)
  $\rightsquigarrow$ Heisenberg model

finite clusters: ED, QMC

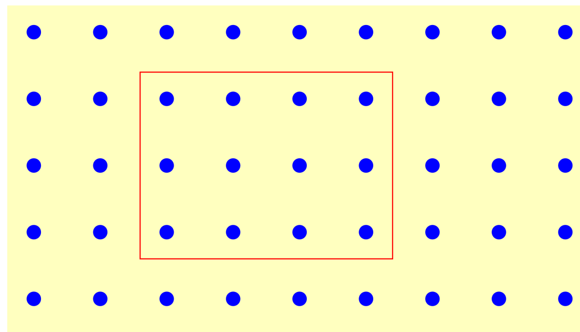

$d \longrightarrow 1$: Bethe ansatz, DMRG

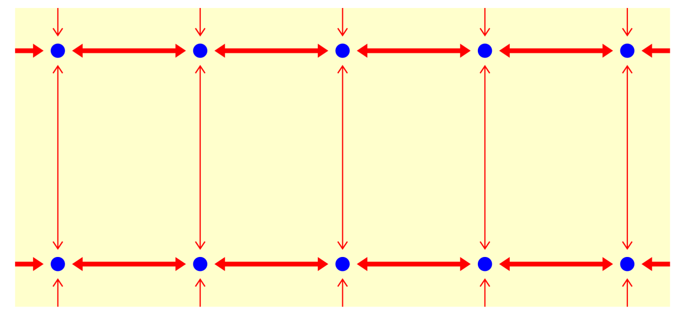

Dynamical mean-field theory (DMFT): local self-energy $\Sigma(\boldsymbol{k}, \omega) \equiv \Sigma(\omega)$

[Metzner, Vollhardt, PRL (1989), Georges, Kotliar, PRL (1992), Jarrell, PRL (1992)]

+	non-perturbative $\rightsquigarrow$ valid at MIT
+	dynamical on-site correlations preserved
+	in thermodynamic limit
+/−	exact for coordination $Z \longrightarrow \infty$

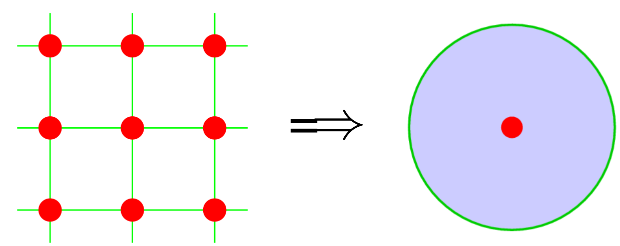

Iterative solution of DMFT equations

0. Initialize self-energy
1. Solve Dyson equation
2. Solve single impurity Anderson model (SIAM)

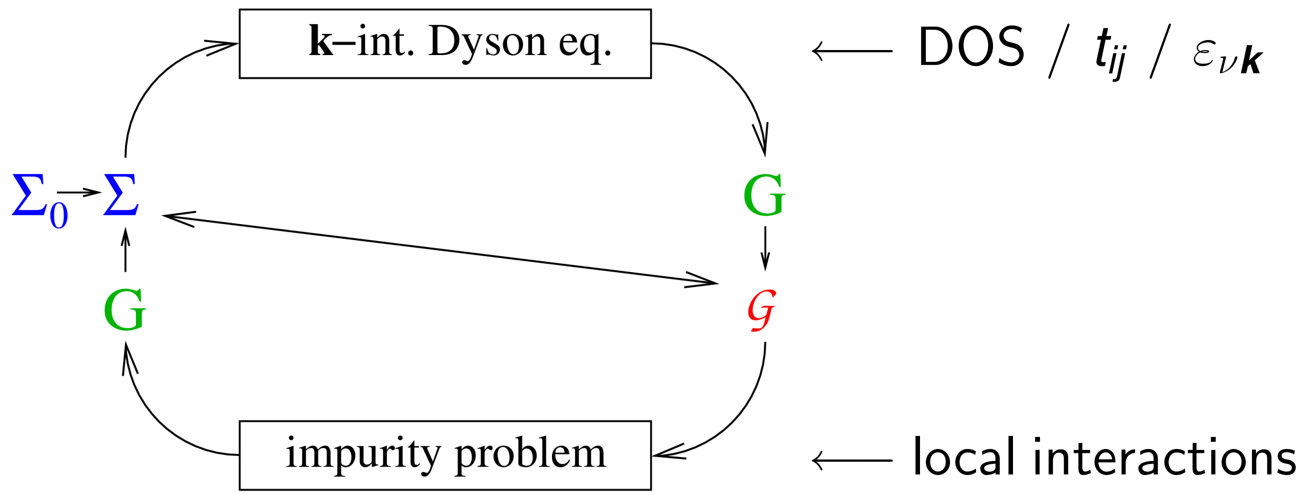

Iterative solution of DMFT equations

0. Initialize self-energy
1. Solve Dyson equation
2. Solve single impurity Anderson model (SIAM)

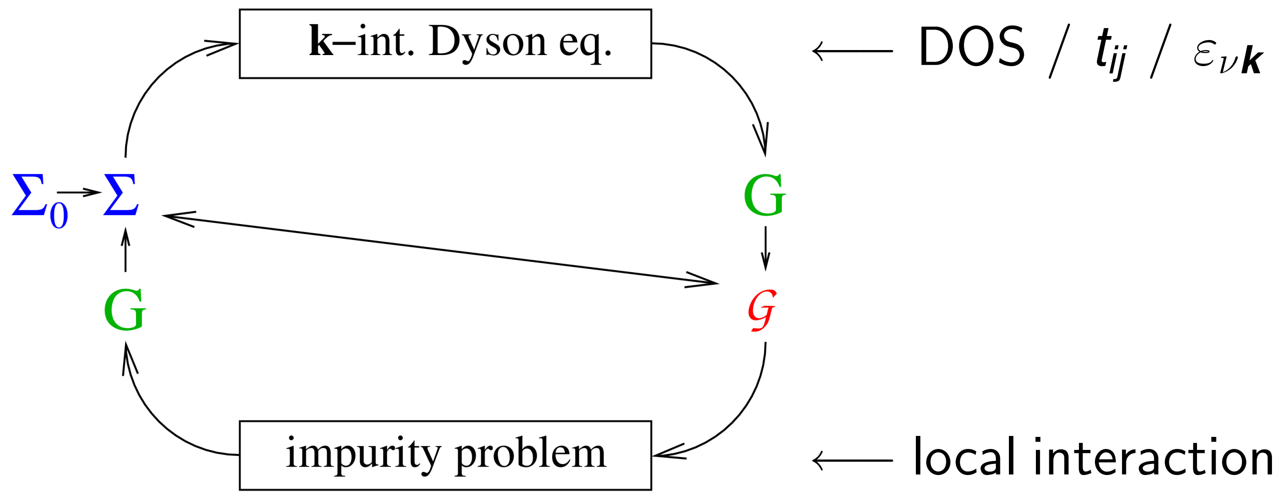

Impurity solver:

- Iterative perturbation theory (IPT; not controlled)
- Quantum Monte Carlo (QMC)
- Exact diagonalization (ED; large finite-size errors)
- Numerical renormalization group (NRG; 1-2 bands)
- Density matrix renormalization group (DMRG)
- Self-energy functional theory (SFT) + ED

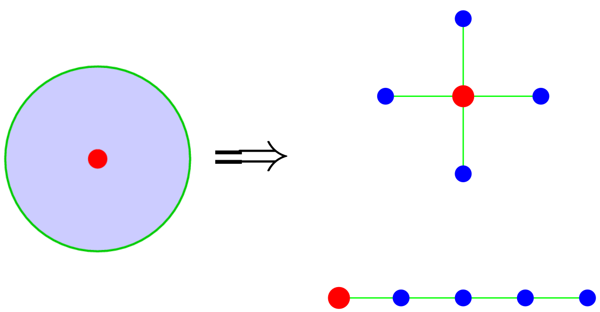

Mathematical excursion: Monte Carlo methods

General task: evaluation of (high-dimensional) sums/integrals

Simple example: quadrature of a convex function (in $d = 1$)

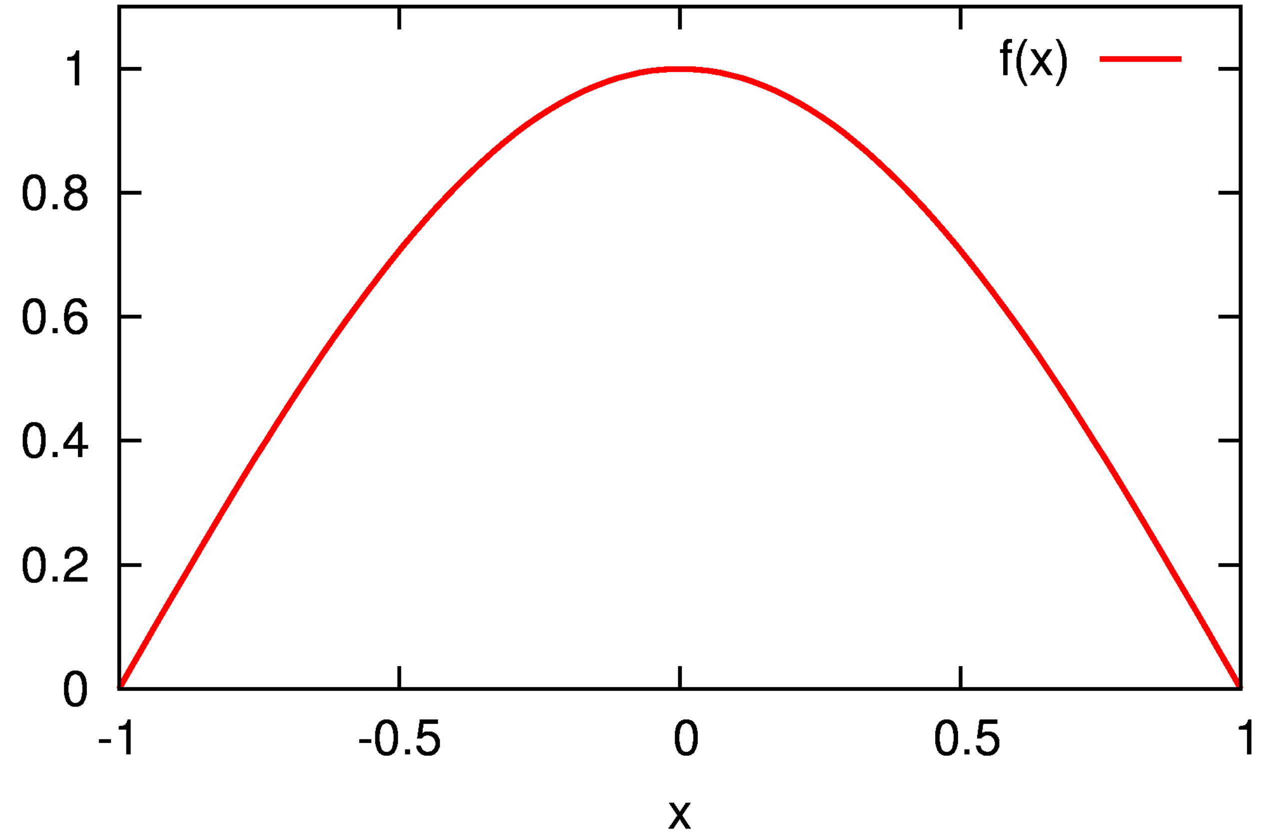

$$I = \int_a^b f(x)\,dx = ?$$

Mathematical excursion: Monte Carlo methods

General task: evaluation of (high-dimensional) sums/integrals

Simple example: quadrature of a convex function (in $d = 1$)

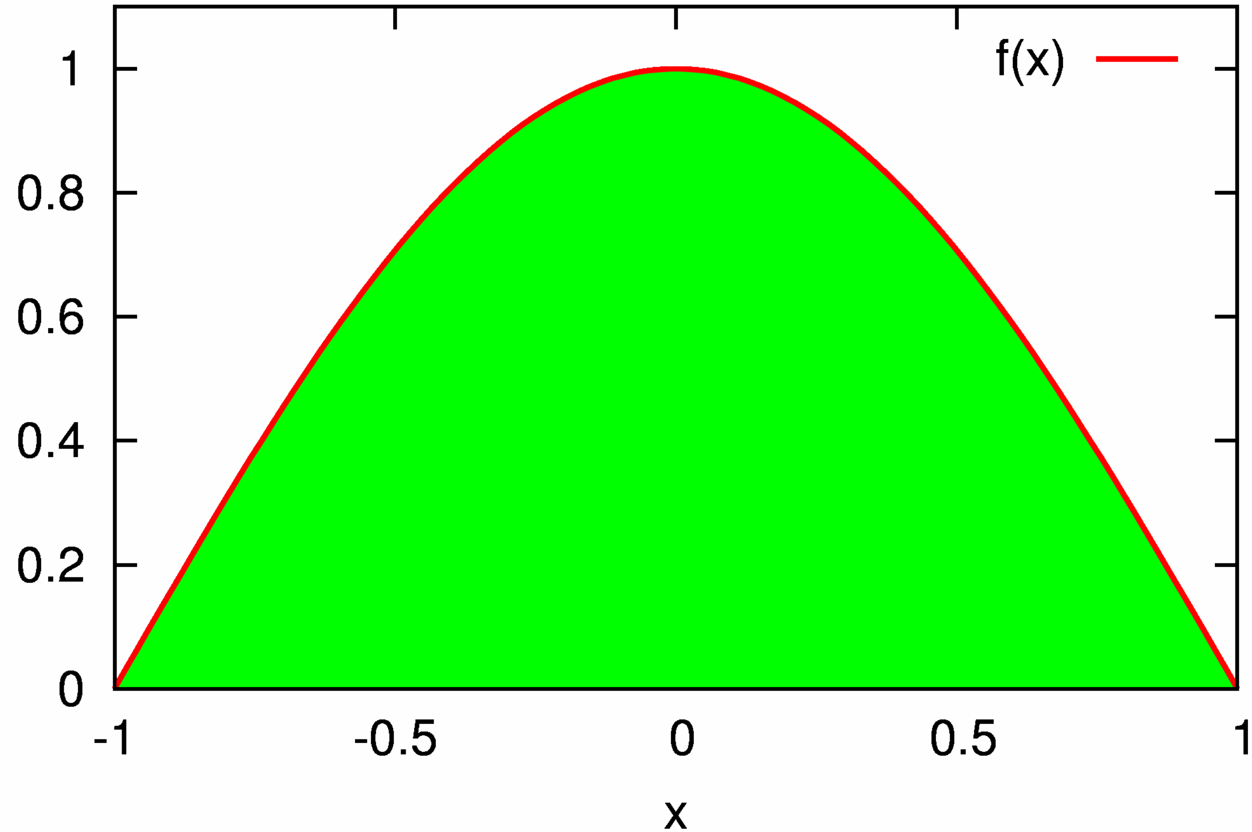

$$I = \int_a^b f(x)\, dx = ?$$

Mathematical excursion: Monte Carlo methods

General task: evaluation of (high-dimensional) sums/integrals

Simple example: quadrature of a convex function (in $d = 1$)

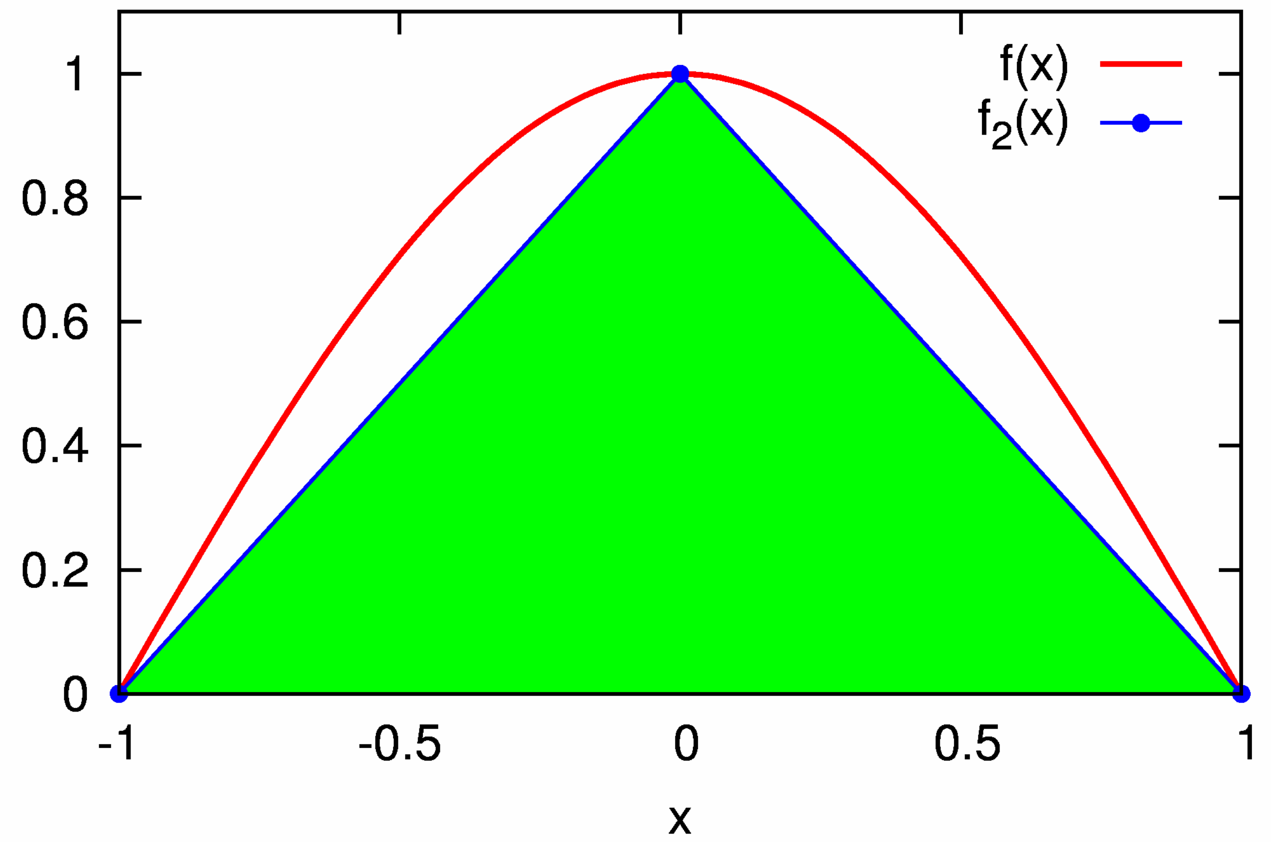

$$I = \int_a^b f(x)\,dx = ?$$

Numerical methods:

- discretization

Mathematical excursion: Monte Carlo methods

General task: evaluation of (high-dimensional) sums/integrals

Simple example: quadrature of a convex function (in $d = 1$)

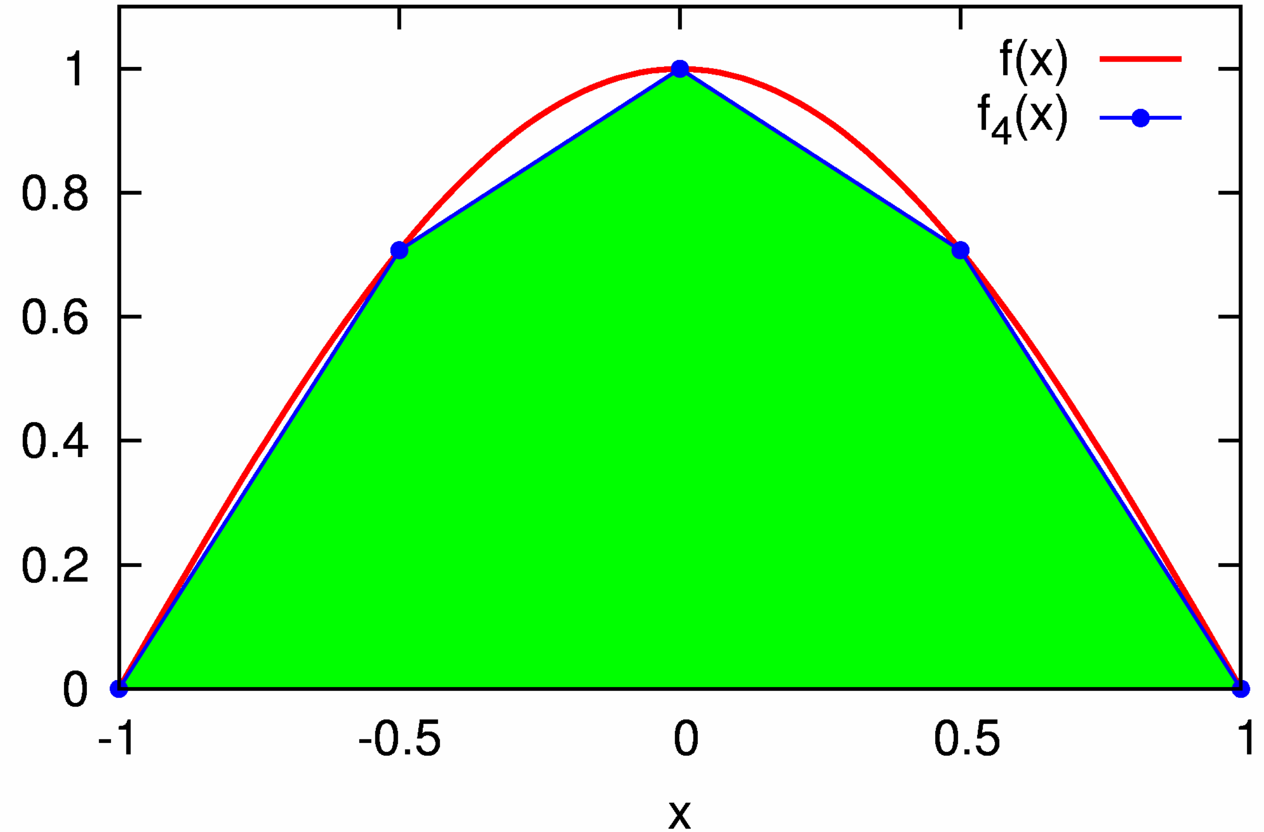

$$I = \int_a^b f(x)\, dx = ?$$

Numerical methods:

- discretization

Mathematical excursion: Monte Carlo methods

General task: evaluation of (high-dimensional) sums/integrals

Simple example: quadrature of a convex function (in $d = 1$)

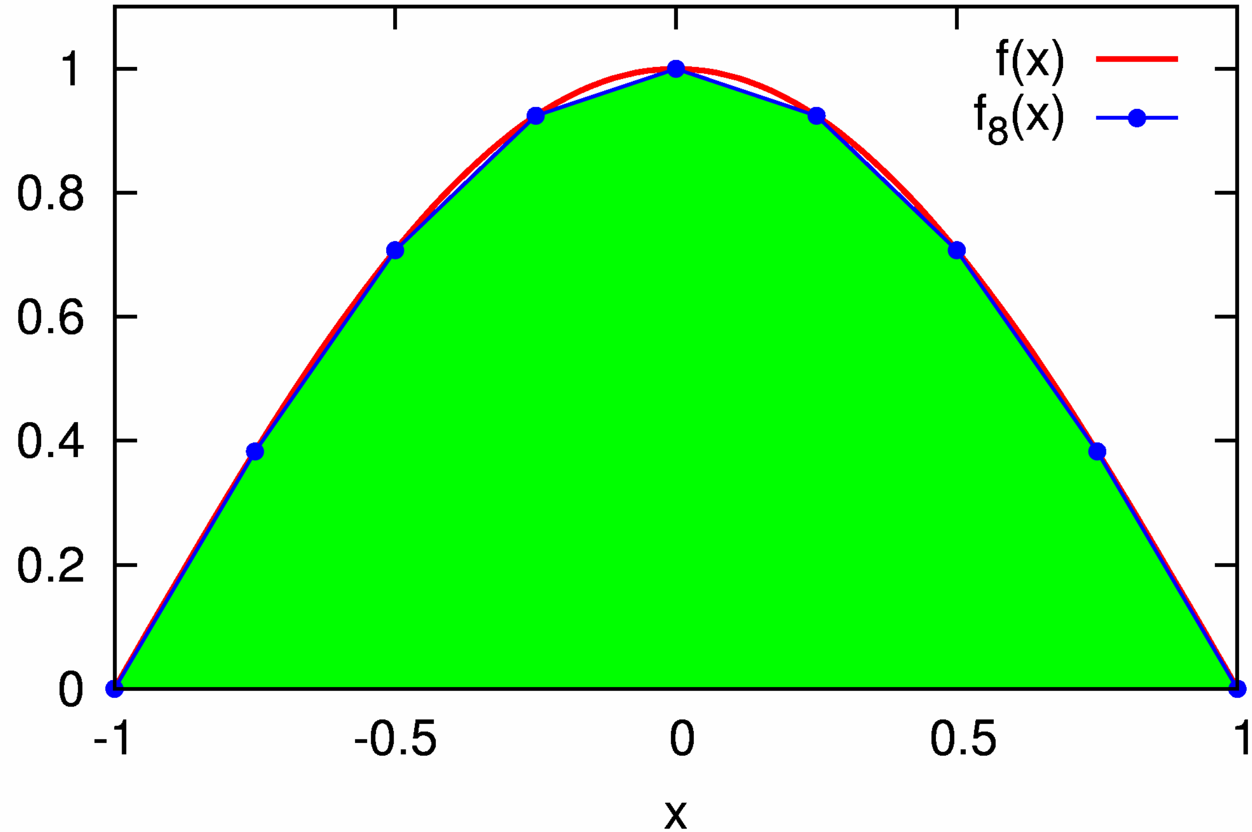

$$I = \int_a^b f(x)\, dx = ?$$

Numerical methods:

- discretization

Mathematical excursion: Monte Carlo methods

General task: evaluation of (high-dimensional) sums/integrals

Simple example: quadrature of a convex function (in $d = 1$)

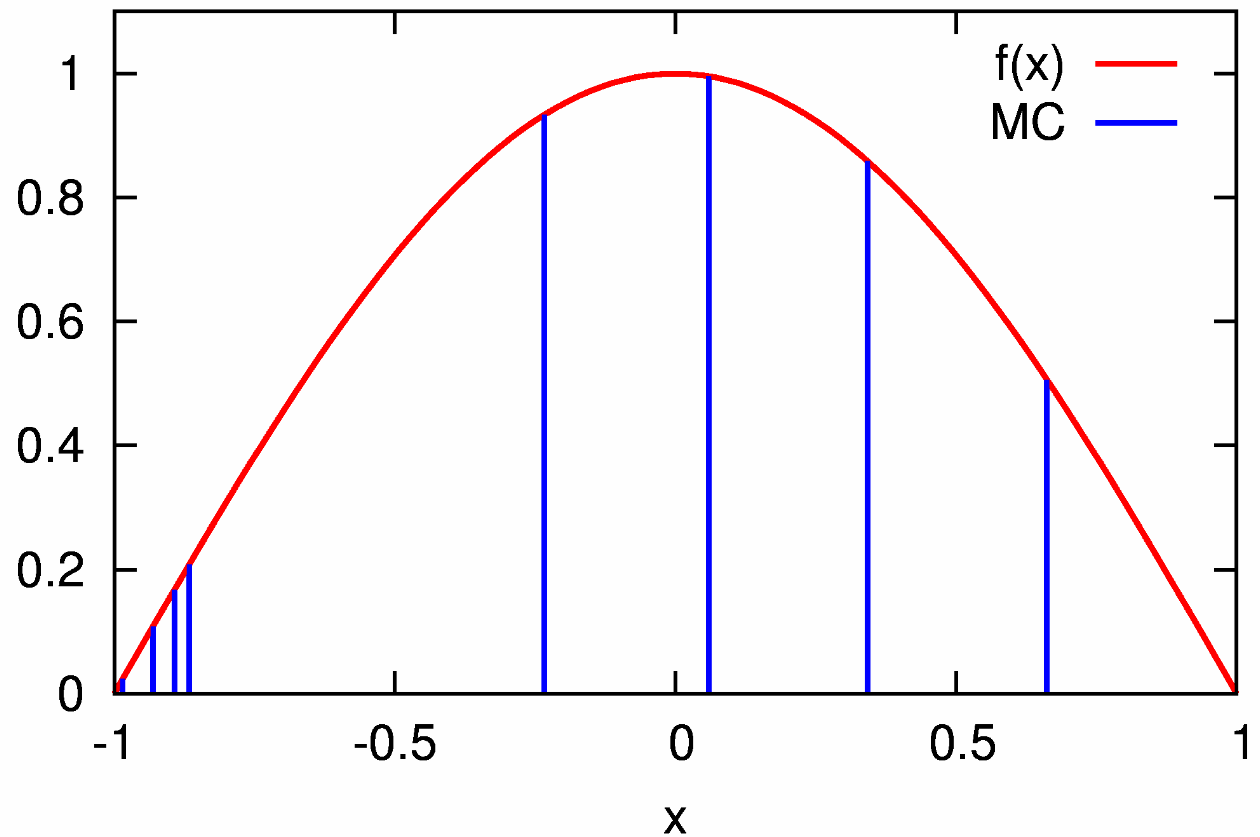

$$I = \int_a^b f(x)\,dx = ?$$

Numerical methods:

- discretization
- Monte Carlo

Convergence of results?

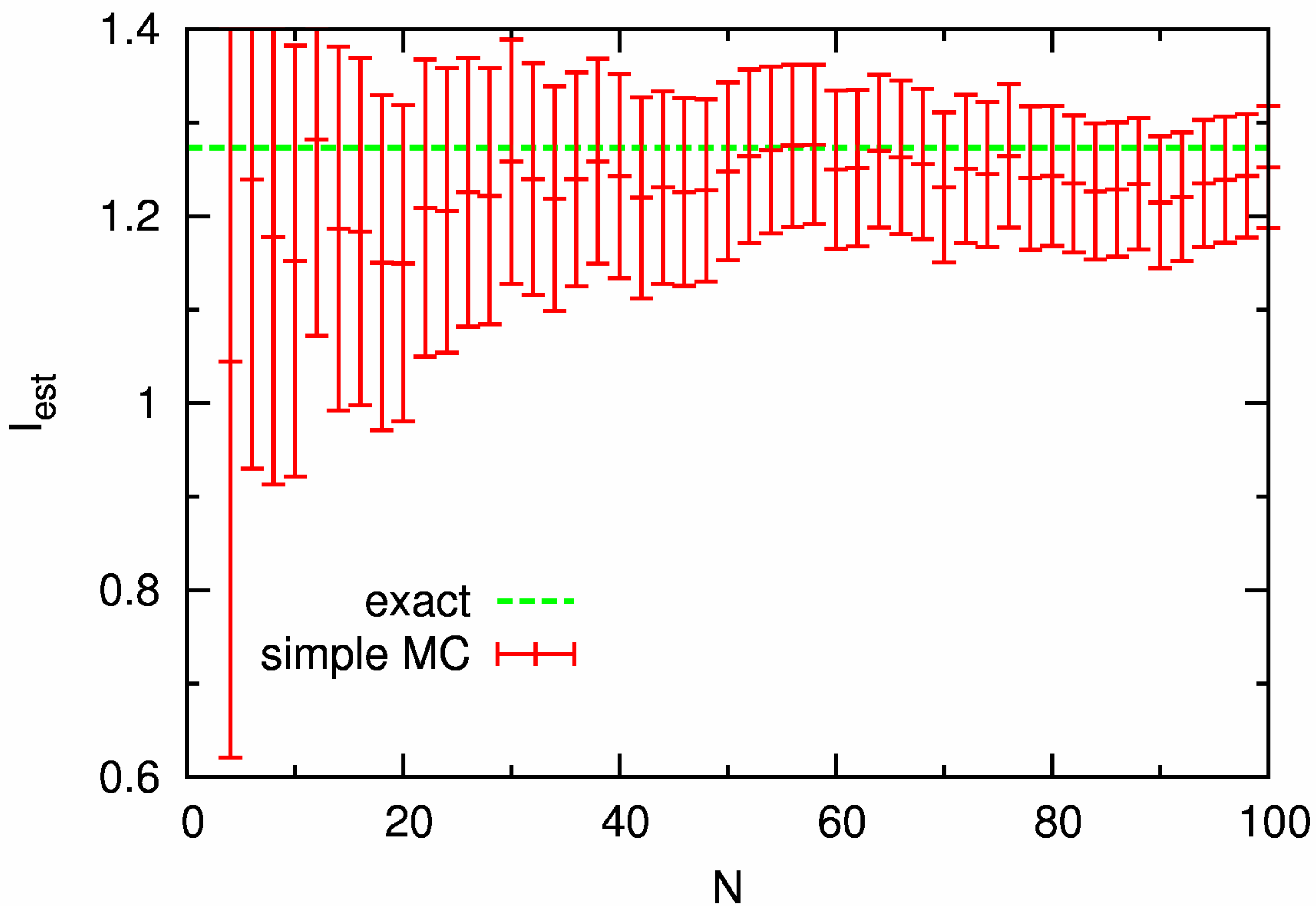

In Monte Carlo: errors $\propto \sqrt{1/N}$

Convergence of results?

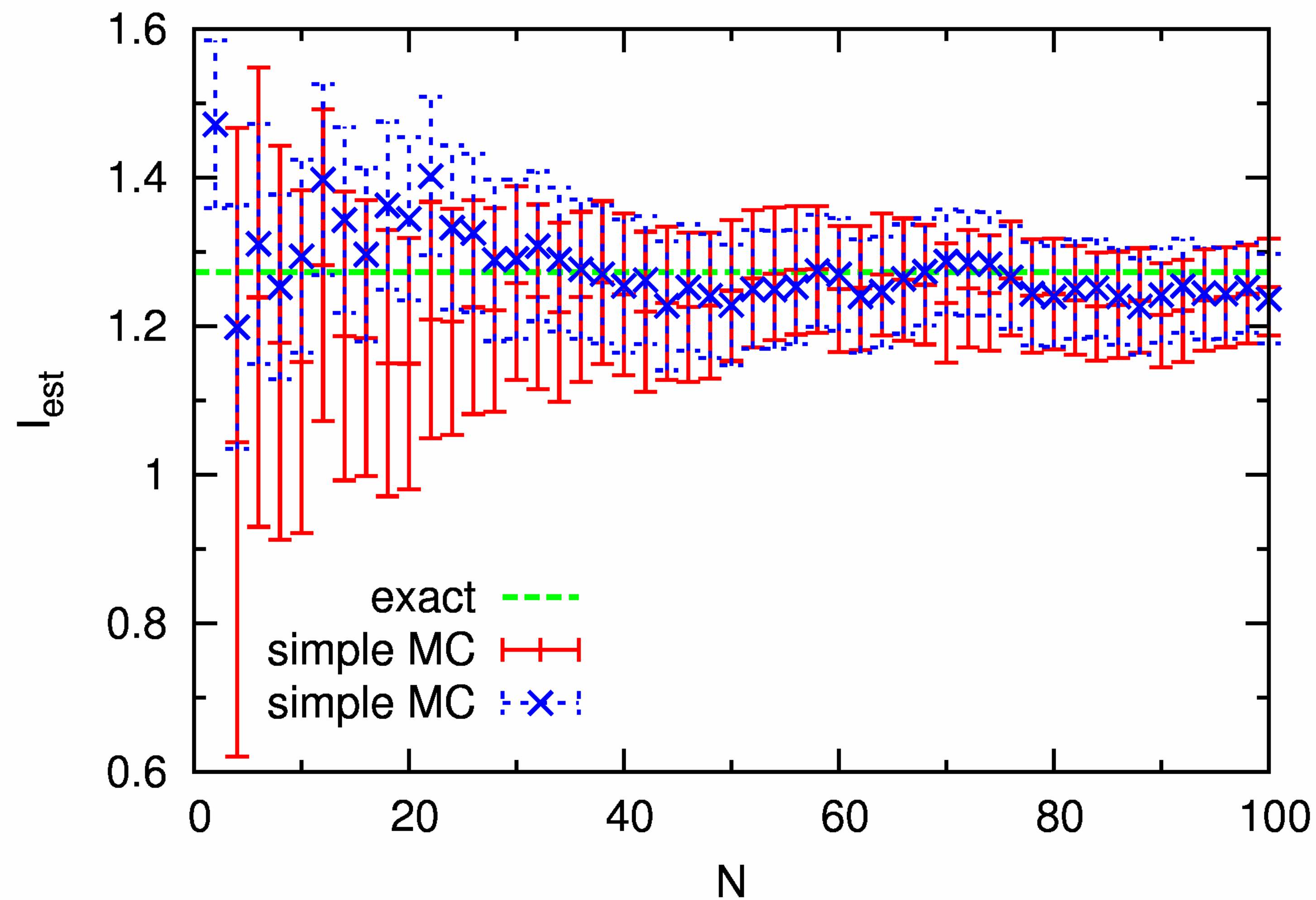

In Monte Carlo: errors $\propto \sqrt{1/N}$

MC results are non-deterministic: only meaningful within statistical error bars!

In this case, the deterministic method converges much faster (and very regularly)

Convergence of results?

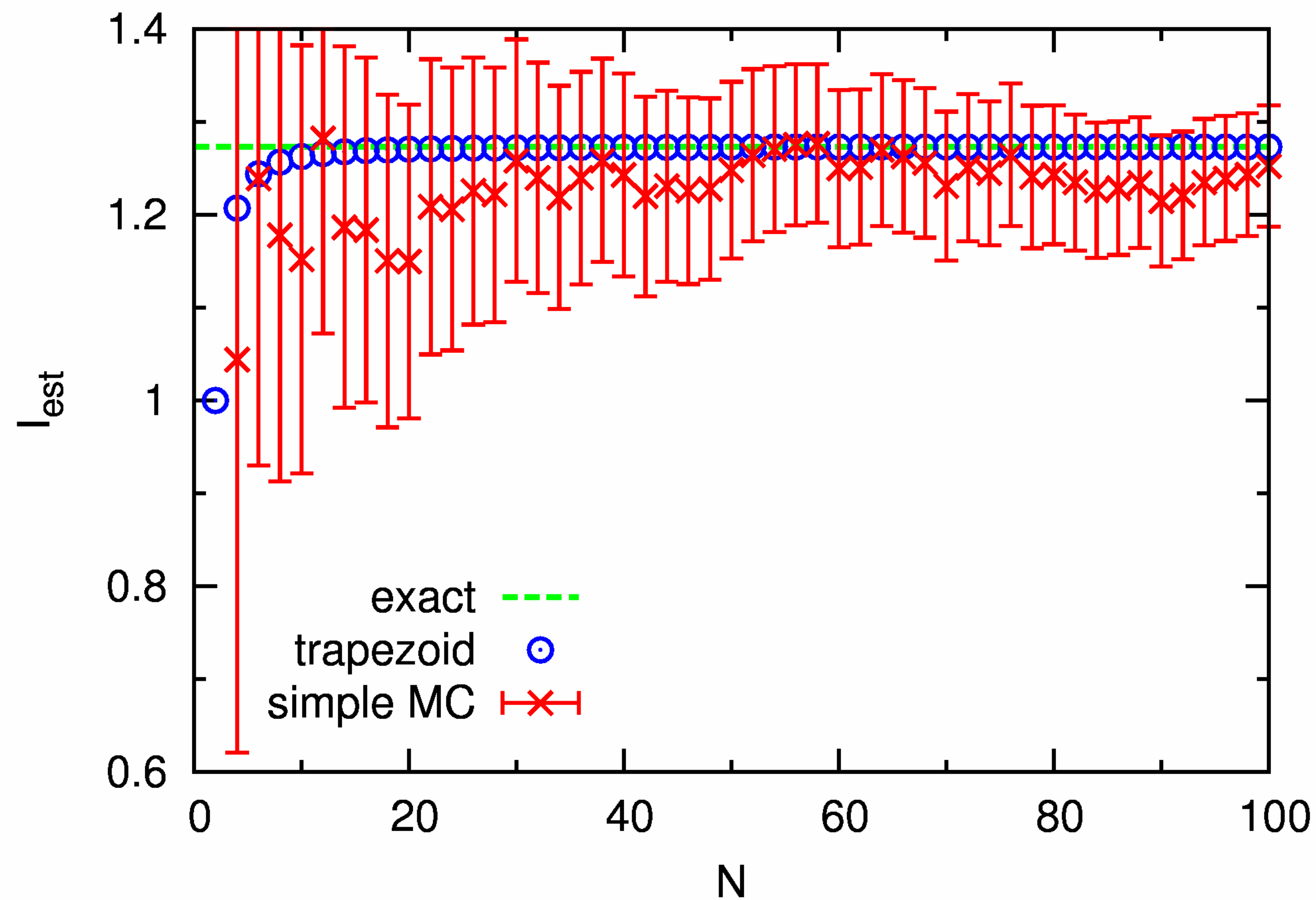

In Monte Carlo: errors $\propto \sqrt{1/N}$

MC results are non-deterministic: only meaningful within statistical error bars!

In this case, the deterministic method converges much faster (and very regularly)

Convergence of results?

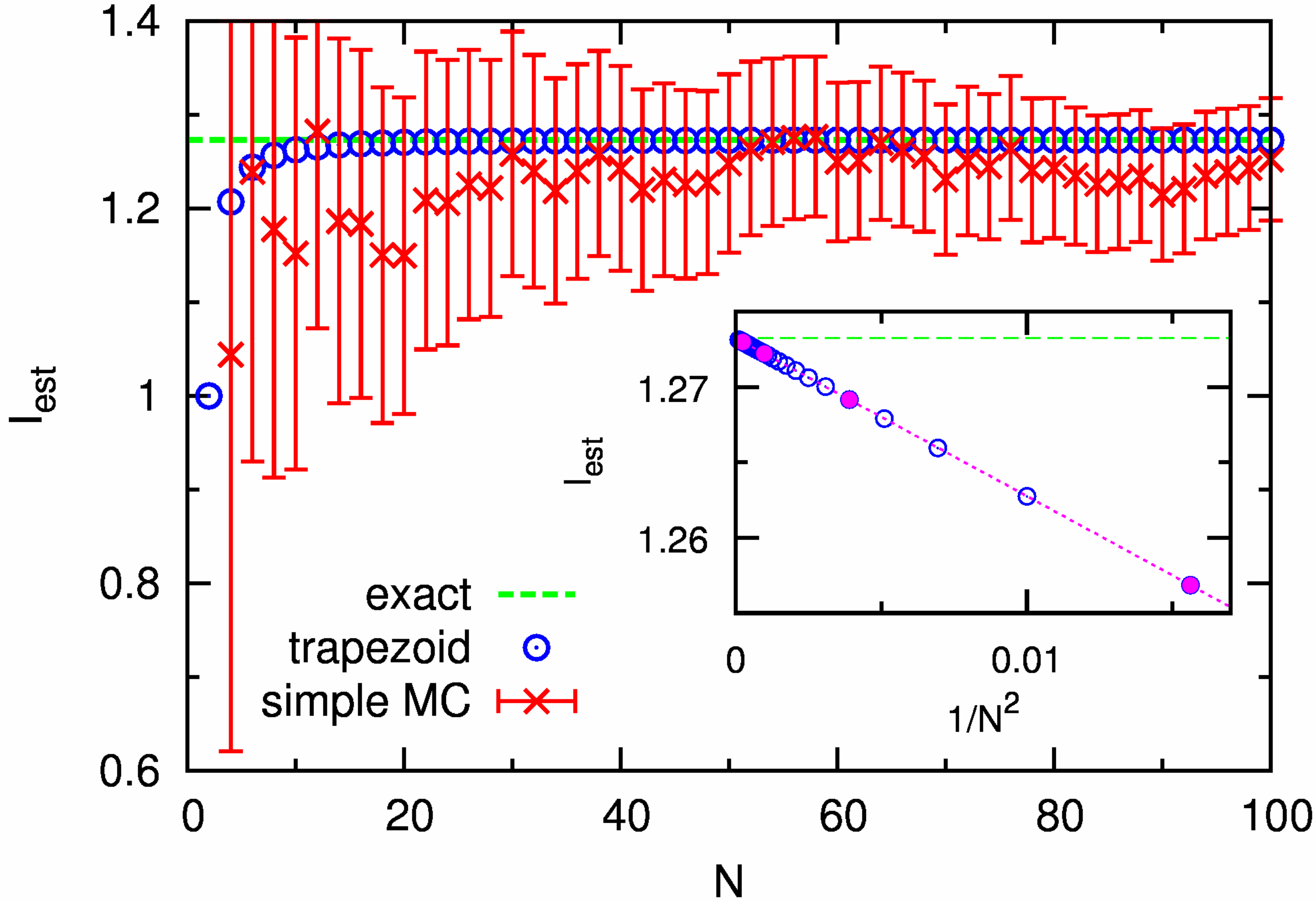

In Monte Carlo: errors $\propto \sqrt{1/N}$

MC results are non-deterministic: only meaningful within statistical error bars!

In this case, the deterministic method converges much faster (and very regularly)

Application of Monte Carlo in Statistical Physics

$$\langle O \rangle = \sum_i p_i \, O_i \,, \qquad p_i = \frac{e^{-E_i/(k_\mathrm{B}T)}}{\mathcal{Z}} \equiv \frac{\tilde{p}_i}{\mathcal{Z}}, \qquad \mathcal{Z} = \sum_i e^{-E_i/(k_\mathrm{B}T)}$$

Simple Monte Carlo: Estimation of both sums from a number N of equally probable configurations. Problem: typically $\sqrt{\mathrm{var}\{p\}} \gg \overline{p}$.

Solution: approach target prob. distribution by Markov chain (needs only p_i/p_j)

Application of Monte Carlo in Statistical Physics

$$\langle O \rangle = \sum_i p_i \, O_i \,, \qquad p_i = \frac{e^{-E_i/(k_B T)}}{\mathcal{Z}} \equiv \frac{\tilde{p}_i}{\mathcal{Z}}, \qquad \mathcal{Z} = \sum_i e^{-E_i/(k_B T)}$$

Simple Monte Carlo: Estimation of both sums from a number N of equally probable configurations. Problem: typically $\sqrt{\mathrm{var}\{p\}} \gg \overline{p}$.

Importance Sampling MC: Probability distribution given by Boltzmann weights p_i. Problem: Normalization $1/\mathcal{Z}$ unknown.

Solution: approach target prob. distribution by Markov chain (needs only p_i/p_j)

Auxiliary-field QMC algorithm [Hirsch, Fye (1986)]

Green function G in imaginary time (fermionic Grassmann variables ψ, ψ^*):

$$G_\sigma(\tau_2 - \tau_1) = \frac{1}{\mathcal{Z}} \int \mathcal{D}[\psi]\,\mathcal{D}[\psi^*]\;\; \psi_\sigma(\tau_1)\psi^*_\sigma(\tau_2)\;\; \exp\left[\mathcal{A}_0 - U \sum_{\sigma\sigma'} \int_0^\beta d\tau\, \psi^*_\sigma \psi_\sigma \psi^*_{\sigma'} \psi_{\sigma'}\right]$$

Auxiliary-field QMC algorithm [Hirsch, Fye (1986)]

Green function G in imaginary time (fermionic Grassmann variables ψ, ψ^*):

$$G_\sigma(\tau_2-\tau_1) = \frac{1}{\mathcal{Z}}\int \mathcal{D}[\psi]\,\mathcal{D}[\psi^*]\;\psi_\sigma(\tau_1)\psi^*_\sigma(\tau_2)\;\exp\Big[\mathcal{A}_0 - U\sum_{\sigma\sigma'}\int_0^\beta d\tau\,\psi^*_\sigma\psi_\sigma\psi^*_{\sigma'}\psi_{\sigma'}\Big]$$

(i) Imaginary-time discretization $\beta = \Lambda\,\Delta\tau$

(ii) Trotter decoupling $e^{-\beta(\hat{T}+\hat{V})} \approx \left[e^{-\Delta\tau\hat{T}}e^{-\Delta\tau\hat{V}}\right]^\Lambda$

Auxiliary-field QMC algorithm [Hirsch, Fye (1986)]

Green function G in imaginary time (fermionic Grassmann variables ψ, ψ^*):

$$G_\sigma(\tau_2 - \tau_1) = \frac{1}{\mathcal{Z}} \int \mathcal{D}[\psi]\,\mathcal{D}[\psi^*]\;\; \psi_\sigma(\tau_1)\psi^*_\sigma(\tau_2)\;\; \exp\Big[\mathcal{A}_0 - U \sum_{\sigma\sigma'} \int_0^\beta d\tau\, \psi^*_\sigma \psi_\sigma \psi^*_{\sigma'} \psi_{\sigma'}\Big]$$

(i) Imaginary-time discretization $\beta = \Lambda\,\Delta\tau$

(ii) Trotter decoupling $e^{-\beta(\hat{T}+\hat{V})} \approx \left[e^{-\Delta\tau \hat{T}} e^{-\Delta\tau \hat{V}}\right]^\Lambda$

(iii) Hubbard-Stratonovich transformation

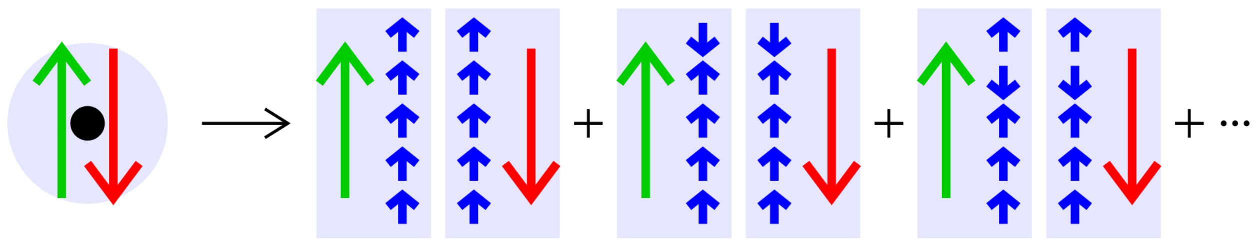

Wick theorem:

$$G = \frac{\sum M \det\{M\}}{\sum \det\{M\}}$$

Auxiliary-field QMC algorithm [Hirsch, Fye (1986)]

Green function G in imaginary time (fermionic Grassmann variables ψ, ψ^*):

$$G_\sigma(\tau_2 - \tau_1) = \frac{1}{\mathcal{Z}} \int \mathcal{D}[\psi]\,\mathcal{D}[\psi^*]\;\; \psi_\sigma(\tau_1)\psi^*_\sigma(\tau_2)\;\; \exp\Big[\mathcal{A}_0 - U \sum_{\sigma\sigma'} \int_0^\beta d\tau\, \psi^*_\sigma \psi_\sigma \psi^*_{\sigma'} \psi_{\sigma'}\Big]$$

(i) Imaginary-time discretization $\beta = \Lambda\,\Delta\tau$

(ii) Trotter decoupling $e^{-\beta(\hat{T}+\hat{V})} \approx \left[e^{-\Delta\tau\,\hat{T}} e^{-\Delta\tau\,\hat{V}}\right]^\Lambda$

(iii) Hubbard-Stratonovich transformation

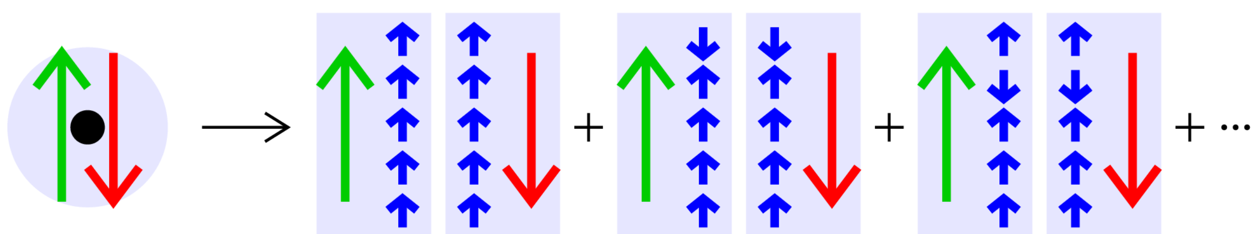

Wick theorem:

$$G = \frac{\sum M \det\{M\}}{\sum \det\{M\}}$$

(iv) MC importance sampling over auxiliary Ising field $\{s\}$: 2^Λ configurations

+ numerically exact, + no sign problem, $-$ effort scales as T^{-3}

(density-type interactions)

Self-consistency cycle using conventional HF-QMC

$\Delta\tau \rightsquigarrow$ bias

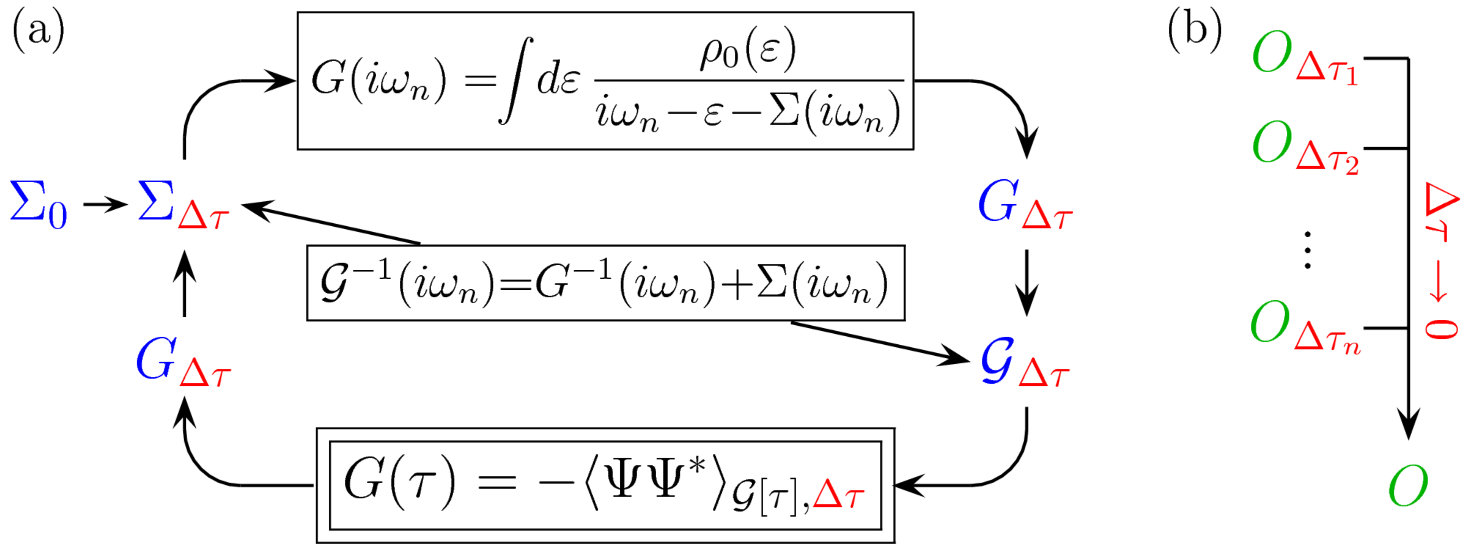

Extrapolation $\Delta\tau \to 0$ can improve accuracy of observable estimates by several orders of magnitude ($\sim$ same cost)

Self-consistency cycle using conventional HF-QMC

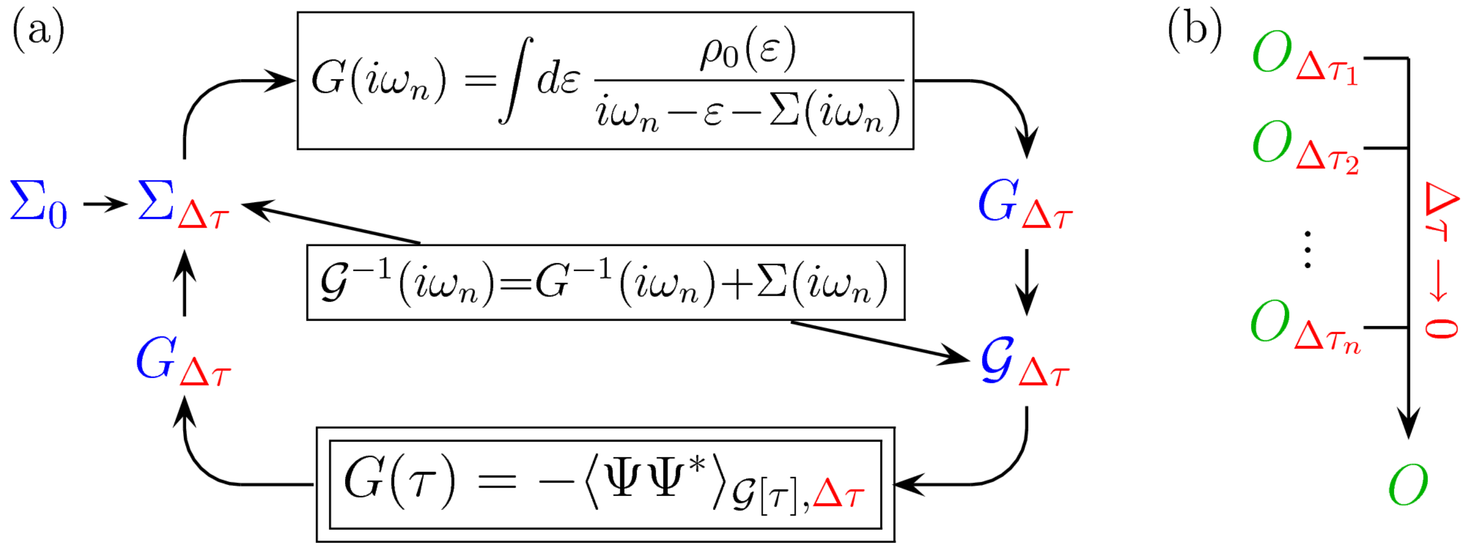

$\Delta\tau \rightsquigarrow$ bias

Extrapolation $\Delta\tau \to 0$ can improve accuracy of observable estimates by several orders of magnitude ($\sim$ same cost)

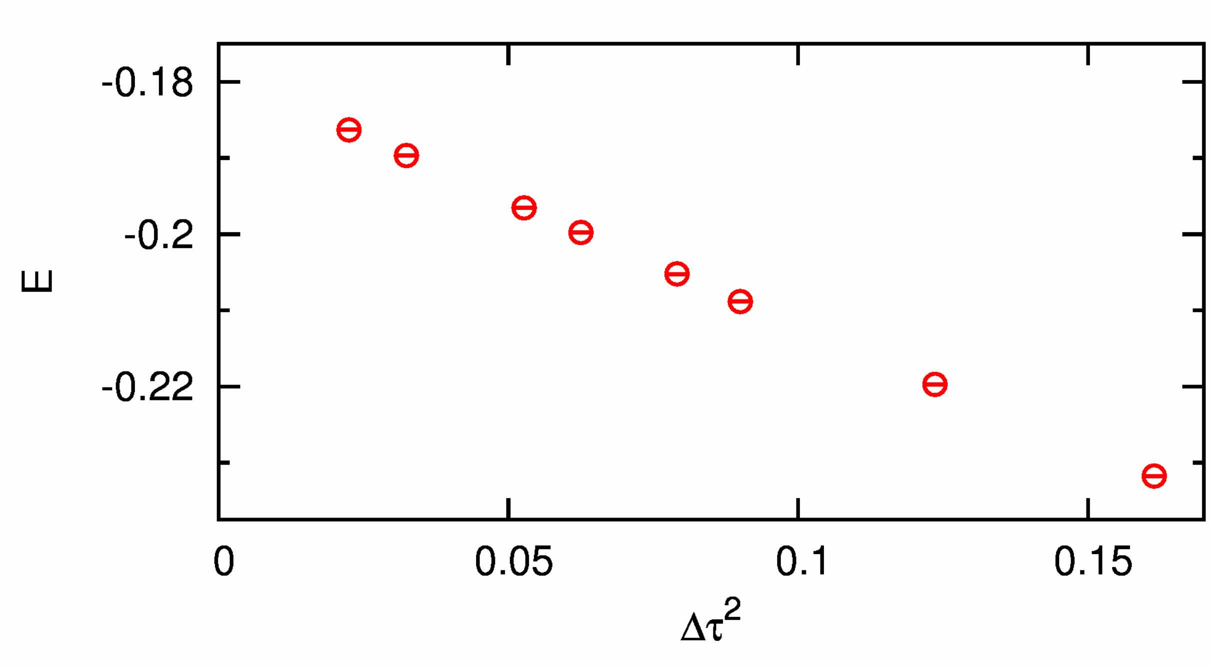

Example: energy E for $U = W = 4$ (Bethe DOS), $T = 1/45$ [NB, PRB (2007)]

Self-consistency cycle using conventional HF-QMC

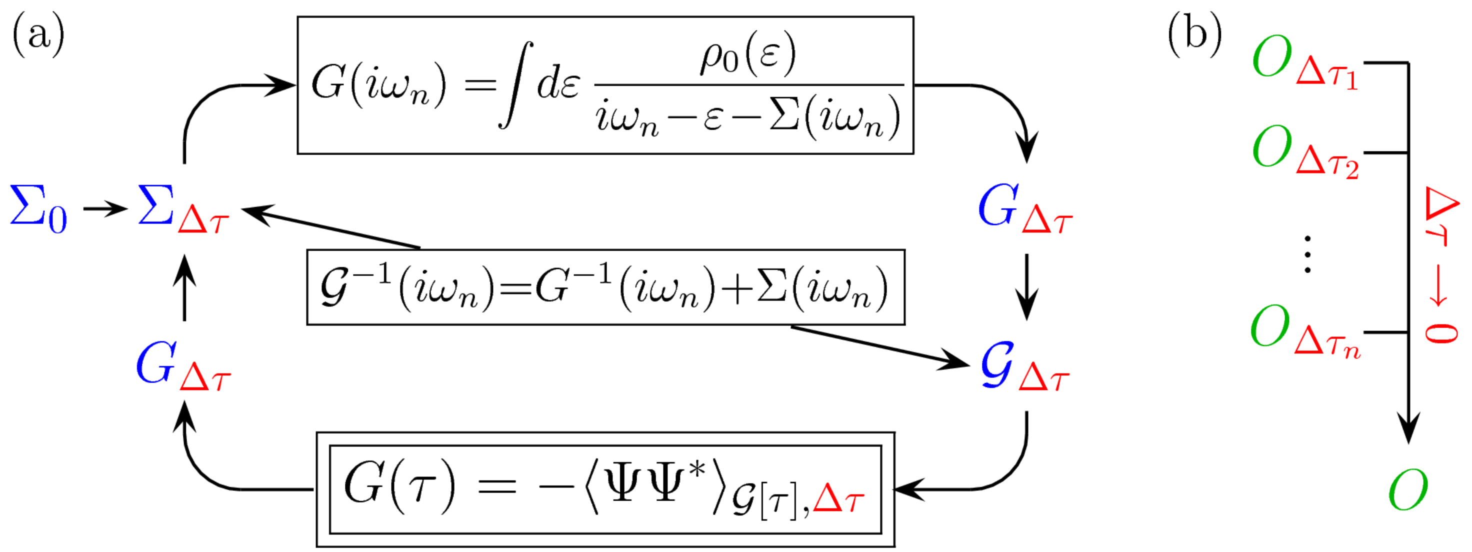

$\Delta\tau \rightsquigarrow$ bias

Extrapolation $\Delta\tau \rightarrow 0$ can improve accuracy of observable estimates by several orders of magnitude ($\sim$ same cost)

Example: energy E for $U = W = 4$ (Bethe DOS), $T = 1/45$ [NB, PRB (2007)]

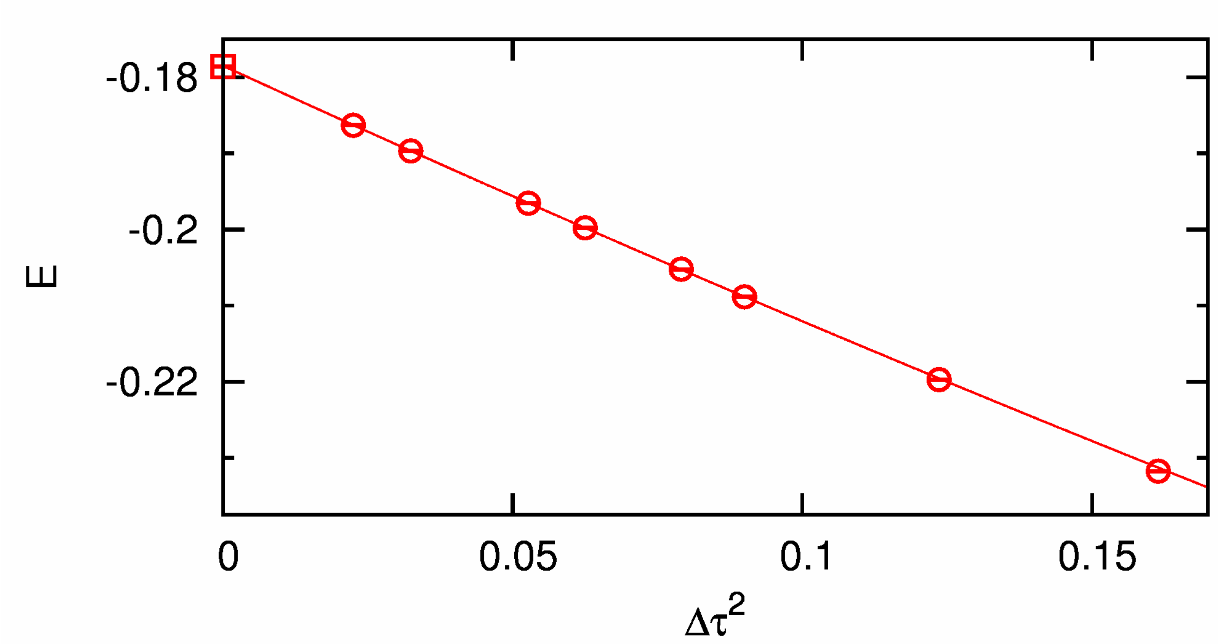

New development: continuous-time QMC algorithms

1. weak-coupling expansion

[Rubtsov, Savkin, Lichtenstein, PRB (2005)]

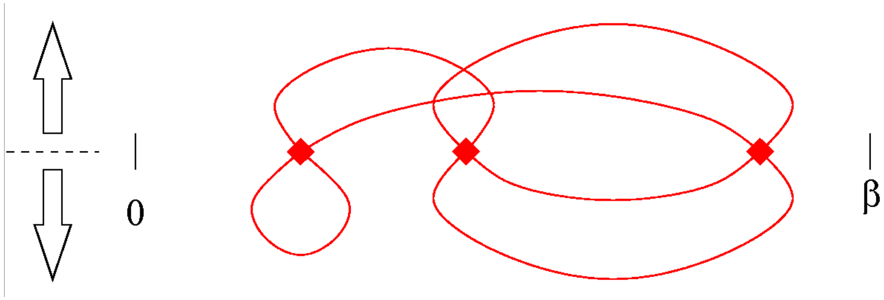

2. hybridization expansion

[Werner et al., PRL (2006)]

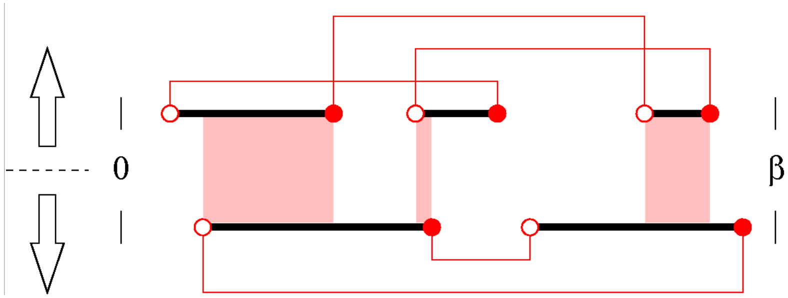

No systematic errors (in principle). Also more efficient than HF-QMC?

New development: continuous-time QMC algorithms

1. weak-coupling expansion

[Rubtsov, Savkin, Lichtenstein, PRB (2005)]

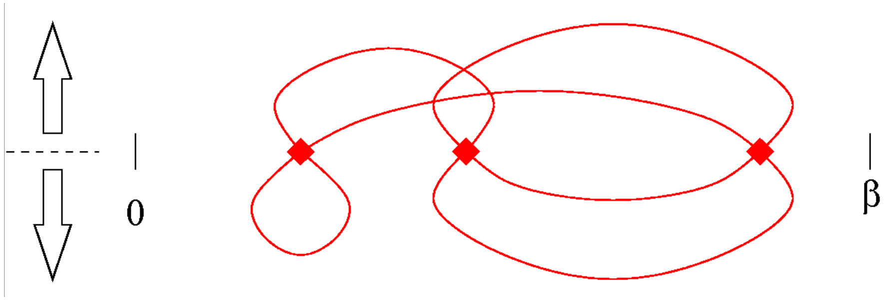

2. hybridization expansion

[Werner et al., PRL (2006)]

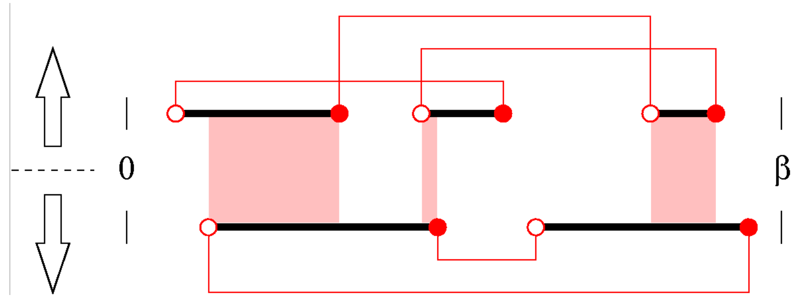

No systematic errors (in principle). Also more efficient than HF-QMC? No!

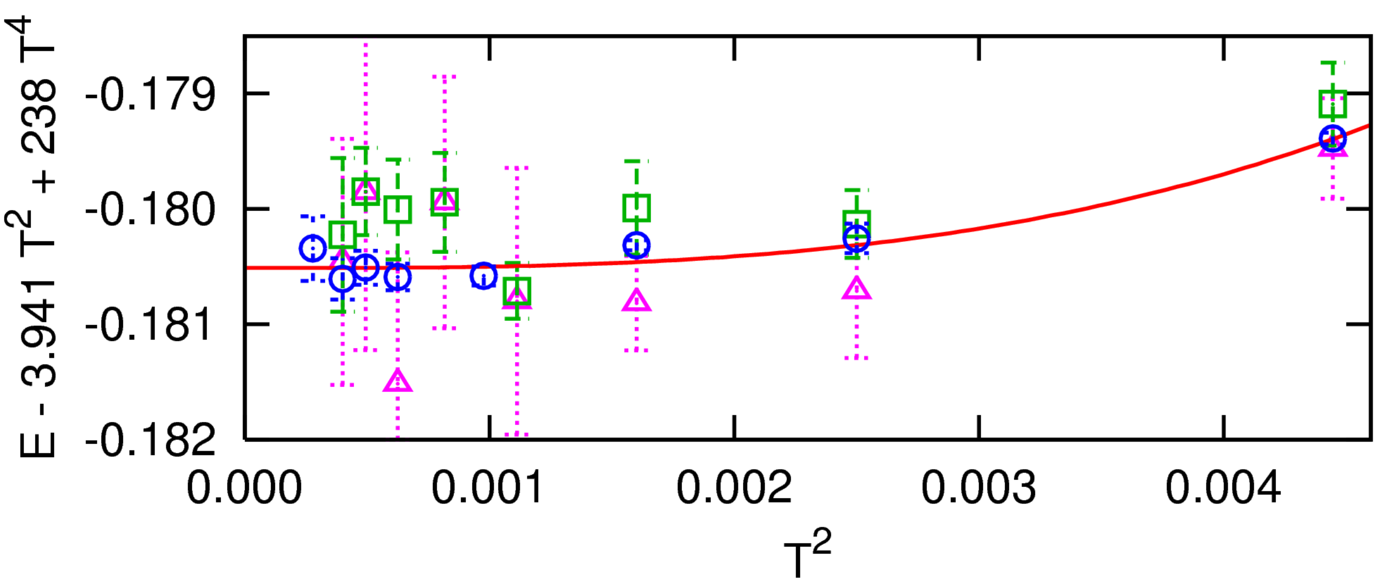

Test case:

1 band, $U = W = 4$

○ HF-QMC ($\Delta\tau \to 0$)

□ weak-coupling CT-QMC

△ hybridization CT-QMC

HF-QMC + extrapolation $\Delta\tau \to 0$ can be more efficient [NB, PRB **76**, 205120 (2007)]

Multigrid Hirsch-Fye quantum Monte Carlo algorithm

State of the art: (a) conventional HF-QMC

(b) *a posteriori* extrapolation of selected observables

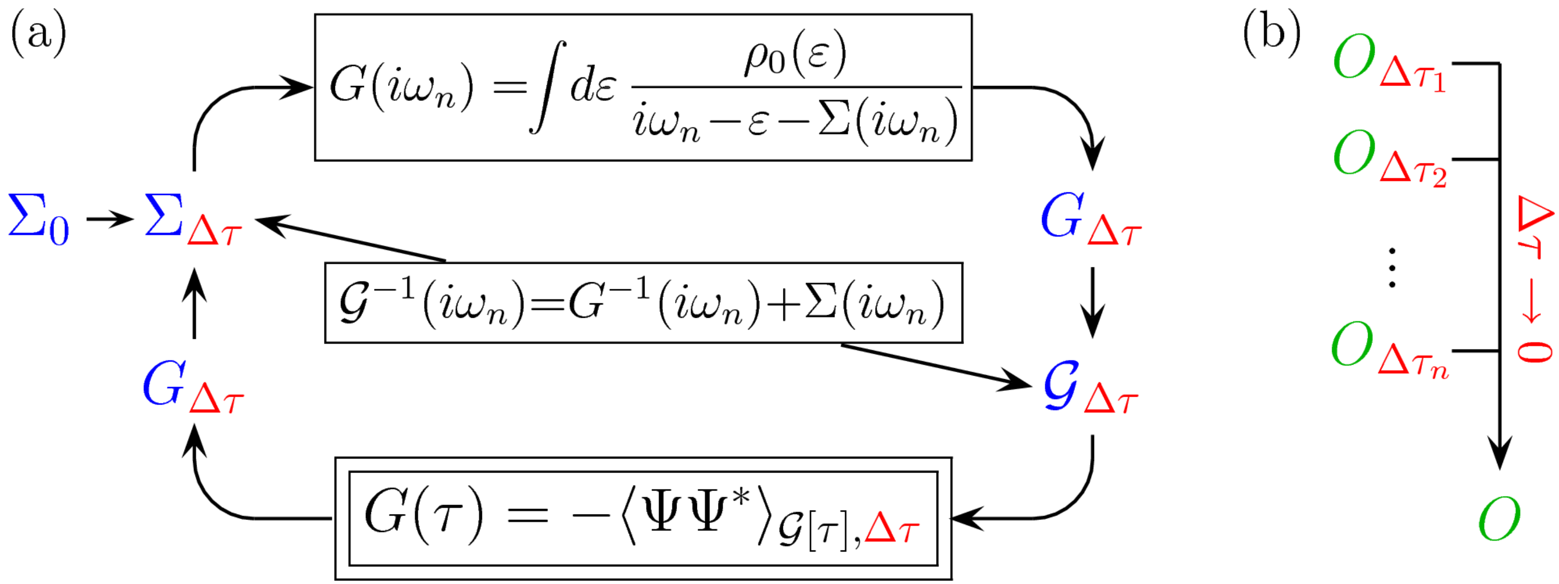

Multigrid Hirsch-Fye quantum Monte Carlo algorithm

State of the art: (a) conventional HF-QMC

(b) *a posteriori* extrapolation of selected observables

(c)

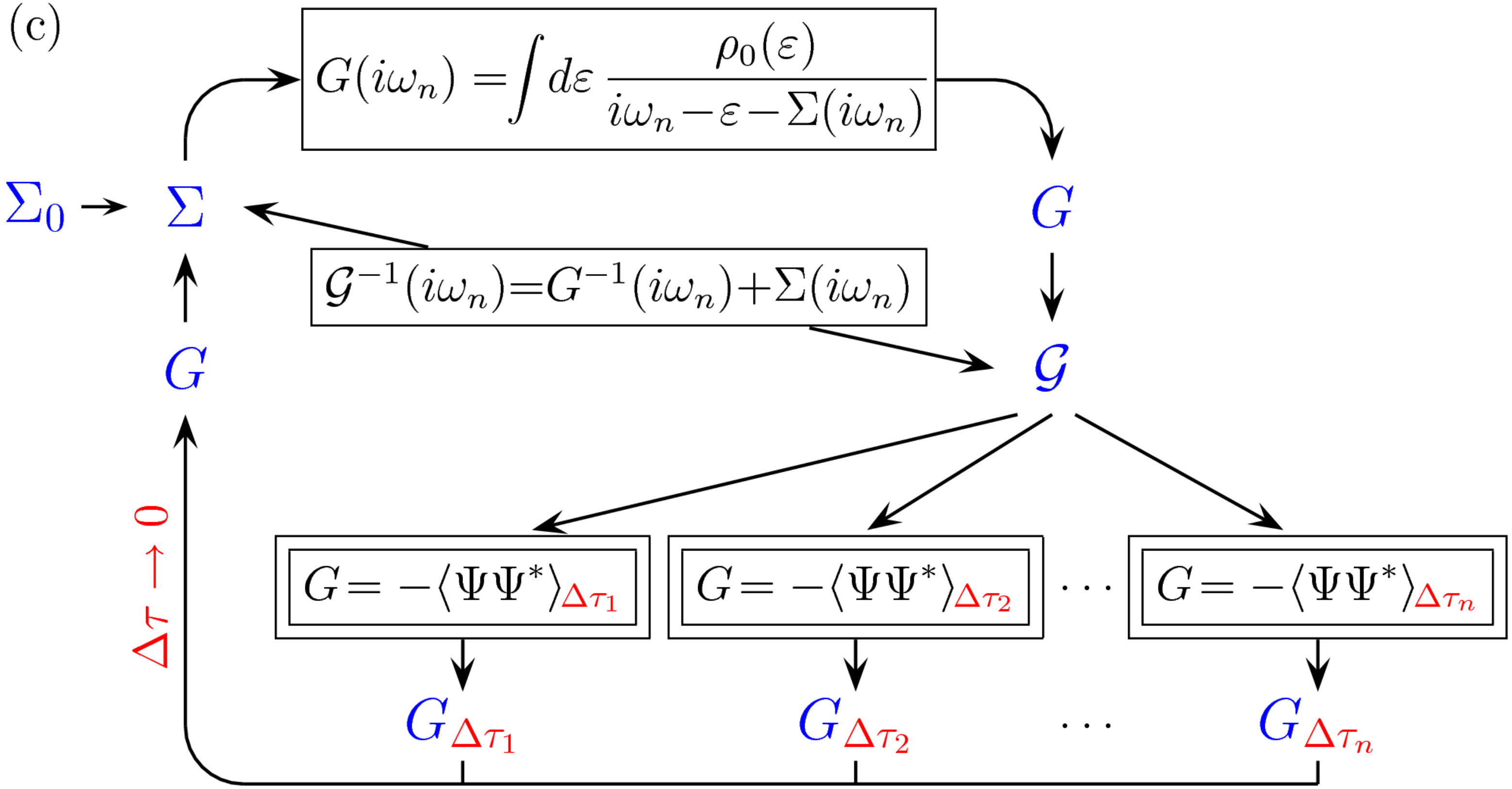

(c) Multigrid HF-QMC: internal elimination of Trotter error

$\rightsquigarrow$ quasi continuous time algorithm [NB, arXiv:0801.1222]

Schematic comparison via generalized Ginzburg-Landau functionals

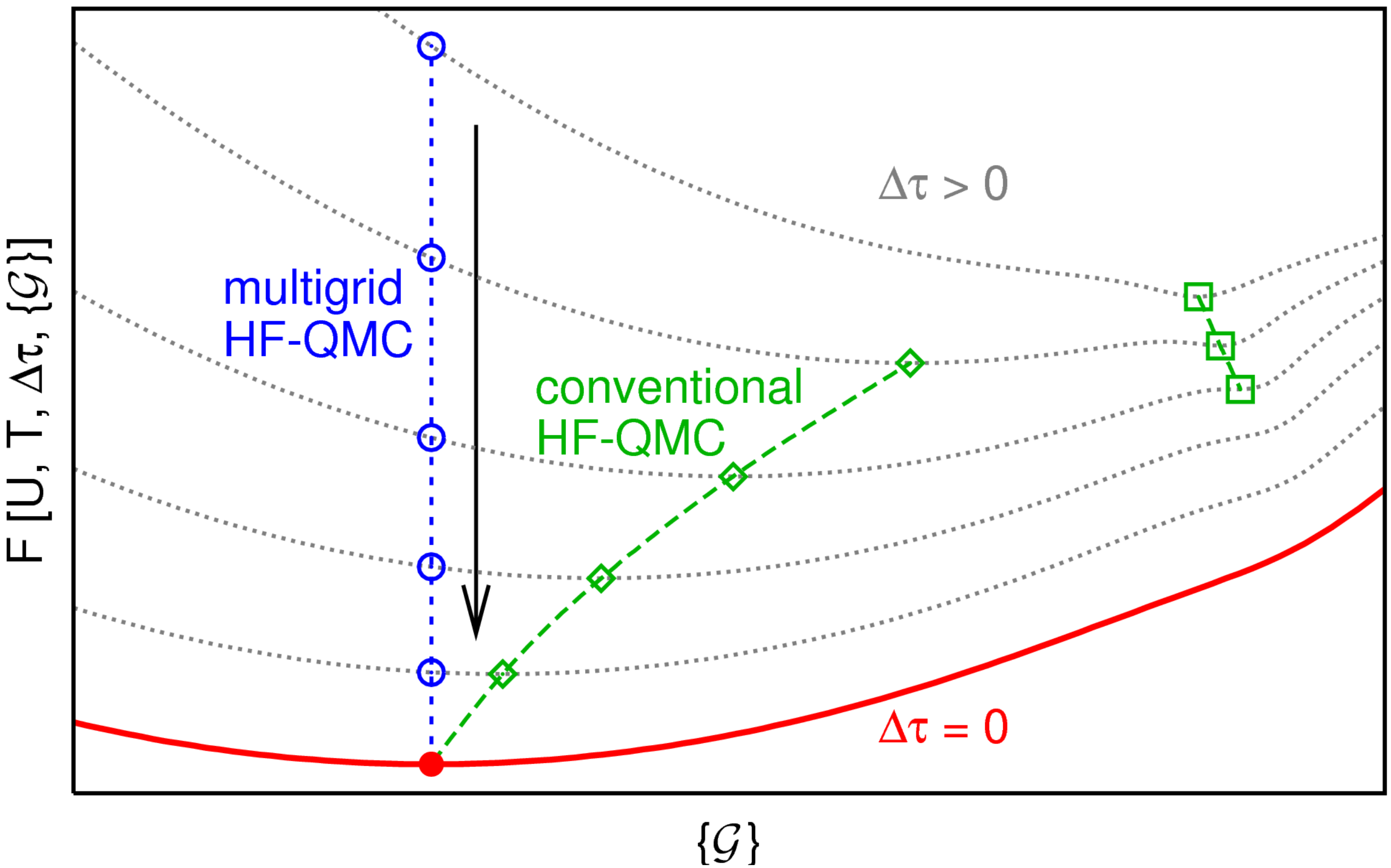

Conventional Hirsch-Fye QMC: DMFT fixed point shifts with $\Delta\tau$

Multigrid Hirsch-Fye QMC: DMFT iteration towards exact fixed point

Schematic comparison via generalized Ginzburg-Landau functionals

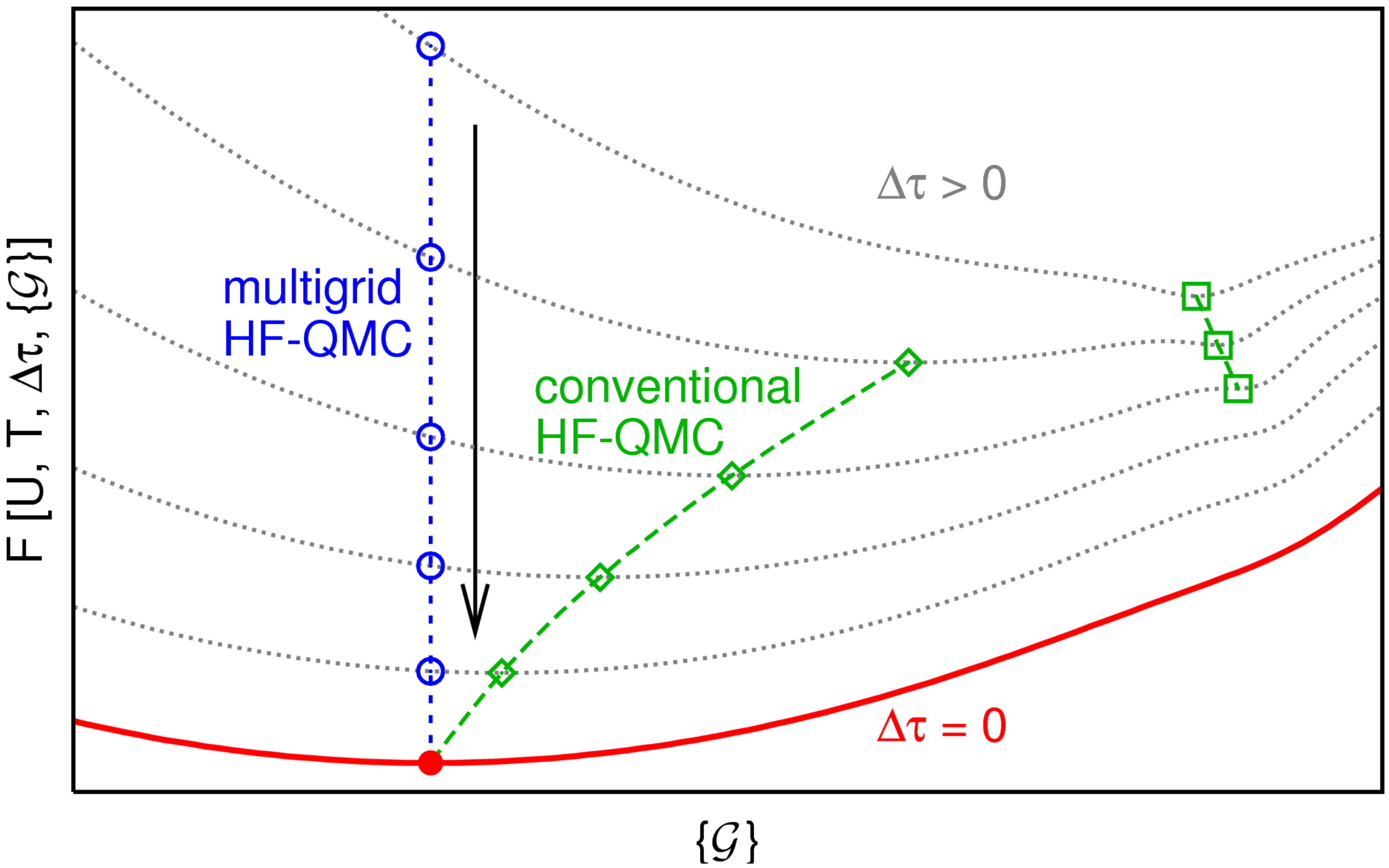

Conventional Hirsch-Fye QMC: DMFT fixed point shifts with $\Delta\tau$

Multigrid Hirsch-Fye QMC: DMFT iteration towards exact fixed point

Implementation: Green function extrapolation, hierarchy of frequency scales

Comparison: double occupancy $D = \langle n_{i\uparrow} n_{i\downarrow} \rangle$ near Mott transition

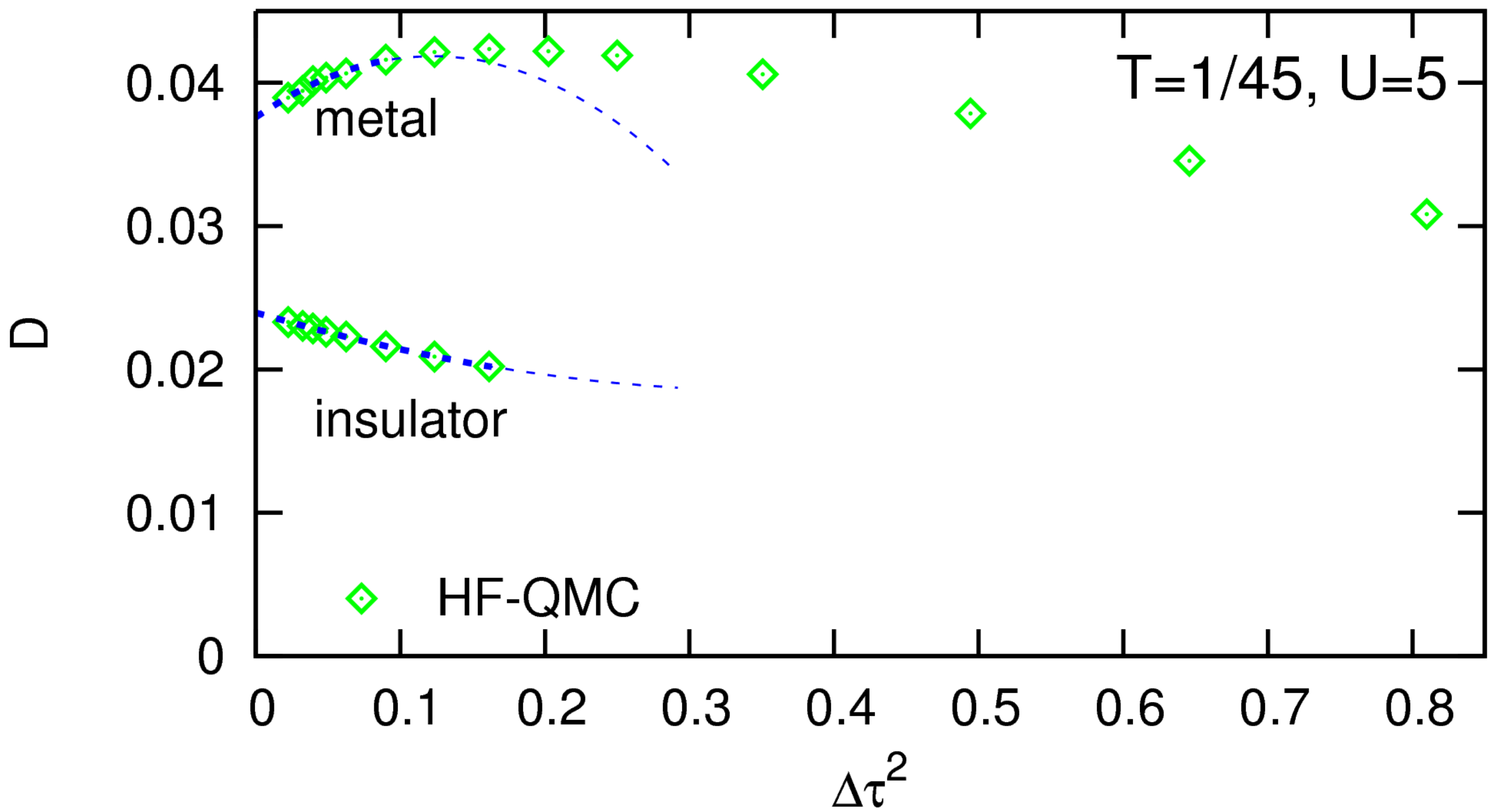

Conventional HF-QMC: no insulating solution for $\Delta\tau \gtrsim 0.4$

very irregular $\Delta\tau$ dependence beyond $\Delta\tau \approx 0.3$

Comparison: double occupancy $D = \langle n_{i\uparrow} n_{i\downarrow} \rangle$ near Mott transition

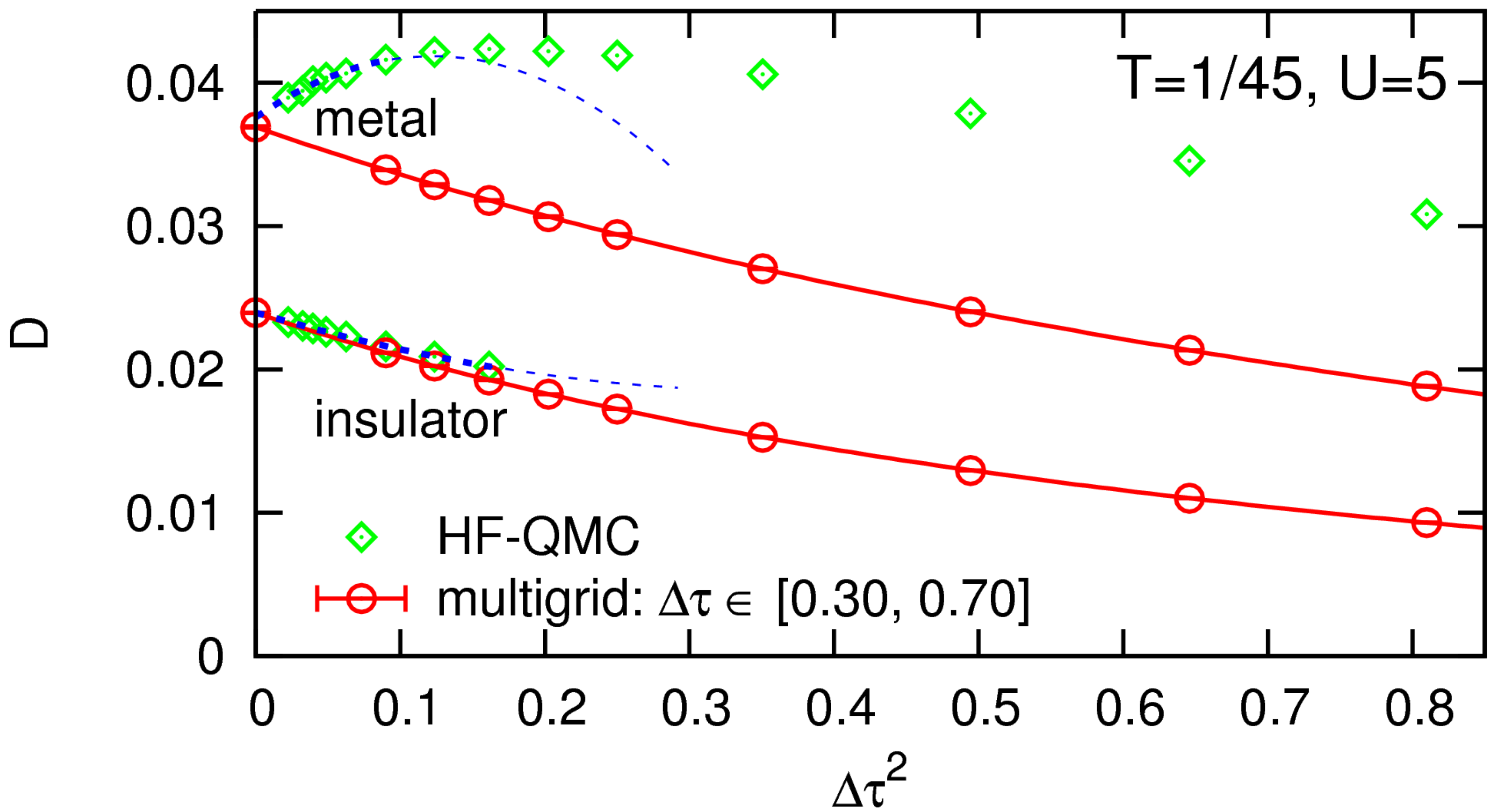

Conventional HF-QMC:	no insulating solution for $\Delta\tau \gtrsim 0.4$
	very irregular $\Delta\tau$ dependence beyond $\Delta\tau \approx 0.3$
Multigrid HF-QMC:	vastly larger useful range of $\Delta\tau$

Systematic study: impact of grid range (on double occupancy)

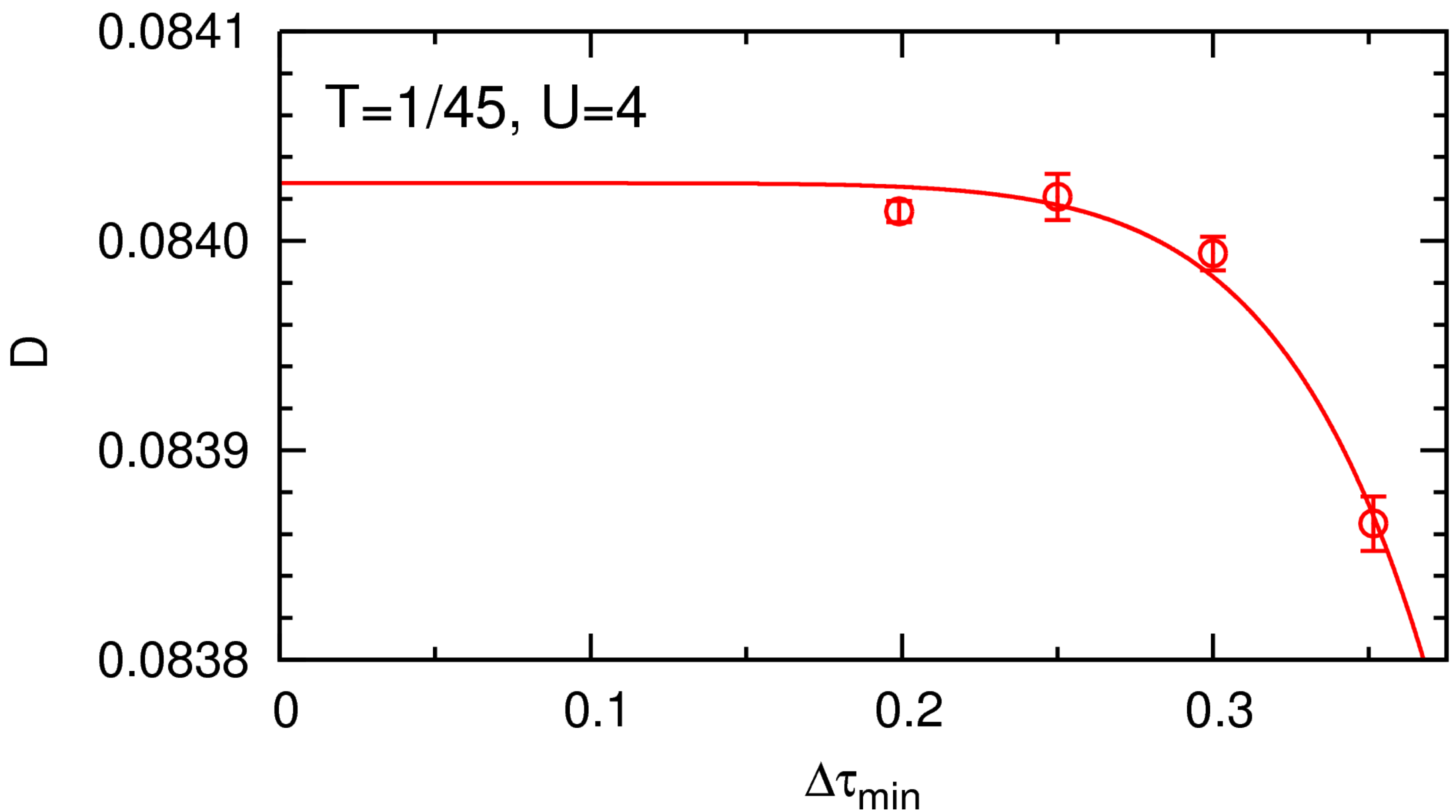

Multigrid HF-QMC usually "numerically exact" for $\tau_{\min} \lesssim 0.3$

No "difficult observables" for multigrid HF-QMC, higher efficiency than CT-QMC

Many successful applications: spectra, high-precision c_v, 8-band calculations, . . .

Ultracold fermions on optical lattices: model systems for strongly correlated materials

Ultracold atoms are much simpler:

Ultracold fermions on optical lattices: model systems for strongly correlated materials

Ultracold atoms are much simpler:

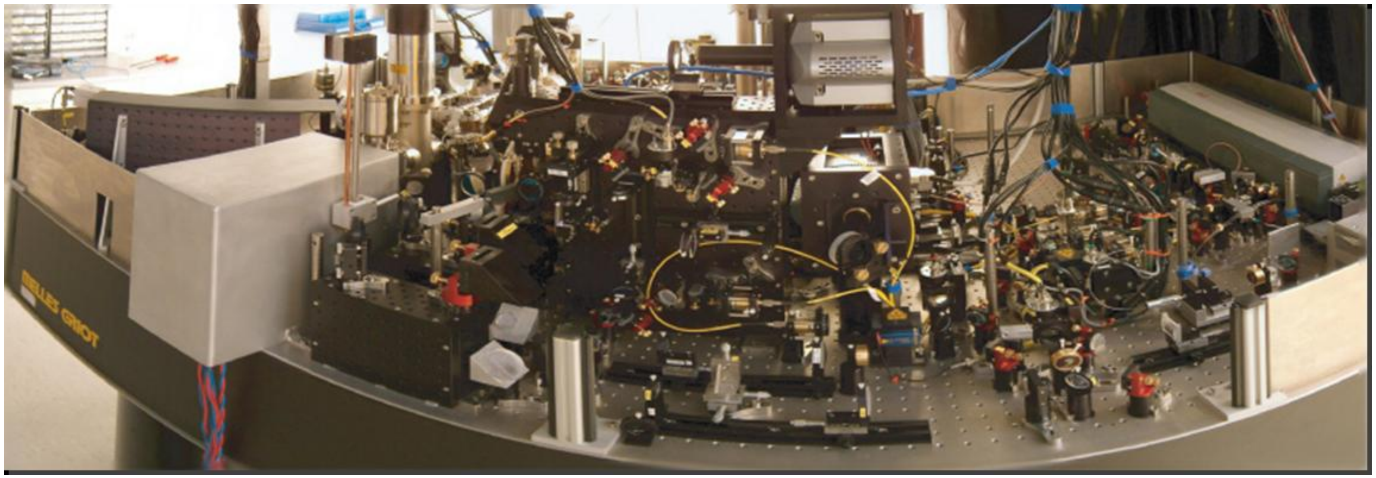

[Photo courtesy of U. Schneider]

Ultracold fermions on optical lattices: model systems for strongly correlated materials

Ultracold atoms are much simpler: 1-band assumption is often accurate

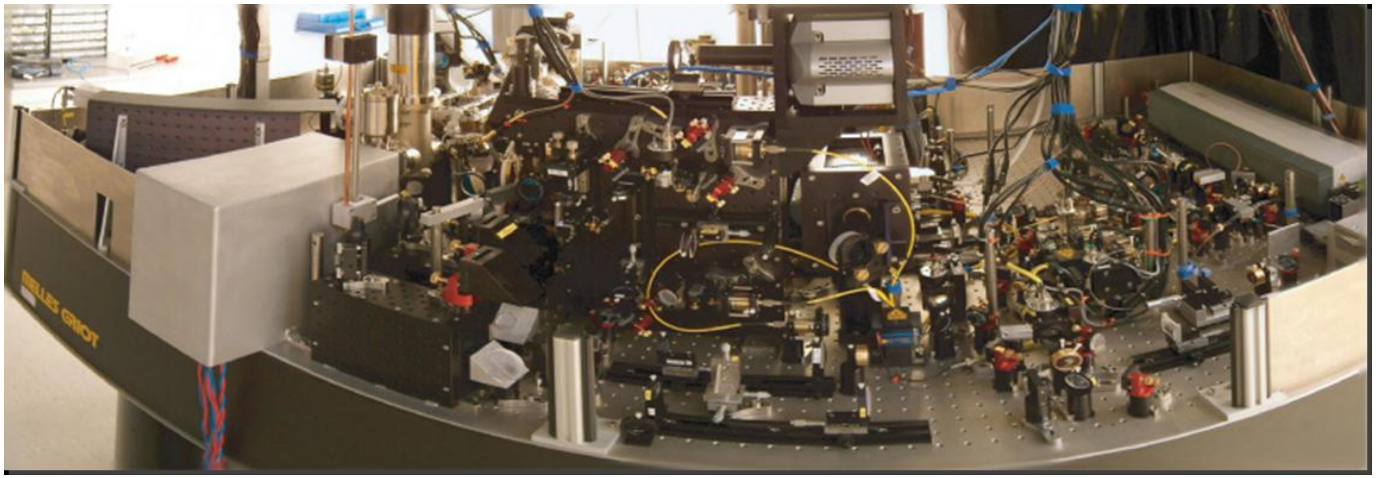

[Photo courtesy of U. Schneider]

Ultracold fermions on optical lattices: model systems for strongly correlated materials

Ultracold atoms are much simpler: 1-band assumption is often accurate

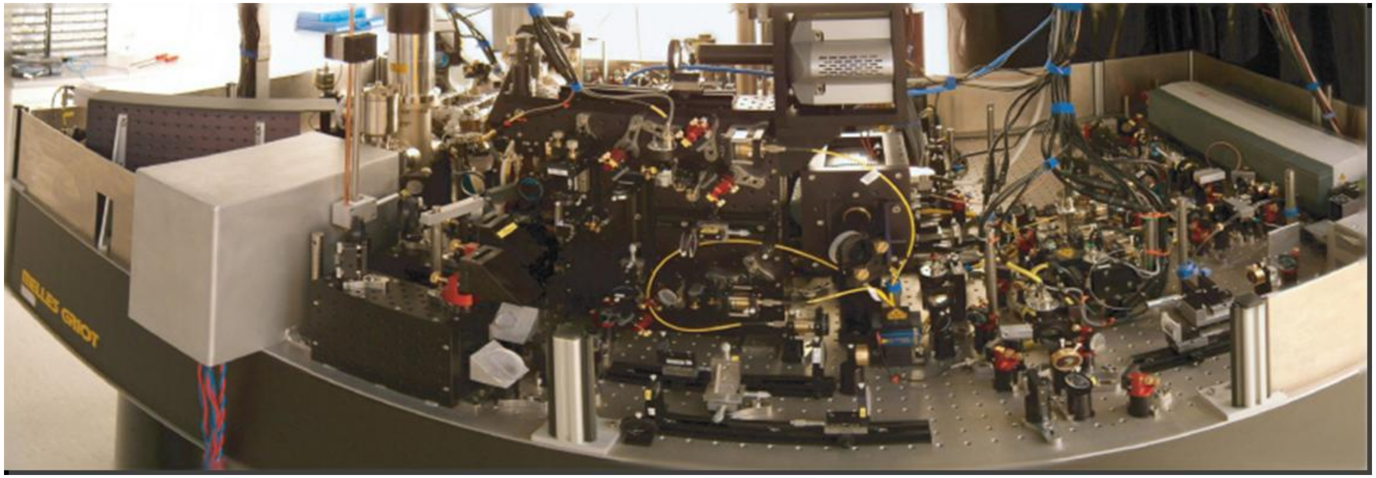

[Photo courtesy of U. Schneider]

But: trapping potential $\rightsquigarrow$ inhomogeneous systems

finite cloud sizes

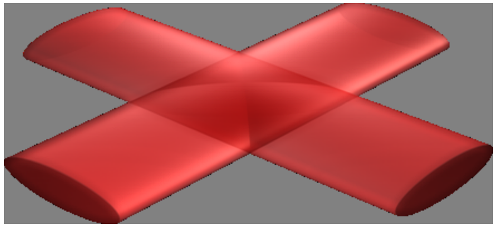

Ultracold fermions on optical lattices: model systems for strongly correlated materials

Ultracold atoms are much simpler: 1-band assumption is often accurate

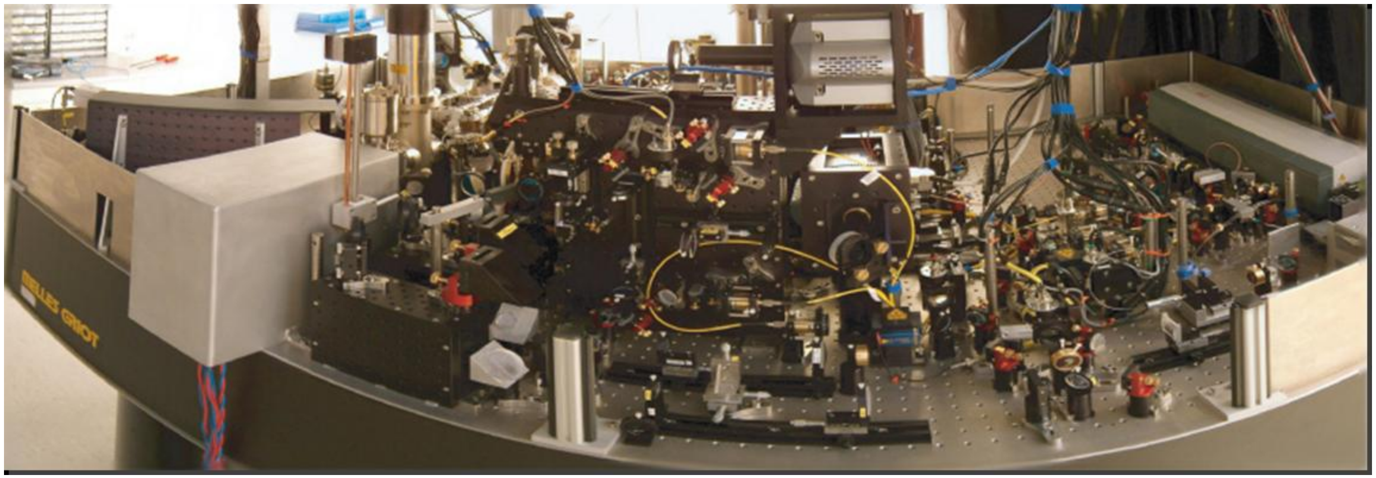

[Photo courtesy of U. Schneider]

But: trapping potential $\rightsquigarrow$ inhomogeneous systems

finite cloud sizes

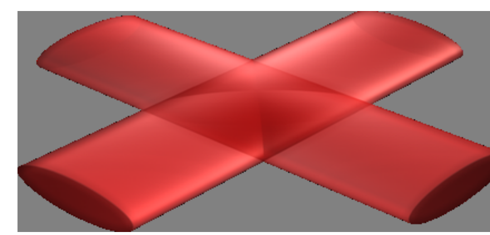

Note: more possibilities, e.g. 3-flavor systems

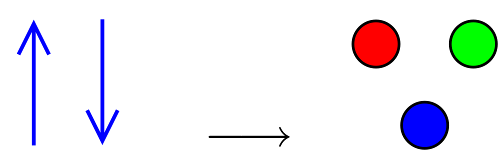

Paramagnetic Mott transitions in 3-flavor mixtures

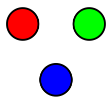

3 flavors: simplest case beyond electronic systems
1st approximation: all flavors equivalent

Paramagnetic Mott transitions in 3-flavor mixtures

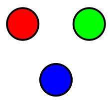

3 flavors: simplest case beyond electronic systems
1^{st} approximation: all flavors equivalent

- Qualitatively new physics: $U < 0$, $n = 1.5$ [Hofstetter, PRB (2004), PRL (2007)]

  Color superconductivity
  Trionic phase
  ...

Paramagnetic Mott transitions in 3-flavor mixtures

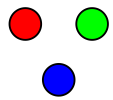

3 flavors: simplest case beyond electronic systems
1st approximation: all flavors equivalent

- Qualitatively new physics: $U < 0$, $n = 1.5$ [Hofstetter, PRB (2004), PRL (2007)]

  Color superconductivity
  Trionic phase
  . . .

- Ordered phases: $U > 0$, $n = 1$

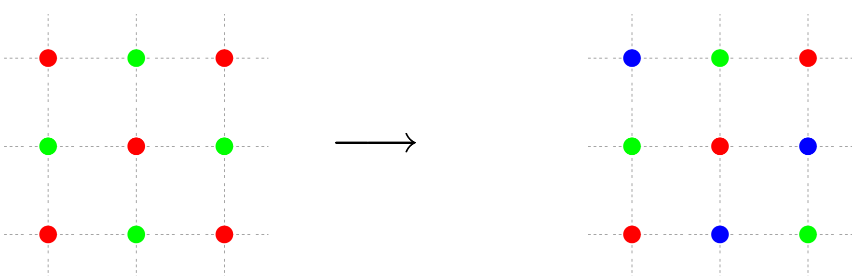

2 spins/flavors

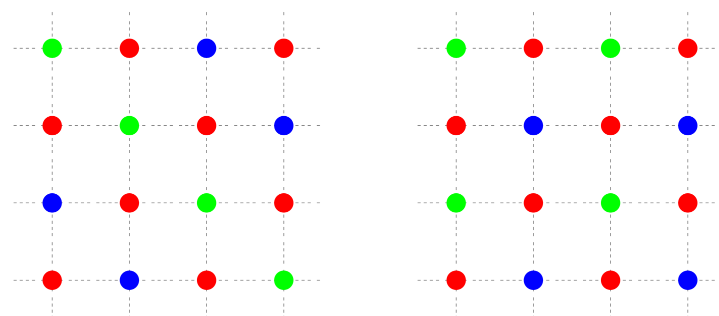

3 spins/flavors

Paramagnetic Mott transitions in 3-flavor mixtures

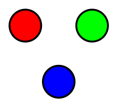

3 flavors: simplest case beyond electronic systems
1$^{\text{st}}$ approximation: all flavors equivalent

- Qualitatively new physics: $U < 0$, $n = 1.5$ [Hofstetter, PRB (2004), PRL (2007)]

  Color superconductivity
  Trionic phase
  . . .

- Ordered phases: $U > 0$, $n = 1$

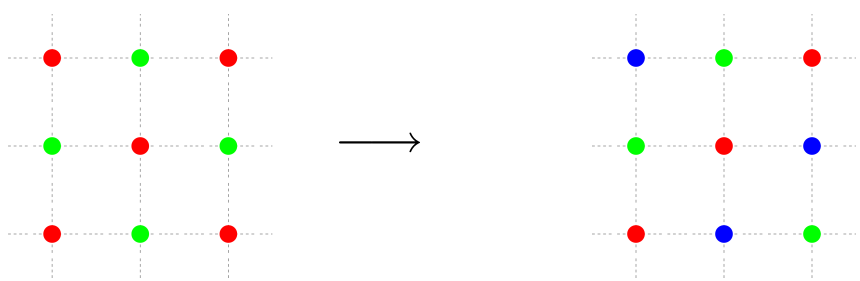

2 spins/flavors

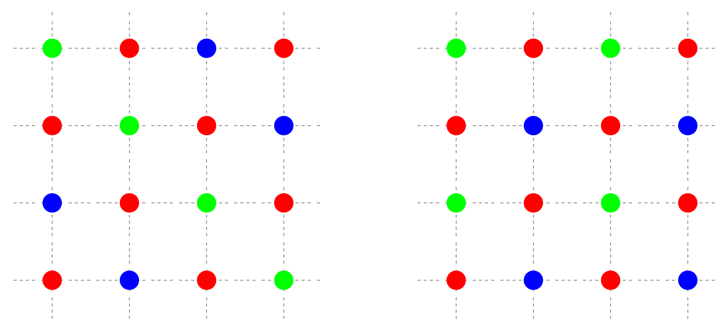

3 spins/flavors

Most "electron-like": $U > 0$, paramagnetic phase

Results at low T: particle density n and compressibility $\kappa = \frac{dn}{d\mu}$ (vs. μ)

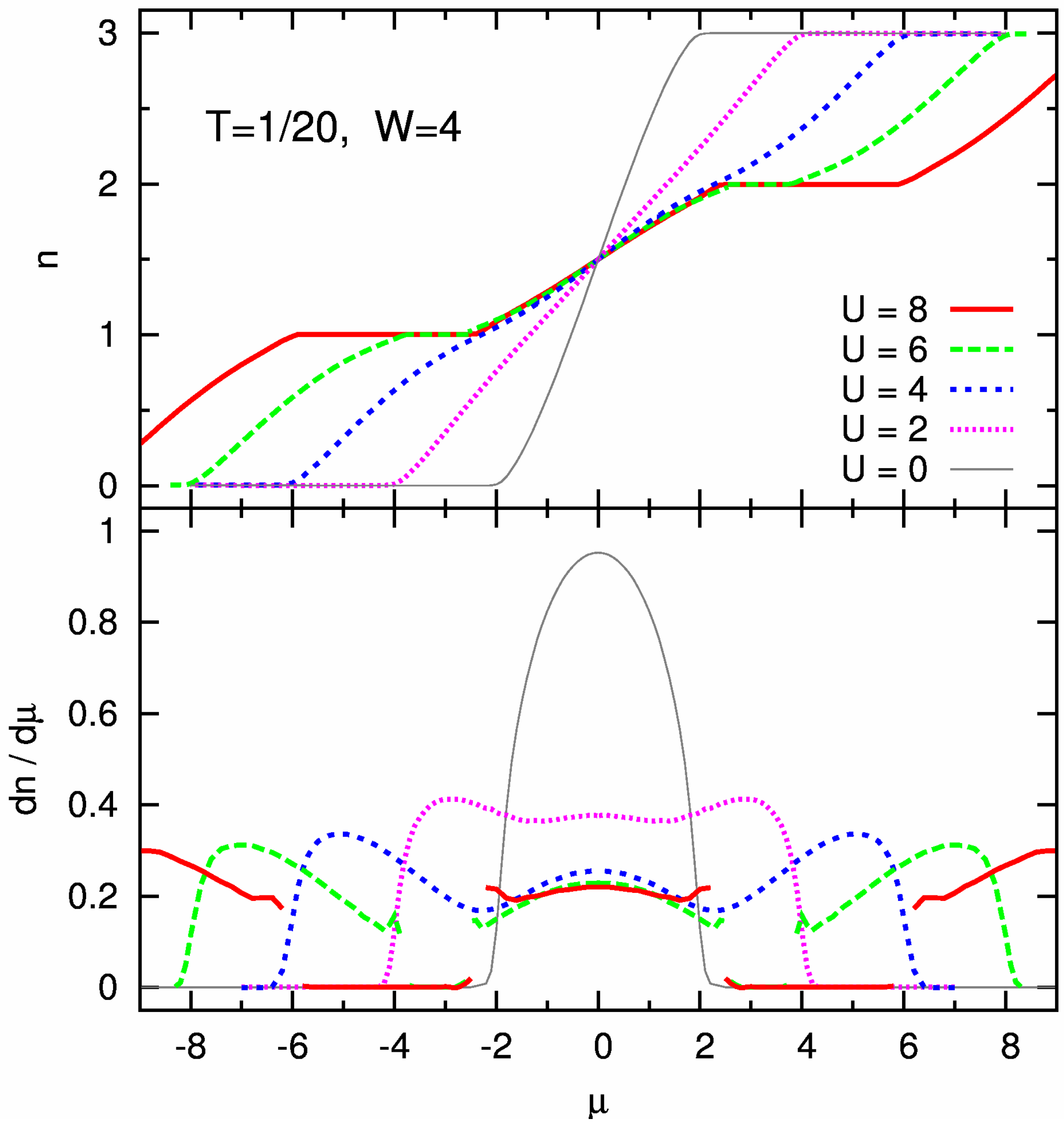

HF-QMC, Bethe DOS ($W = 4$)

Plateaus at integer filling ($U \gtrsim 5.5$)

$\rightsquigarrow$ incompressible Mott phases

[E. Gorelik, N. Blümer, arXiv:0904.4610]

Results at low T: particle density n and compressibility $\kappa = \frac{dn}{d\mu}$ (vs. μ)

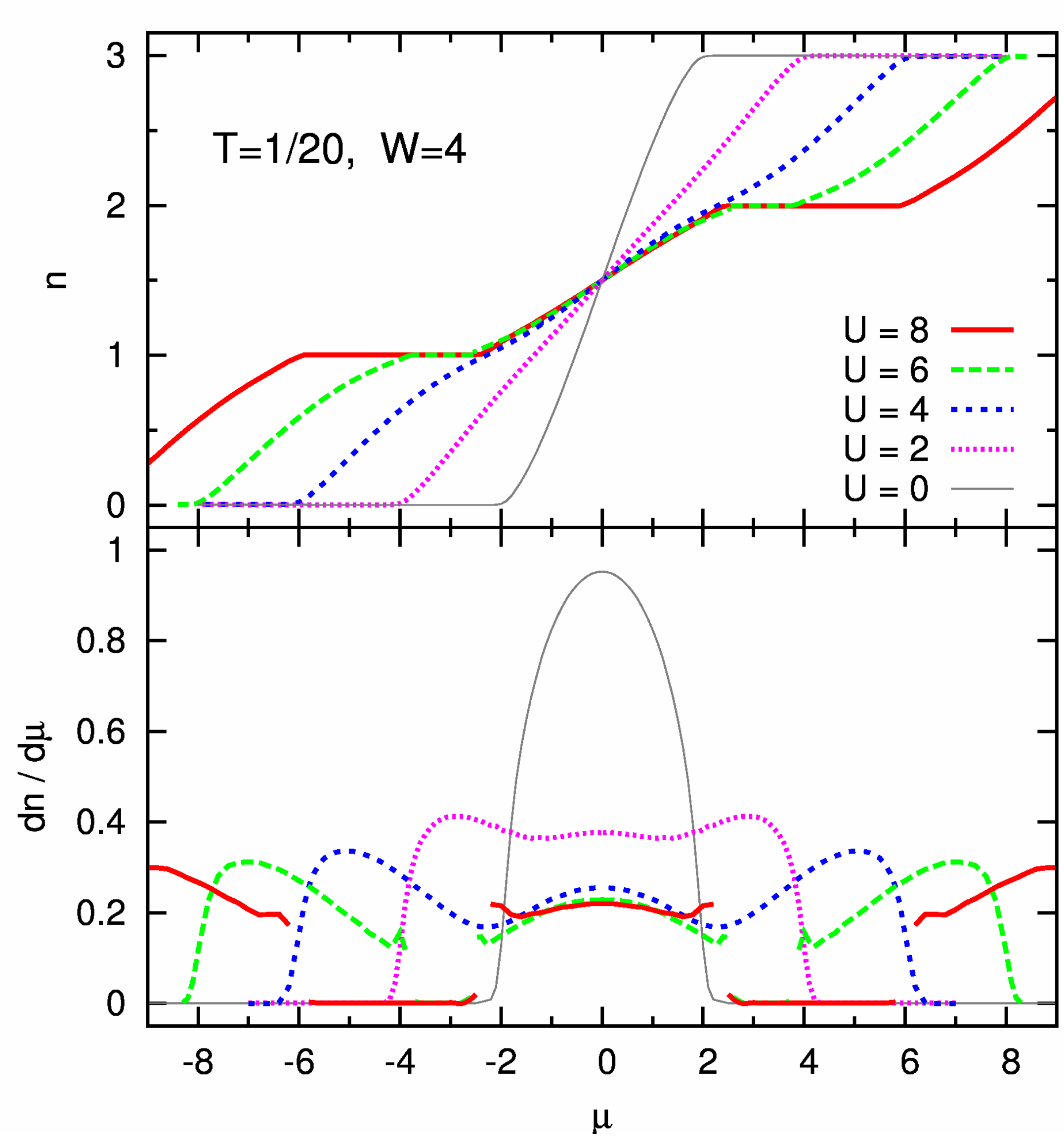

HF-QMC, Bethe DOS ($W = 4$)

Plateaus at integer filling ($U \gtrsim 5.5$)

$\rightsquigarrow$ incompressible Mott phases

$1 < n < 2$: semi-compressible phase

κ independent of μ, U, T

[E. Gorelik, N. Blümer, arXiv:0904.4610]

Results at low T: particle density n and compressibility $\kappa = \frac{dn}{d\mu}$ (vs. μ)

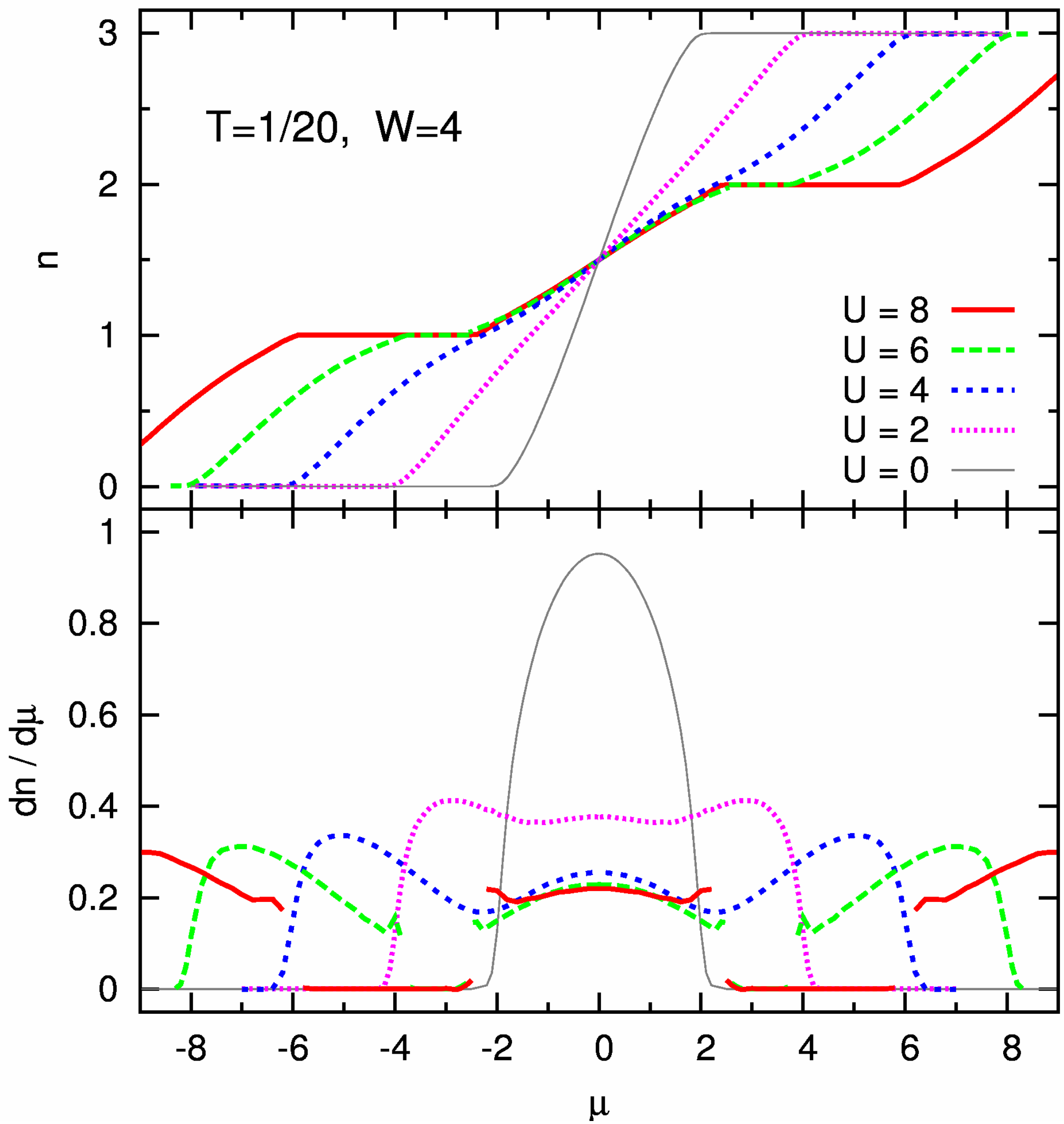

HF-QMC, Bethe DOS ($W = 4$)

Plateaus at integer filling ($U \gtrsim 5.5$)

$\rightsquigarrow$ incompressible Mott phases

$1 < n < 2$: semi-compressible phase

κ independent of μ, U, T

Contrast with SU(4) system:

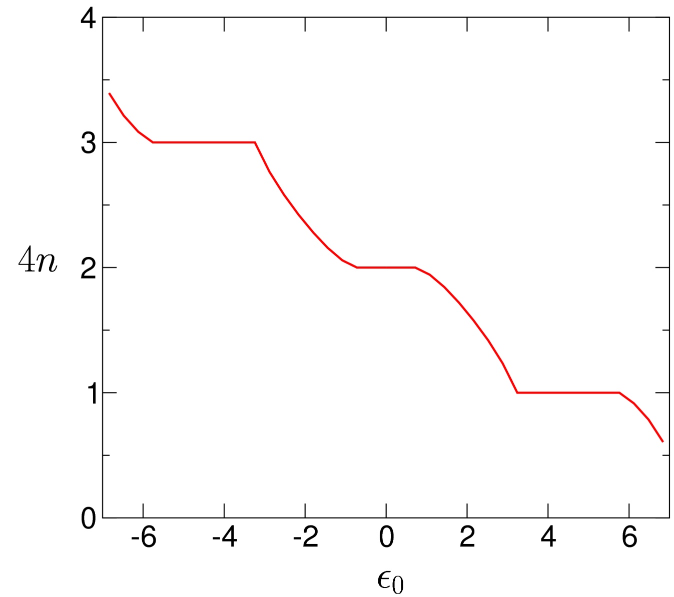

[E. Gorelik, N. Blümer, arXiv:0904.4610]

[Florens, Georges, PRB **70**, 035114 (2004)]

T dependence of density n and compressibility κ

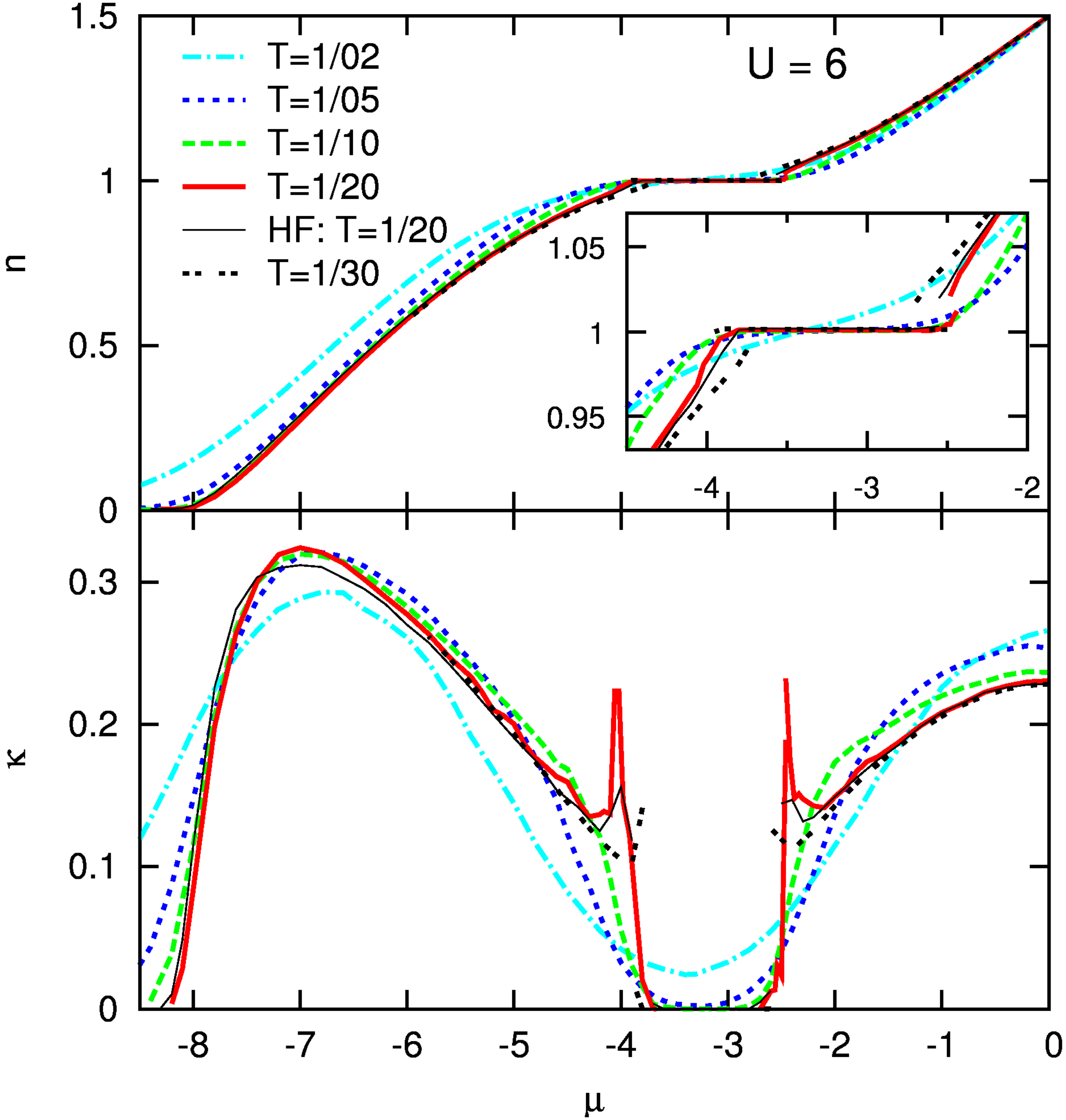

Multigrid HF-QMC results

(also HF-QMC at T = 1/20):

Critical temperature $T^{*} \approx 1/20$

T dependence of density n and compressibility κ

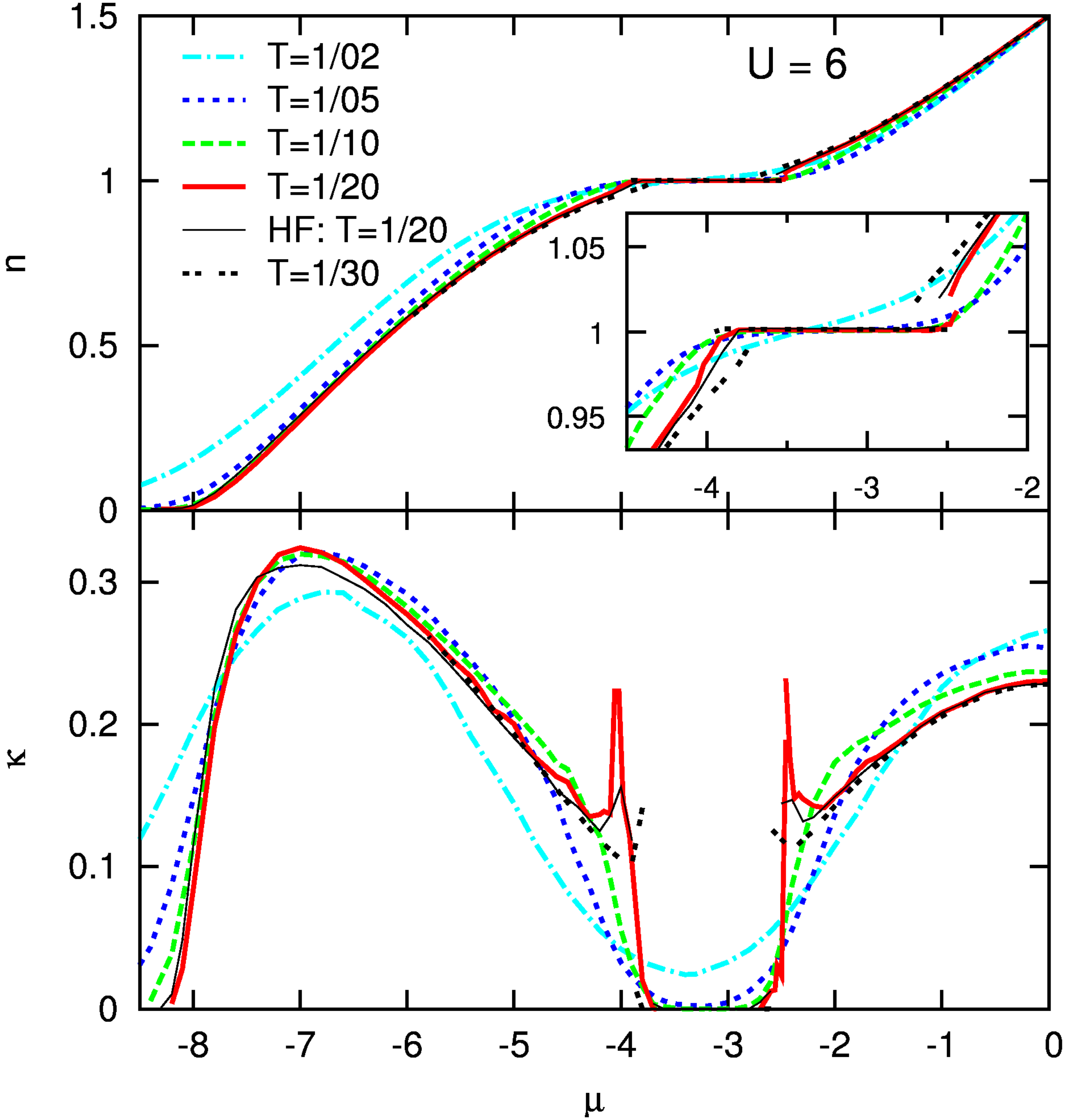

Multigrid HF-QMC results

(also HF-QMC at T = 1/20):

Critical temperature $T^* \approx 1/20$

Important for experiments:

Signatures of Mott transition persist to high temperatures:

nearly complete suppression of κ (at $n \approx 1$) up to $T \approx 1/5$.

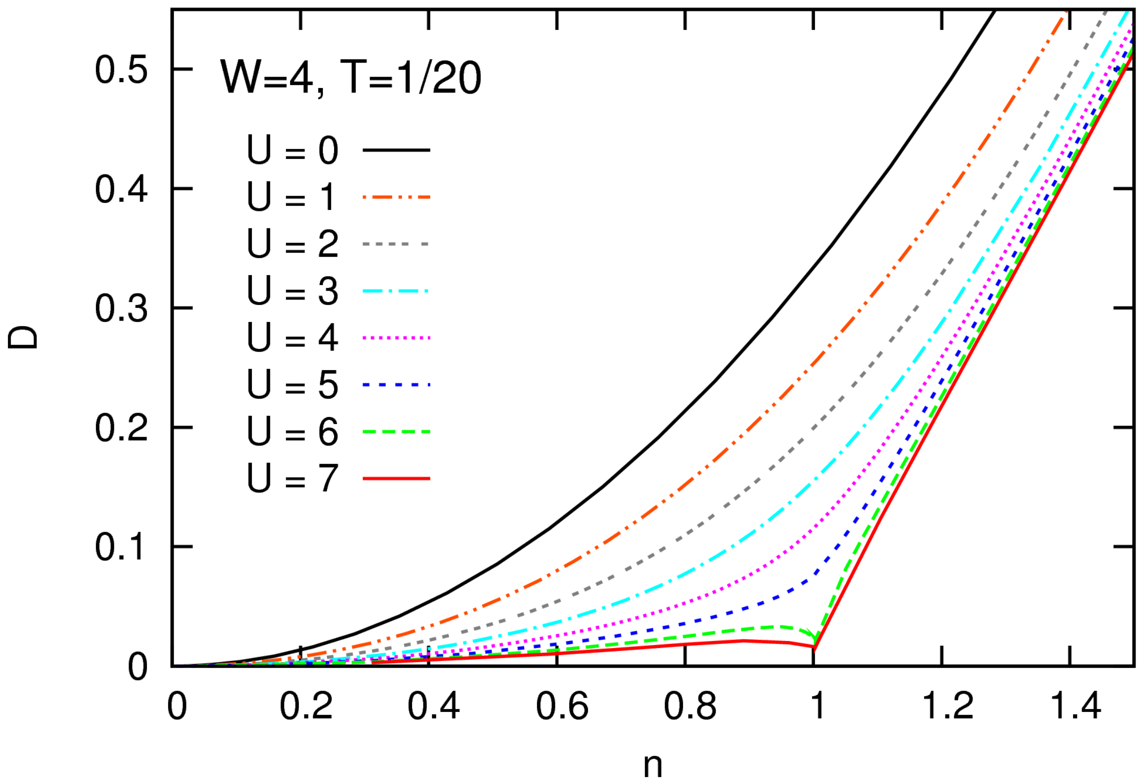

3-spin/flavor system:

Pair occupancy vs. density

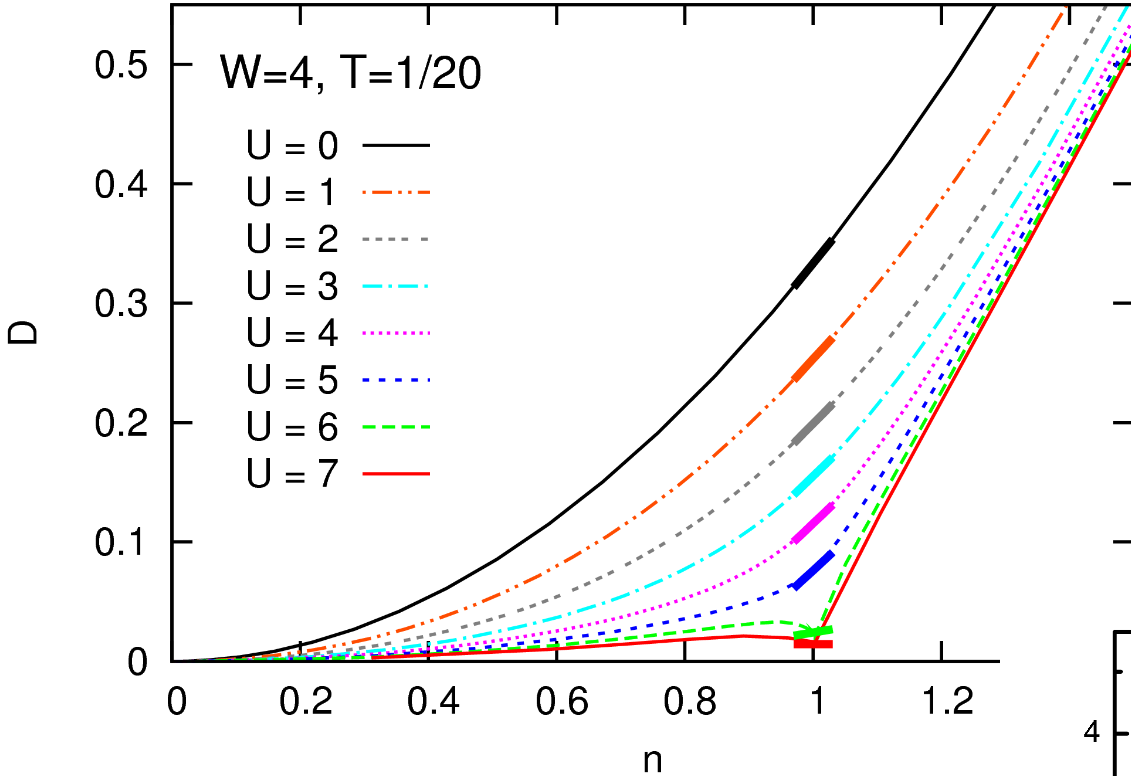

3-spin/flavor system:

Pair occupancy vs. density

Experiment: 2-spin system

Transition to an incompressible phase

[Jördens et al., Nature (2008)]

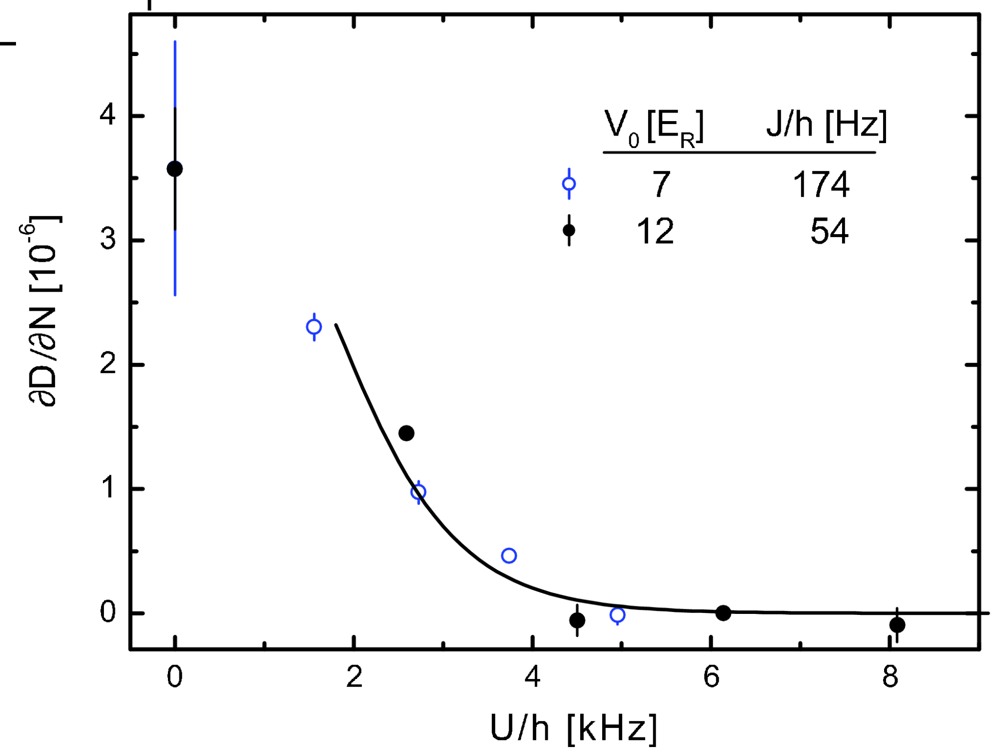

Local spectral function

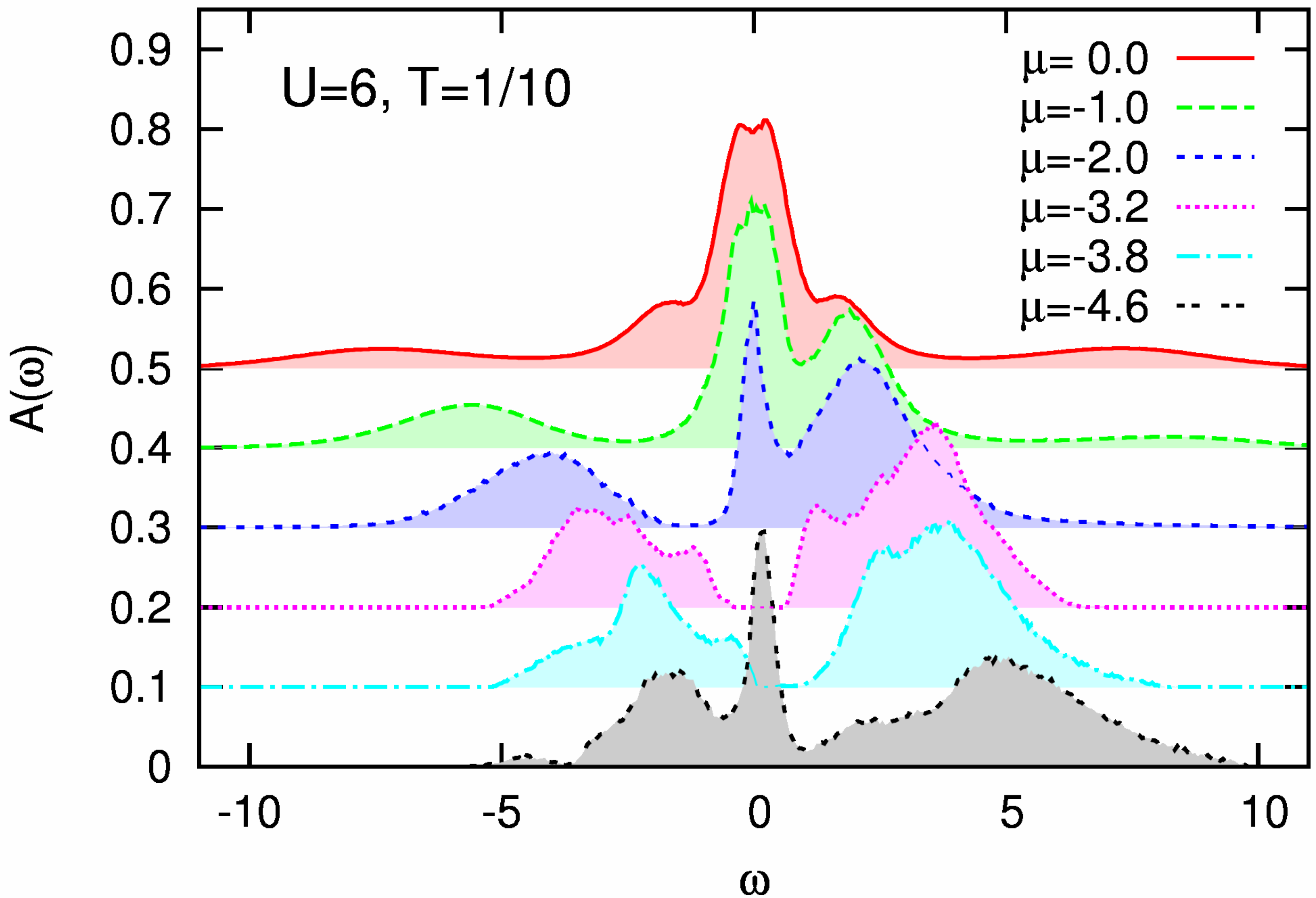

Melting of an antiferromagnet in an optical trap

Now include trapping potential, e.g.: $V_i = V r_i^2$

$$H = -\sum_{(ij),\sigma} t_{ij}\, c^{\dagger}_{i\sigma} c_{j\sigma} + U \sum_{i=1}^{N} n_{i\uparrow} n_{i\downarrow} + \sum_{i,\sigma} V_i\, n_{i\sigma}$$

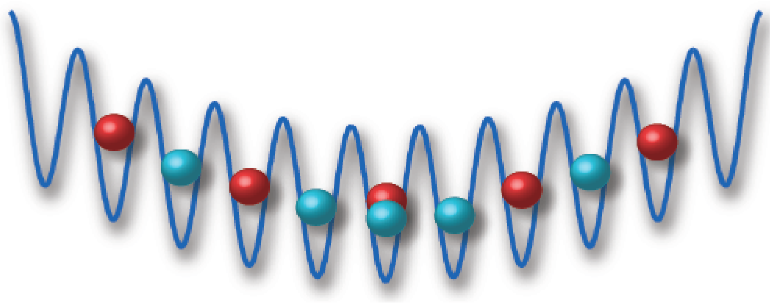

Melting of an antiferromagnet in an optical trap

Now include trapping potential, e.g.: $V_i = V r_i^2$

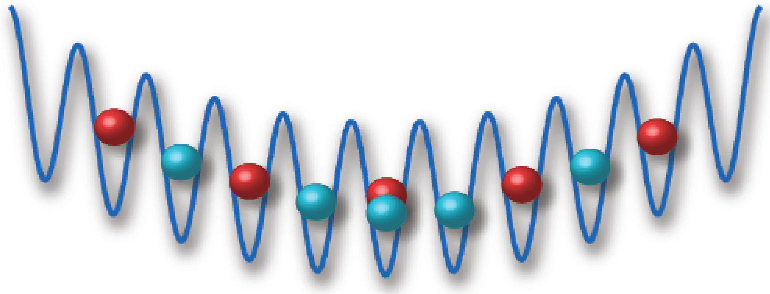

$$H = -\sum_{(ij),\sigma} t_{ij}\, c^\dagger_{i\sigma} c_{j\sigma} + U \sum_{i=1}^{N} n_{i\uparrow} n_{i\downarrow} + \sum_{i,\sigma} V_i\, n_{i\sigma}$$

Real-space DMFT: use local self-energy in inhomogeneous system

$\rightsquigarrow$ N single-site impurities, coupled by modified lattice Dyson equation:

$$\Big[G_\sigma(i\omega_n)\Big]^{-1}_{ij} = \big(\mu_\sigma + i\omega_n\big)\delta_{ij} - t_{ij} - \big(V_i + \Sigma_{i\sigma}(i\omega_n)\big)\delta_{ij}$$

[M. Snoek, I. Titvinidze, C. Toke, K. Byczuk, and W. Hofstetter, New Journal of Physics (2008); R. Helmes, T. A. Costi, and A. Rosch, PRL (2008)]

Also: inhomogeneous DMFT (for Falicov-Kimball model) [Freericks]

Melting of an antiferromagnet in an optical trap

Now include trapping potential, e.g.: $V_i = V r_i^2$

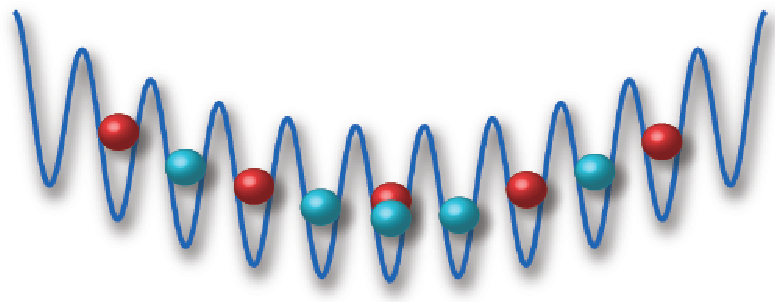

$$H = -\sum_{(ij),\sigma} t_{ij}\, c^\dagger_{i\sigma} c_{j\sigma} + U \sum_{i=1}^{N} n_{i\uparrow} n_{i\downarrow} + \sum_{i,\sigma} V_i\, n_{i\sigma}$$

Real-space DMFT: use local self-energy in inhomogeneous system

$\rightsquigarrow$ N single-site impurities, coupled by modified lattice Dyson equation:

$$\Big[G_\sigma(i\omega_n)\Big]^{-1}_{ij} = \big(\mu_\sigma + i\omega_n\big)\delta_{ij} - t_{ij} - \big(V_i + \Sigma_{i\sigma}(i\omega_n)\big)\delta_{ij}$$

[M. Snoek, I. Titvinidze, C. Toke, K. Byczuk, and W. Hofstetter, New Journal of Physics (2008); R. Helmes, T. A. Costi, and A. Rosch, PRL (2008)]

Also: inhomogeneous DMFT (for Falicov-Kimball model) [Freericks]

Note: impurity problem is site-parallel, lattice Dyson equation is frequency-parallel

All previous implementations: RDMFT+NRG

NRG: problematic at elevated temperatures

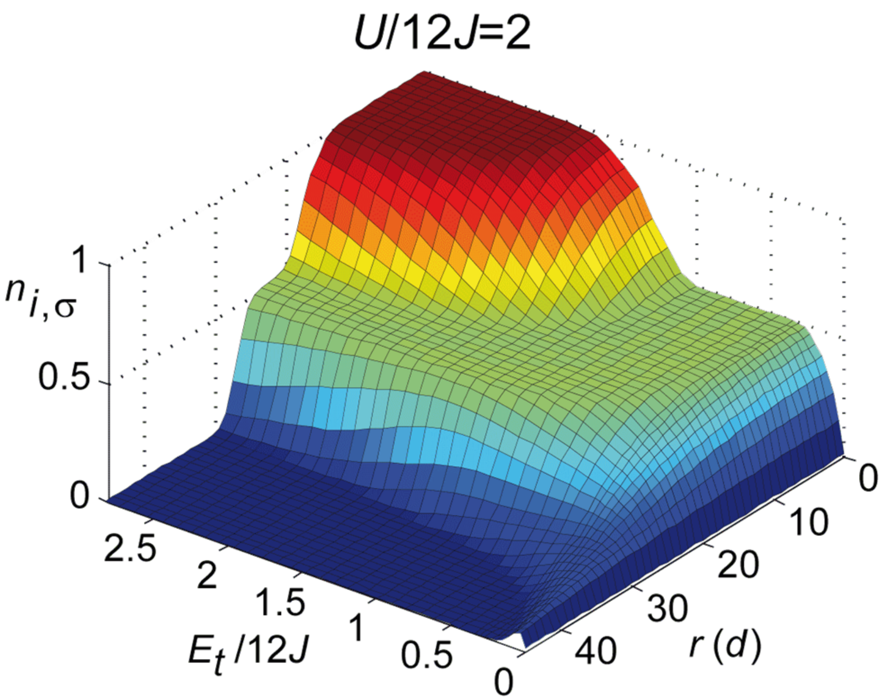

$T = 0.07t$

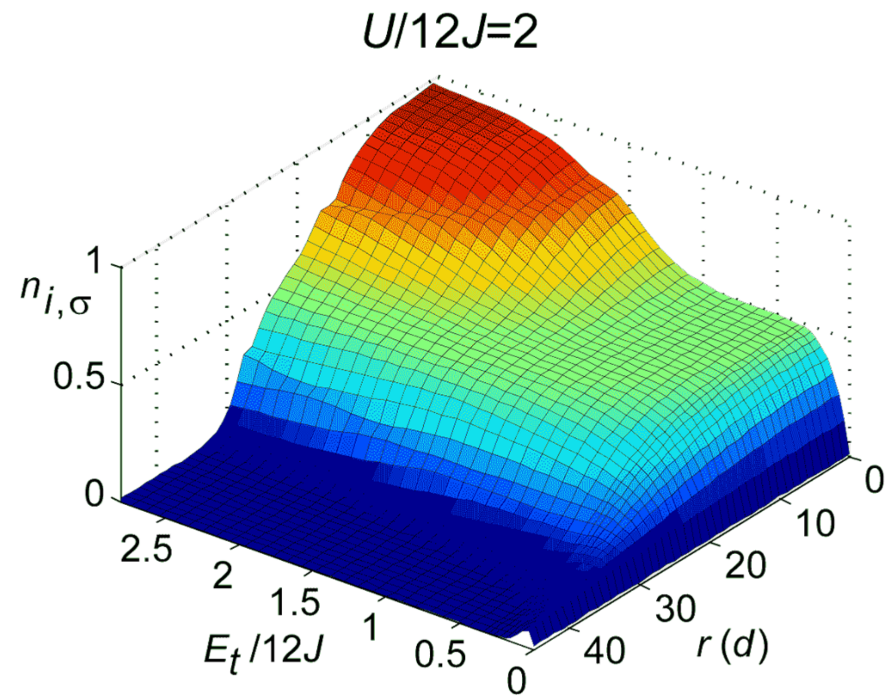

$T = 0.15t$

Additional plateau/kinks at $n_\sigma \approx 0.8$ for $T = 0.15t$ [Rosch group, courtesy of U. Schneider]

However: experimental temperatures are high $\rightsquigarrow$ advantage for QMC!

Real-space DMFT results for paramagnetic phase: QMC vs. NRG

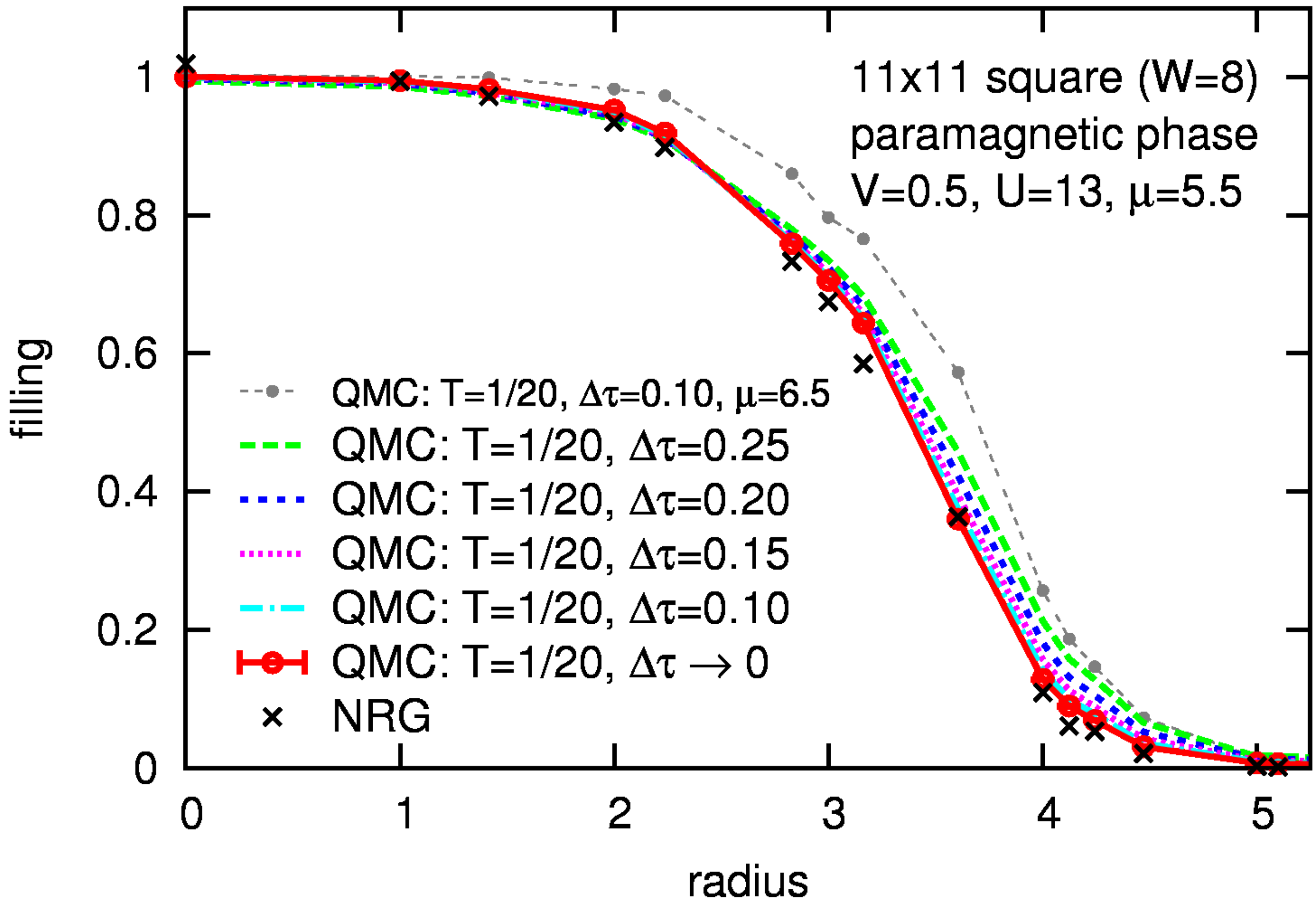

Good agreement QMC $\leftrightarrow$ NRG (after choosing same μ)

[NRG data by I. Titvinidze (collaboration within SFB/TR 49)]

Real-space DMFT results for AF phase: QMC vs. NRG

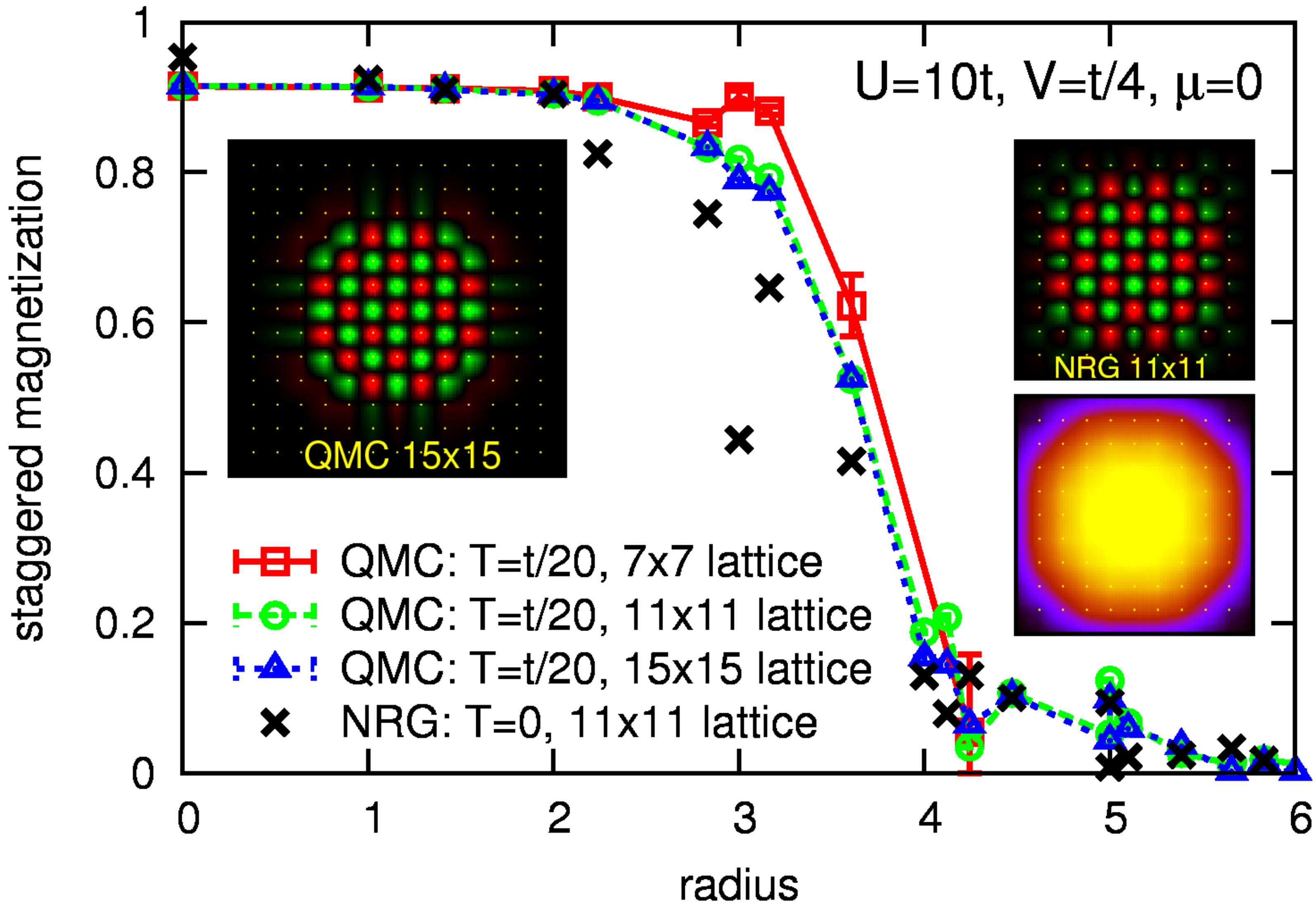

Finite-size effects surprisingly small; QMC apparently more accurate (even at low T)

Melting of a central antiferromagnetic phase

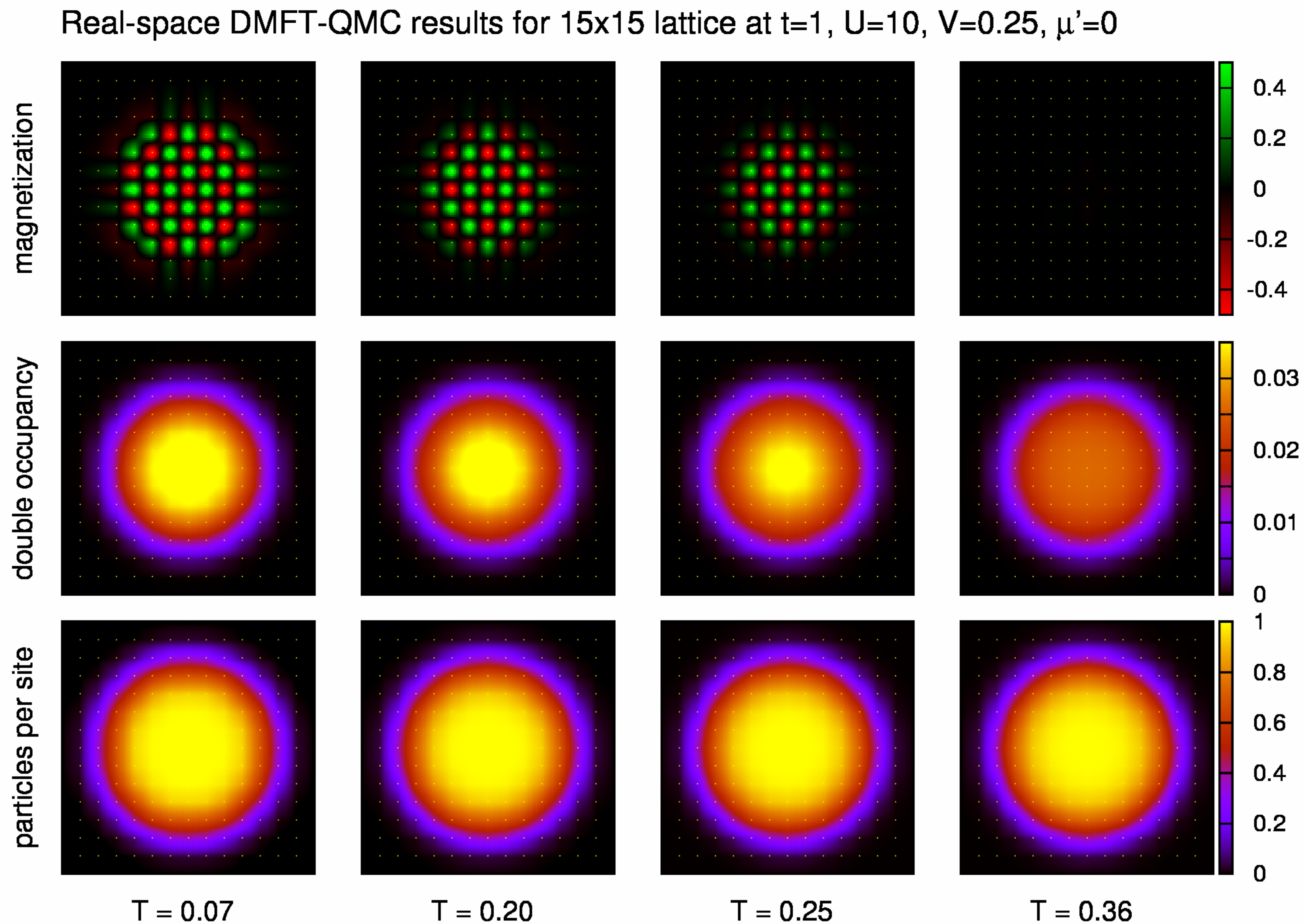

Antiferromagnetic order signaled by enhanced double occupancy - entropy?

Entropy: no direct computation, but from relations such as $dS/d\mu = dN/dT$

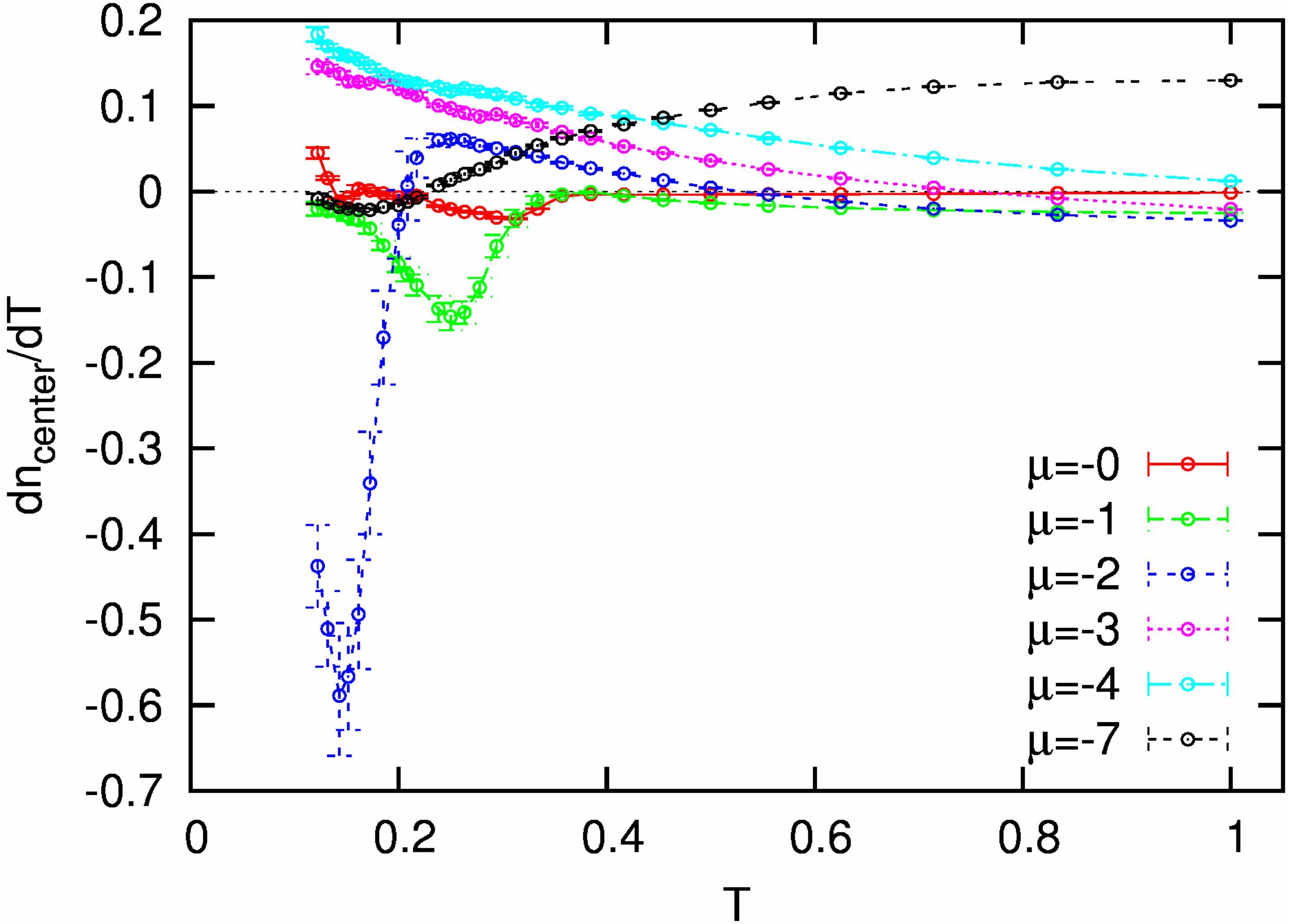

Example: derivative of central density (at $U = 10$, $V = 0.25$) for various μ

Strong negative peak at Neel temperature ($\rightsquigarrow$ need fine integration grid)

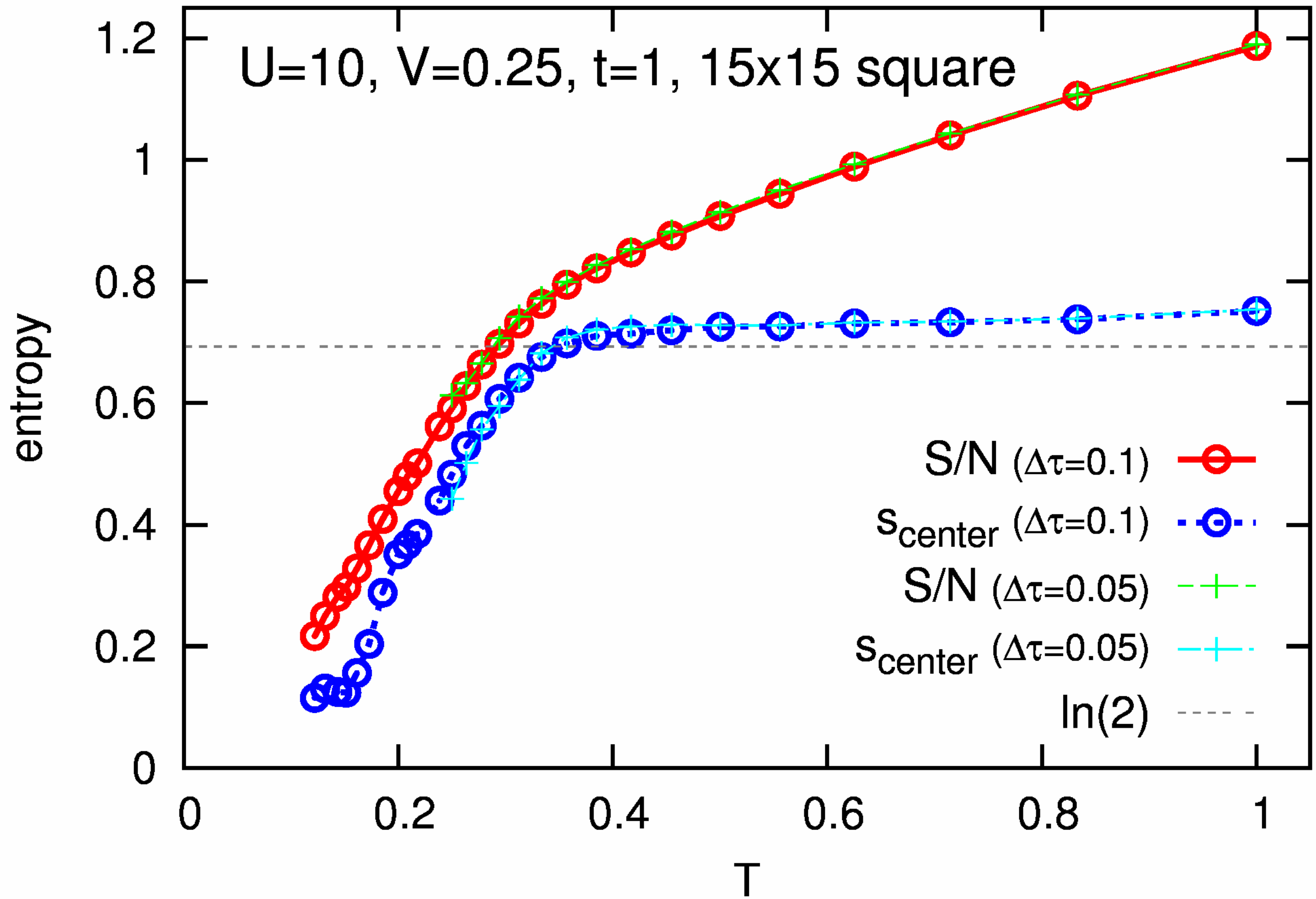

very small discretization dependence

Real-space DMFT-QMC results for 15x15 lattice at t=1, U=10, V=0.25, μ'=0

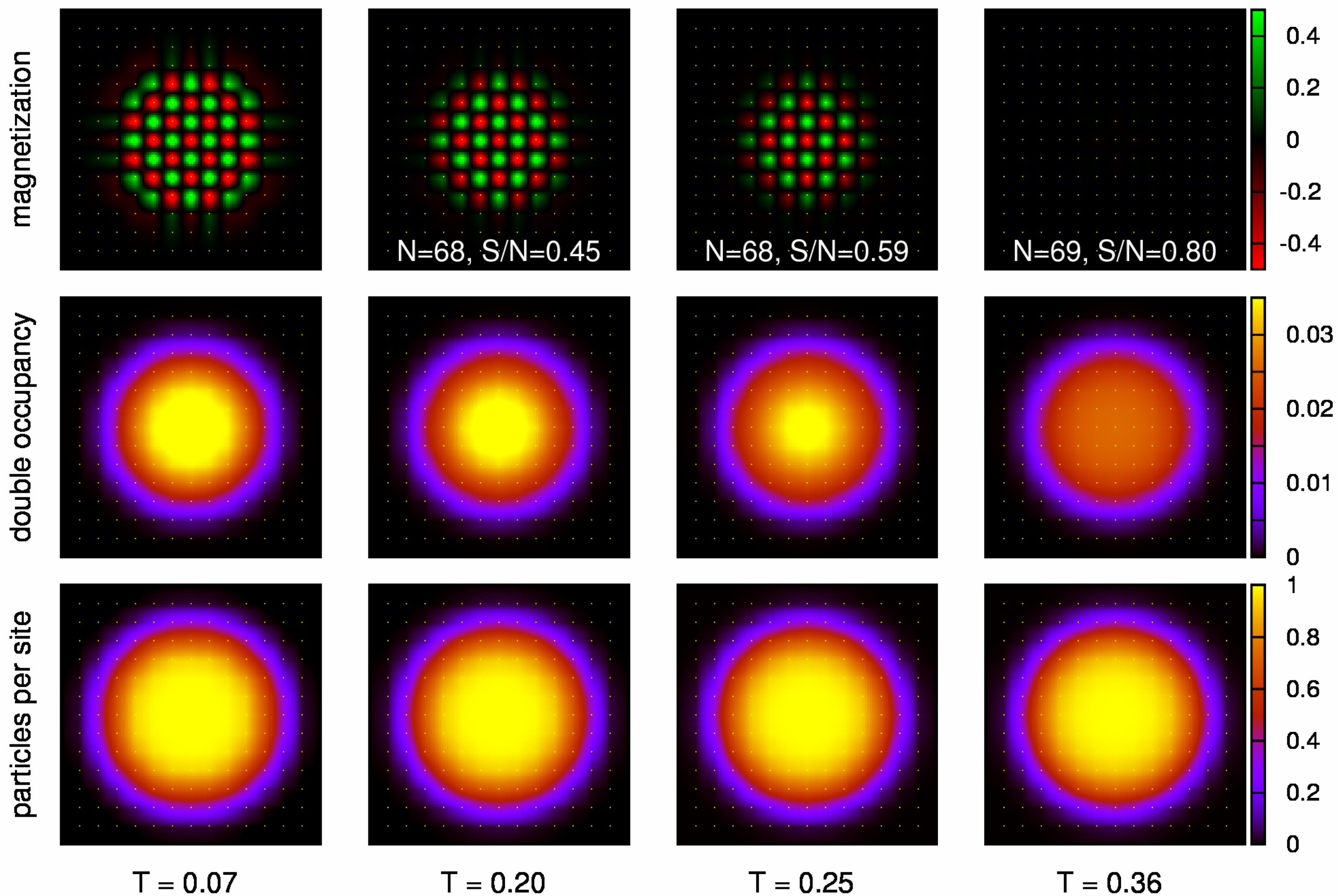

Effect of filling on the antiferromagnetic phase

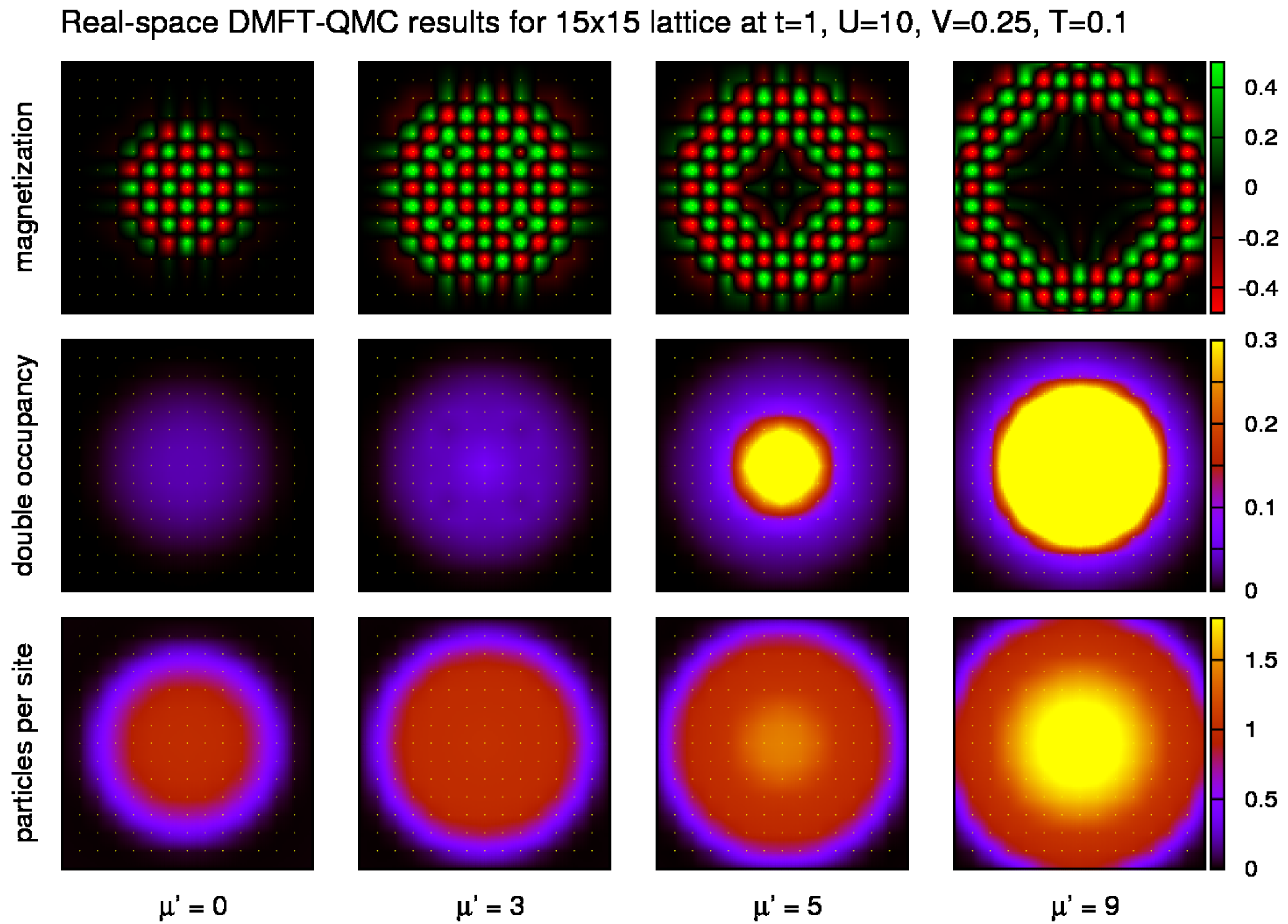

Buildup of metallic core → AF ring/shell

Effect of imbalance on the antiferromagnetic phase

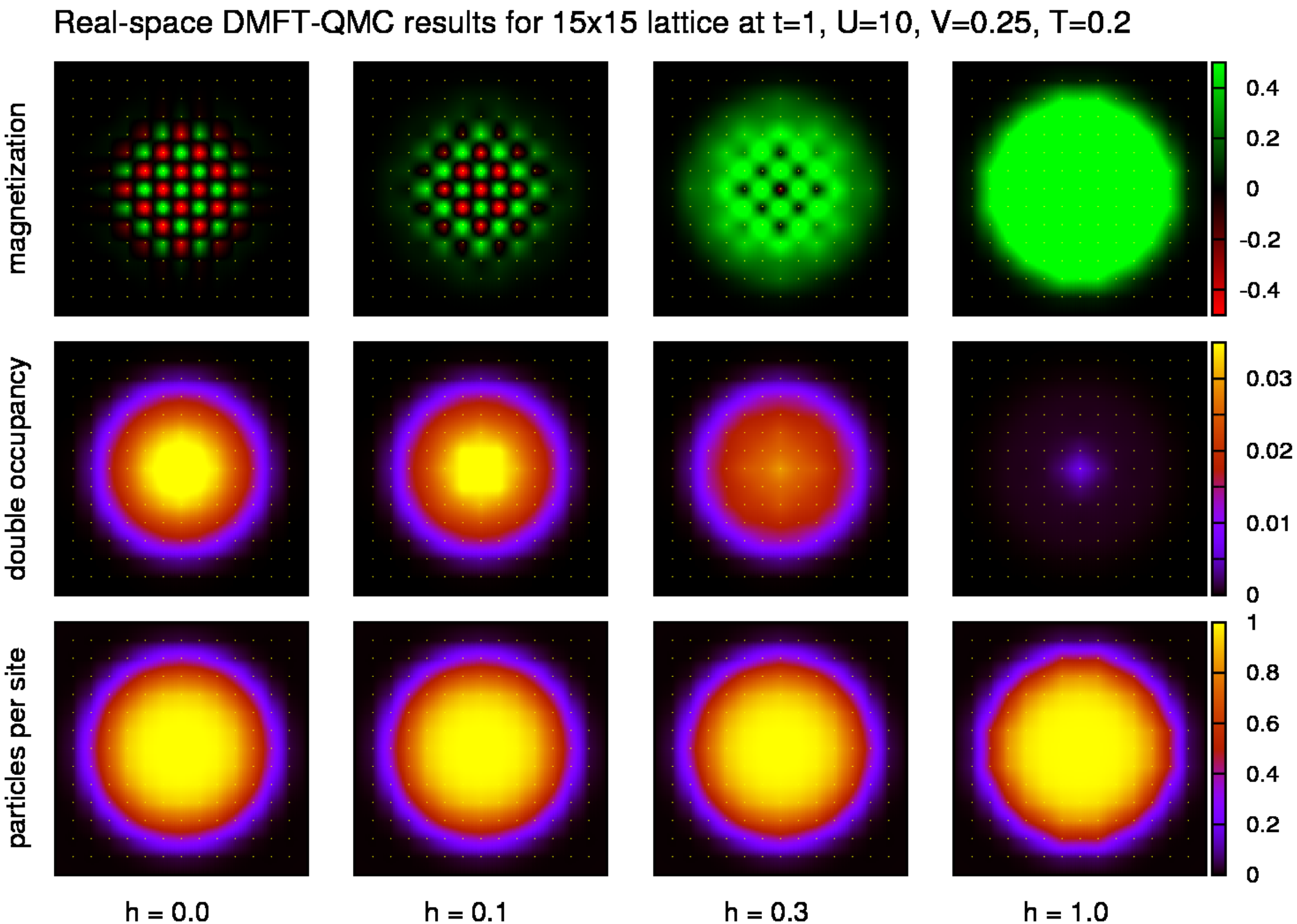

AF survives strong imbalance ($h = 0.3$); $h = 1$ nearly fully polarized

RDMFT: strong proximity effects (not in local μ approximation)

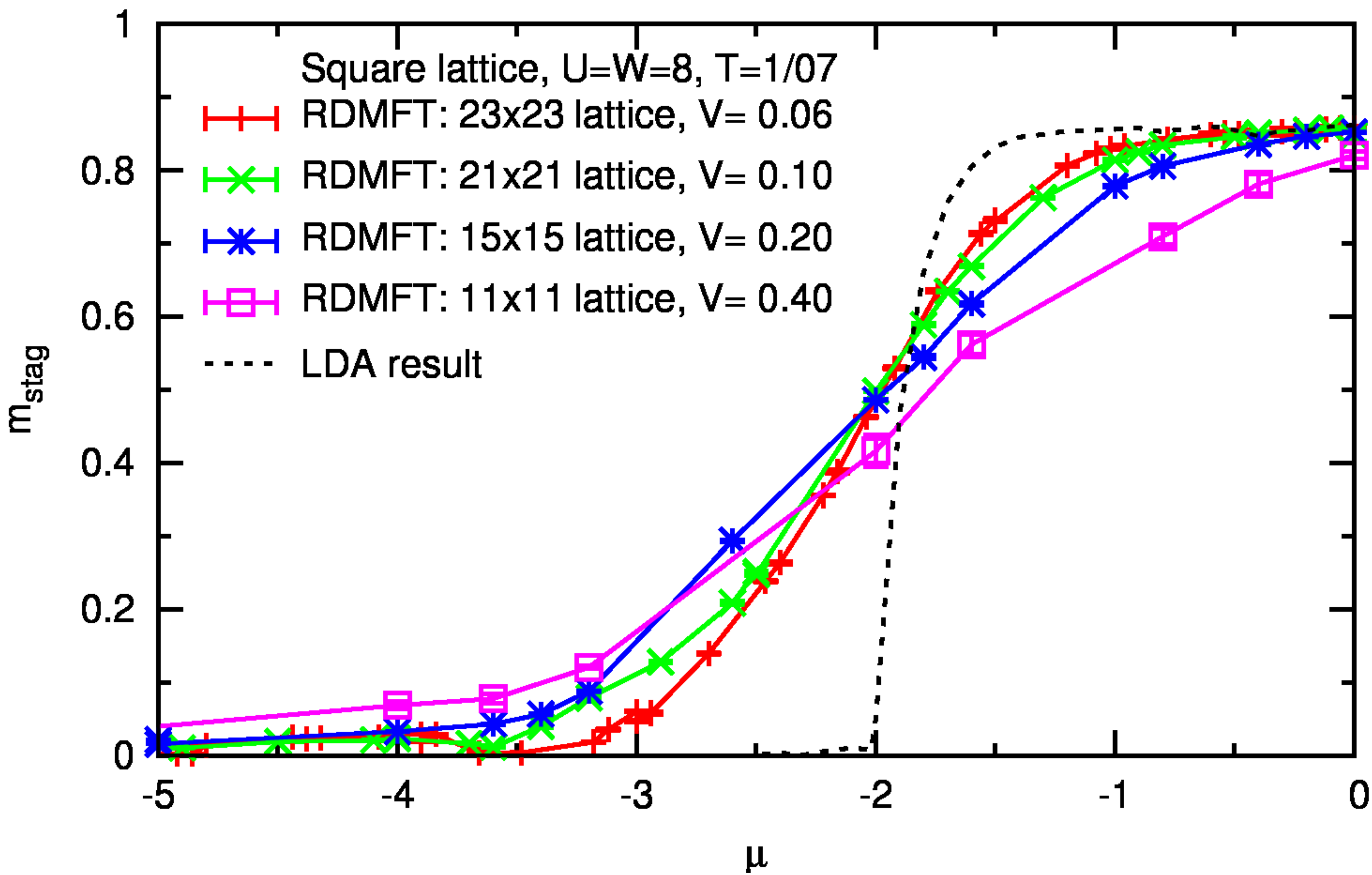

Summary

Multigrid HF-QMC method: numerically exact (quasi CT) + efficient

Mott transition for 3 degenerate flavors in (U, T, μ) space

Novel semi-compressible phase, spectra, small lattice effects

Real-space DMFT

Efficient and flexible RDMFT-QMC code

Melting of an antiferromagnet, entropy, imbalance – LDA deficient

Summary

Multigrid HF-QMC method: numerically exact (quasi CT) + efficient

Mott transition for 3 degenerate flavors in (U, T, μ) space

Novel semi-compressible phase, spectra, small lattice effects

Real-space DMFT

Efficient and flexible RDMFT-QMC code

Melting of an antiferromagnet, entropy, imbalance – LDA deficient

Outlook

3D calculations for realistic trap parameters and system sizes

Inequivalent spins/flavors: OSMT-like physics, ordered phases

Impact of higher Bloch bands

Spin-off: solids with large unit cells (distortions, surfaces, impurities, . . .)

Thanks to: Peter van Dongen Forschungsfonds 2007 and DFG (in SFB/TR 49)

Illustration: interpolation and extrapolation of Green functions

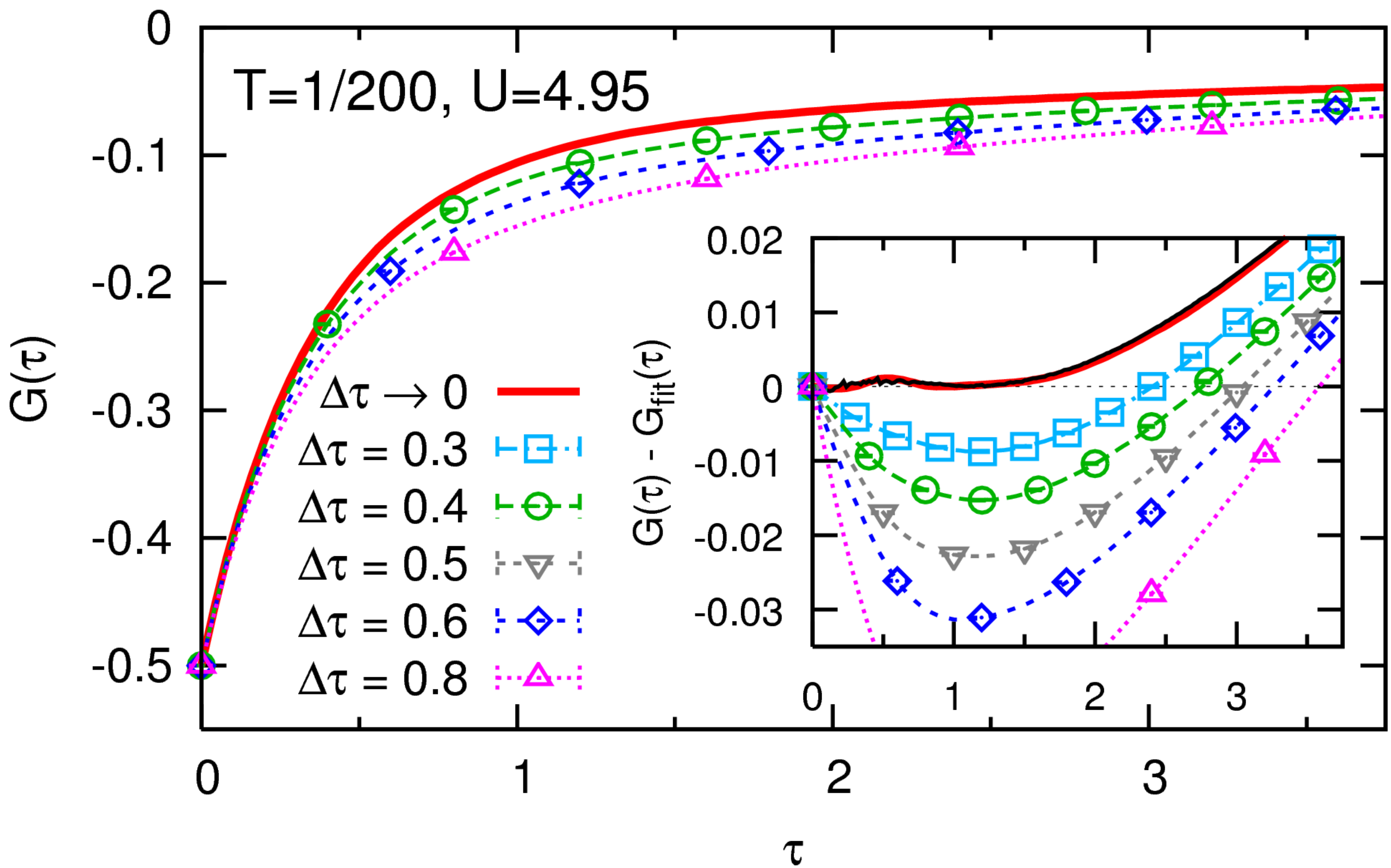

[NB, arXiv:0712.1290]

Excellent agreement with hybridization expansion CT-QMC [Werner et al., PRL (2006)]

Low-τ resolution limited by $\Delta\tau$? No!

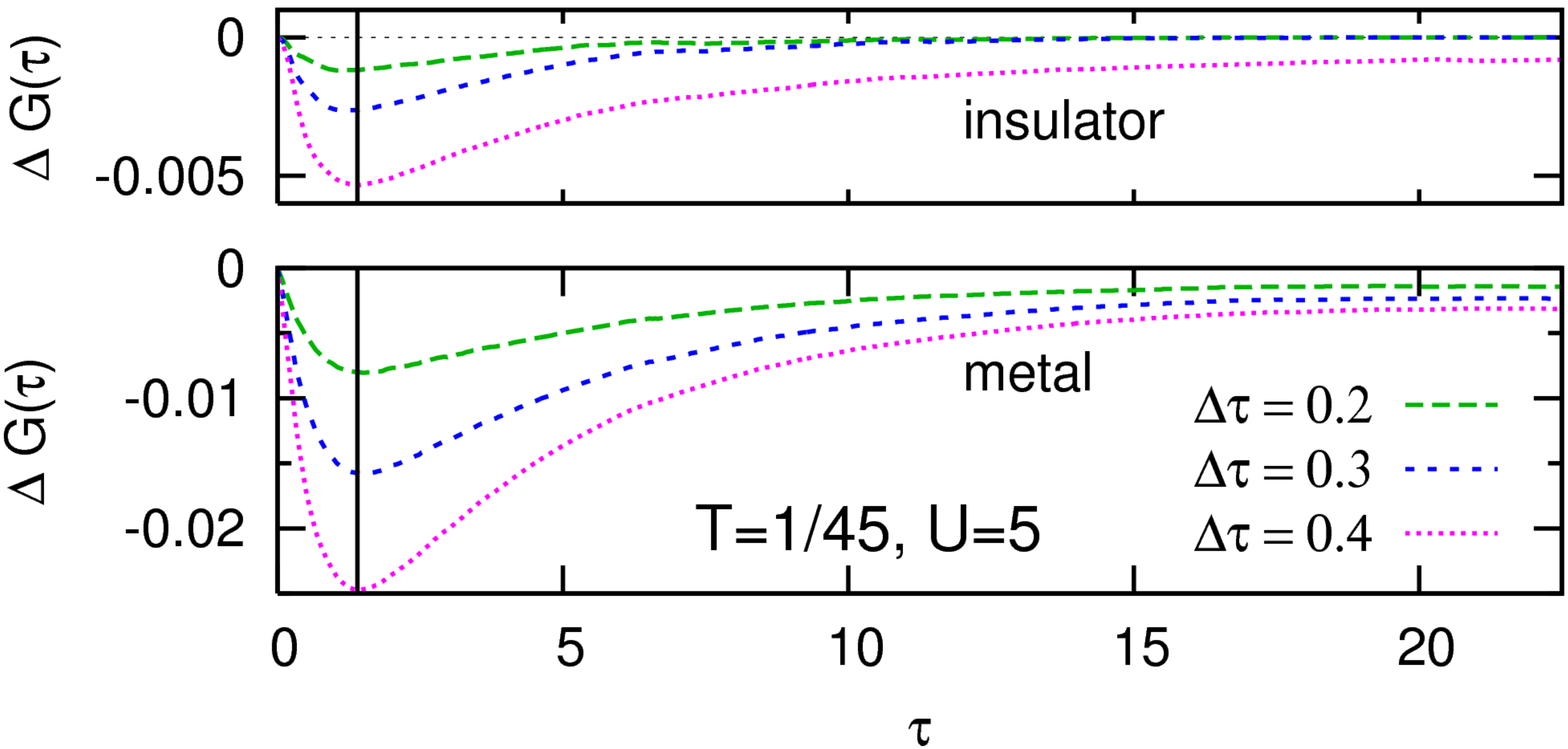

Uniform $\Delta\tau$ dependence, position of max. error independent of $\Delta\tau$ and phase!

Entropy distribution

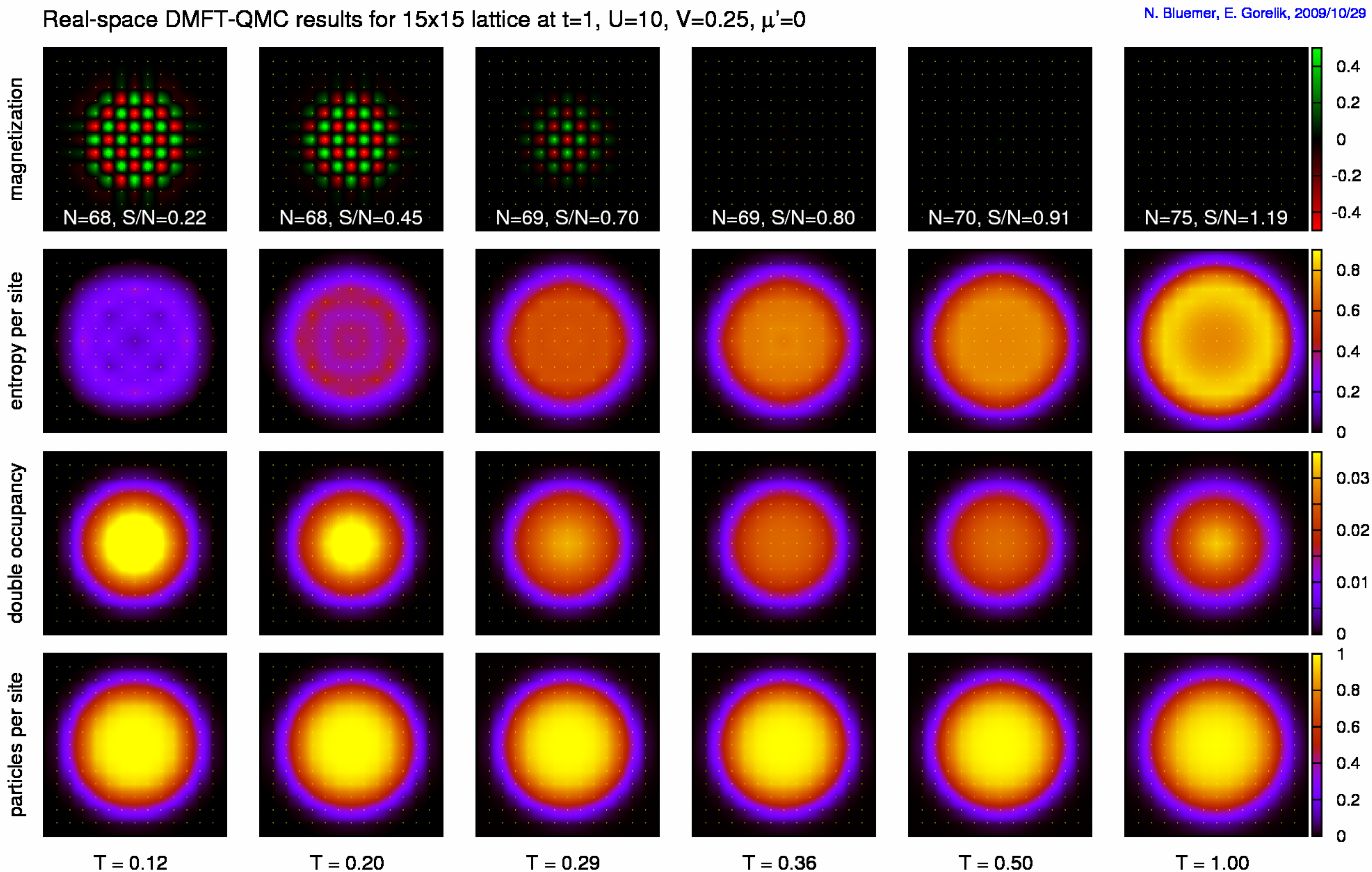

Benchmarks

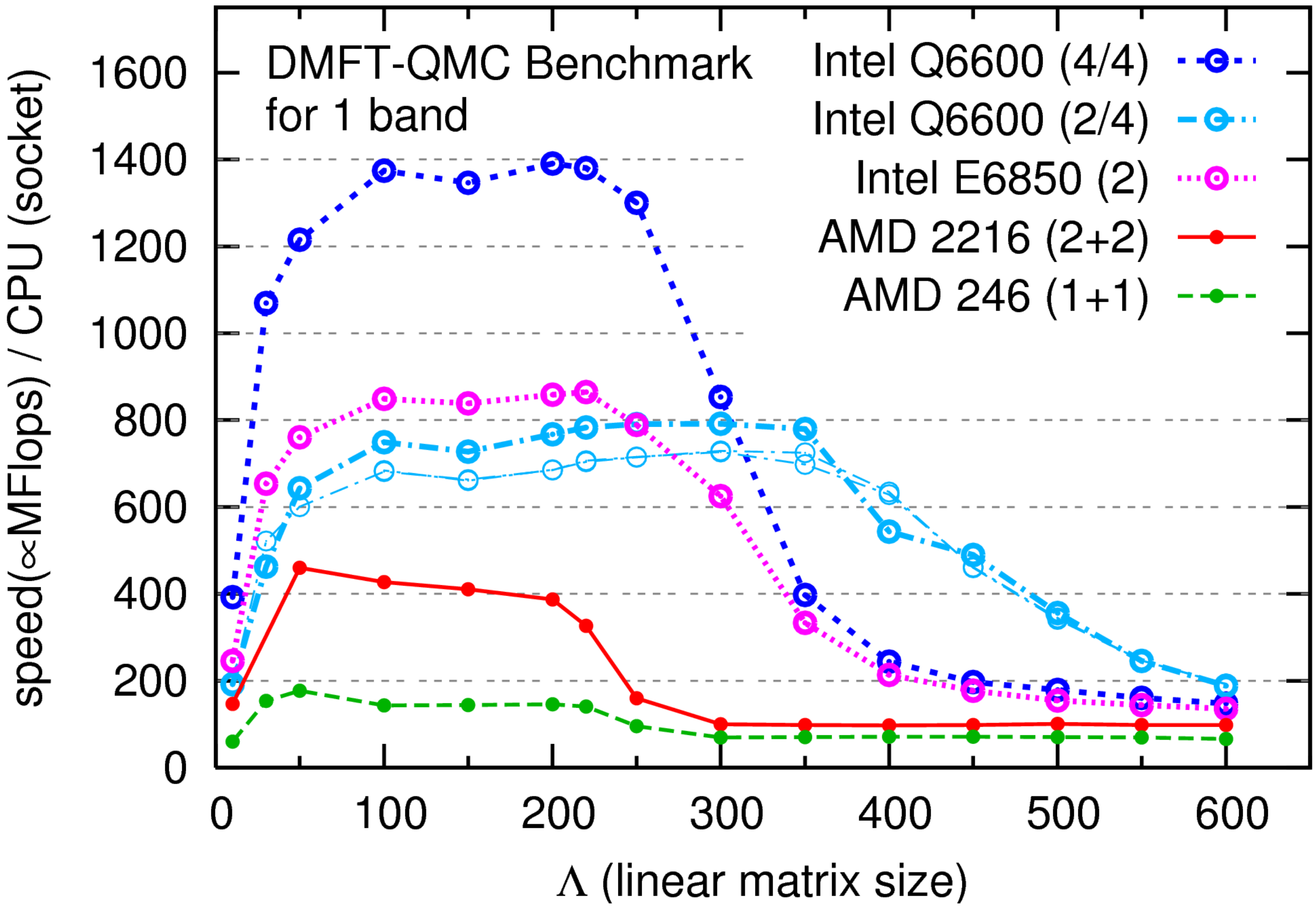

HF-QMC profits strongly from modern large-cache architectures

New (4/2008): hybrid parallelization (MPI + OpenMP)

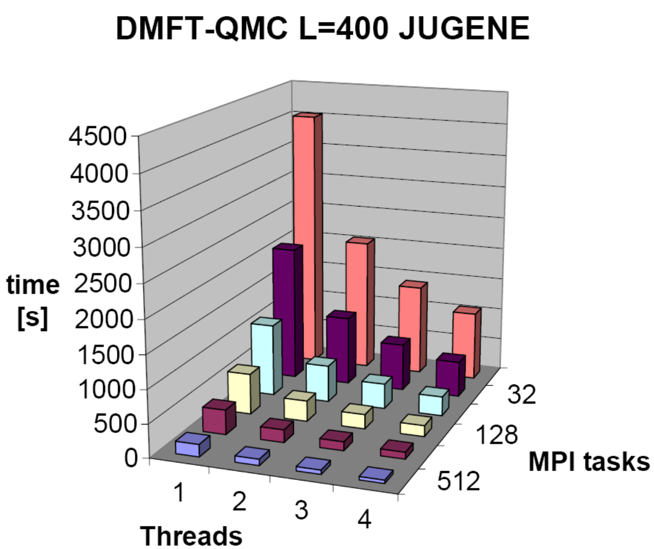

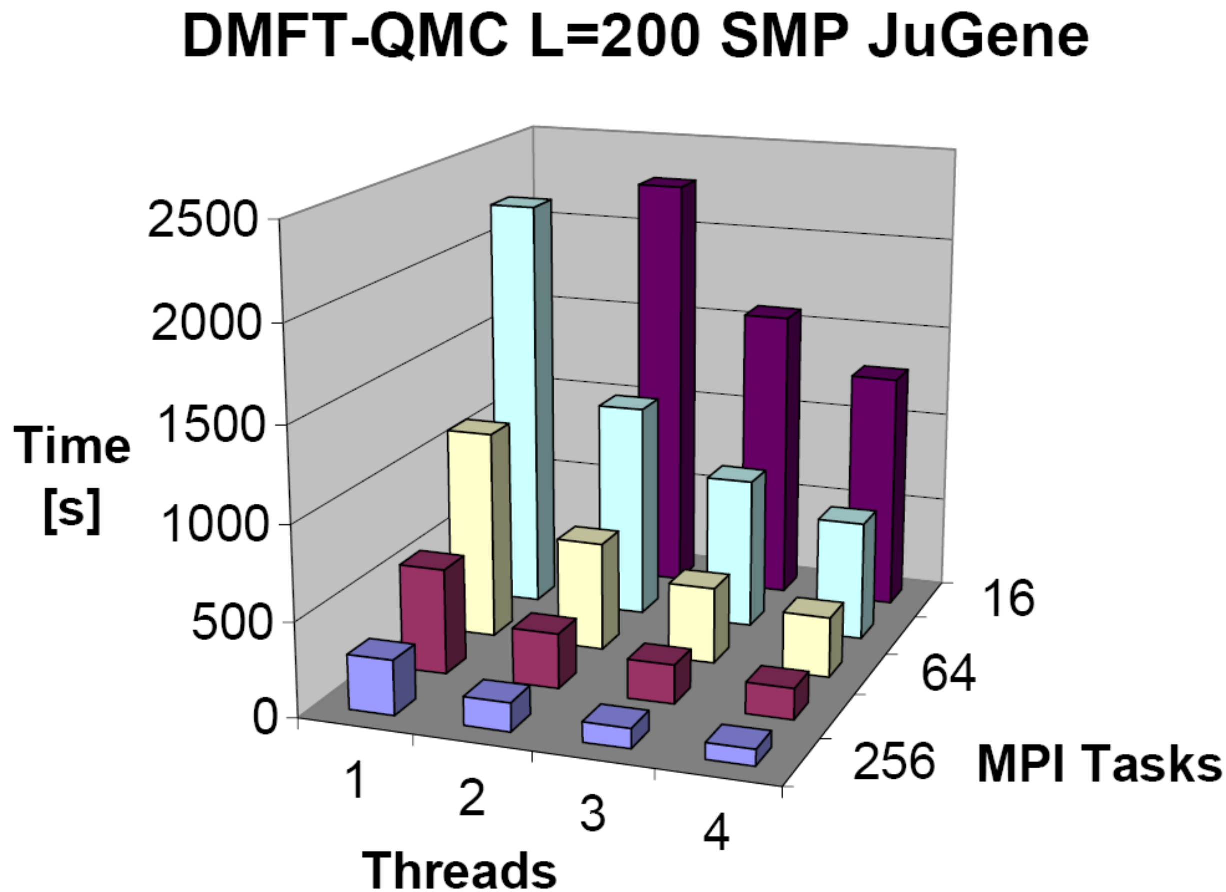

Very good scaling: speed roughly linear with number of CPU cores

Superlinear scaling on JUMP